Barbara Kramer

Collagen vascular diseases associated with interstitial lung diseases -

Analysis of alveolar epithelial cellular stress mechanisms.

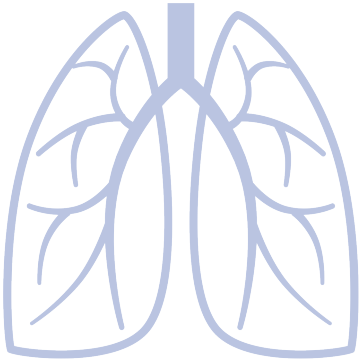

Inauguraldissertation zur Erlangung des Grades eines
Doktors der Medizin
des Fachbereichs Medizin der Justus-Liebig-Universität Gießen

edition scientifique
VVB LAUFERSWEILER VERLAG

1. Auflage 2017

1st Edition 2017

édition linguistique
VVB LAUFERSWEILER VERLAG

STAUFENBERGRING 15, D-35396 GIESSEN
Tel: 0641-5599888 Fax: 0641-5599890
email: redaktion@doktorverlag.de

www.doktorverlag.de

Collagen vascular diseases associated with interstitial lung diseases -

Analysis of alveolar epithelial
cellular stress mechanisms.

INAUGURAL-DISSERTATION

zur Erlangung des Grades eines
Doktors der Medizin
des Fachbereichs Medizin
der Justus-Liebig-Universität Gießen

vorgelegt von

Barbara Kramer

aus Olpe

Gießen 2017

Aus dem Zentrum für Innere Medizin
Medizinische Klinik II,
Direktor: Prof. Dr. med. W. Seeger
Universities of Giessen und Marburg Lung Center (UGMLC)

Gutachter: Prof. Dr. A. Günther

Gutachter: Prof. Dr. M. Wygrecka

Tag der Disputation: 15.11.2016

Meiner Familie

I Content

I Content I
II Figures IV
III Tables V
IV Abbreviations VI
V Summary XI
VI Zusammenfassung XII
1. Introduction 1
1.1 Interstitial lung diseases 1
1.2 ILD in collagen vascular diseases 3
1.3 Idiopathic pulmonary fibrosis 4
1.4 Nonspecific interstitial pneumonia 6
1.5 Molecular mechanisms underlying IPF and NSIP 8
1.5.1 Role of AECII in development of lung fibrosis 8
1.5.2 Endoplasmic reticulum (ER)-Stress and apoptosis 9
1.6 Collagen vascular diseases 10
1.6.1 Polymyositis and Dermatomyositis 10
1.6.1.1 Jo-1 syndrome 11
1.6.1.2 Lung involvement 11
1.6.1.3 Autoantibody against histidyl-tRNA-Synthethase 12
1.6.2 Systemic sclerosis 12
1.6.2.1 Lung involvement 13
1.6.2.2 Function of topoisomerases 14
2. Aim of the study 16
3. Material and Methods 17
3.1 Materials 17
3.1.1 Cell line 17
3.1.2 Human lung sections 17
3.1.2.1 Patient data 17
3.1.3 Machines / Software 18
3.1.4 Reagents 18
3.1.4.1 Chemicals and reagents 18
3.1.4.2 Transfection reagents 20

3.1.4.3 Antibodies....20
3.1.4.4 Buffer....21
3.1.4.5 Gels....23
3.1.4.6 Kits....24
3.2 Methods....24
3.2.1 Cell culture....24
3.2.2 siRNA Transfection....24
3.2.3 Protein Inhibition....25
3.2.4 Protein extraction and quantification....26
3.2.5 Polyacrylamide Gel Electrophoresis of Protein (SDS-Page)....26
3.2.6 Immunoblotting....27
3.2.7 Densitometry....28
3.2.8 RNA isolation and measurement....28
3.2.9 cDNA synthesis 28
3.2.10 Reverse transcription polymerase chain reaction (RT-PCR) 29
3.2.10.1 Semiquantitative reverse transcription polymerase chain reaction . .30
3.2.10.2 Quantitative reverse transcription polymerase chain reaction 31
3.2.10.3 DNA agarose gel electrophoresis....32
3.2.10.4 Measurement of fluoresecence with SYBR-Green....33
3.2.10.5 Melting curve analysis 33
3.2.10.6 Analysis of data....33
3.2.11 Immunohistochemistry....34
3.2.12 Statistical analysis....36
4. Results....37
4.1 Gene silencing in A549 cells....37
4.1.1 HisRS – Silencing and analysis of ER-stress and DNA-damage....38
4.1.1.1 HisRS - Silencing 38
4.1.1.2 Analysis of ER-stress and DNA-damage after HisRS knockdown……39
4.1.2 Topoisomerase 1 – Silencing and analysis of ER-stress 40
4.1.2.1 Topoisomerase 1 – Silencing 40
4.1.2.2 Analysis of ER-stress after Topoisomerase 1 knockdown 41
4.1.3 Topoisomerase 2α – Silencing and analysis of ER-stress 42
4.1.3.1 Topoisomerase 2α – Silencing....42
4.1.3.2 Analysis of ER-stress after Topoisomerase 2α knockdown....43
4.1.4 Topoisomerase 2β – Silencing and analysis of ER-stress 44

4.1.4.1 Topoisomerase 2β – Silencing.....44
4.1.4.2 Analysis of ER-stress after Topoisomerase 2β knockdown.....45
4.2 Protein Inhibition with topotecan and etoposide in A549 cells.....46
4.2.1 Analysis of ER-stress and apoptosis after topotecan treatment in A549 cells 46
4.2.2 Analysis of ER-stress and apoptosis after etoposide treatment in A549 cells 50
4.3 Analysis of ER-stress in a patient with SSc associated ILD 54
5. Discussion.....57
5.1 ILD associated with collagen vascular diseases.....57
5.2 ER-stress and apoptosis of AECII in CVD-ILD 59
5.3 Conclusions and future perspectives in regard to CVD-ILD pathogenesis.....62
6. Appendix.....64
6.1 Additional figures.....64
6.2 Primer sequences.....66
6.3 Dissociation curves.....67
7. References.....68
8. Erklärung.....78
9. Danksagung.....79

II Figures

Figure 1: A schematic for the general classification of the DPLDs [4].....1
Figure 2: Comparison of high-resolution CT features between UIP and NSIP [28].....5
Figure 3: Histologic features of UIP [28].....5
Figure 4: Histologic features of NSIP [28].....7
Figure 5: Dermatomyositis – Typical cutaneous signs [71-73].....11
Figure 6: Raynaud syndrome [76] 11
Figure 7: Systemic sclerosis – Typical cutaneous signs [89-91] 13
Figure 8: Schematic illustration of the action of Topoisomerase Type 1 [98].....14
Figure 9: Schematic illustration of the action of Topoisomerase Type 2 [99].....15
Figure 10: HisRS – Silencing.....38
Figure 11: No ER-stress or DNA damage 72hr after HisRS knockdown.....39
Figure 12: Topoisomerase 1 – Silencing.....40
Figure 13: No ER-stress after Topoisomerase 1 knockdown.....41
Figure 14: Topoisomerase 2α – Silencing.....42
Figure 15: No ER-stress after Topoisomerase 2α knockdown.....43
Figure 16: Topoisomerase 2β – Silencing.....44
Figure 17: No ER-stress after Topoisomerase 2β knockdown 45
Figure 18: Inhibition of Topoisomerase 1 and induction of apoptosis and ER-stress after topotecan treatment in A549 cells 47
Figure 19: Induction of CHOP after topotecan treatment in A549 cells.....48
Figure 20: Inhibition of Topoisomerase 2 and induction of apoptosis and ER-stress after etoposide treatment in A549 cells. 51
Figure 21: Induction of CHOP after etoposide treatment in A549 cells.....52
Figure 22: AECII specific induction of ER stress in patient with SSc-ILD.....54
Figure 23: Silencing of Topo1, Topo2α and Topo2β.....64
Figure 24: Inhibition of Topo1 after topotecan treatment in A549 cells.....65
Figure 25: Isotype controls.....65
Figure 26: Dissociation curves.....67

III Tables

Table 1: Classification of histological and radiological patterns developed for IIP [3].....3
Table 2: Machines / Software.....18
Table 3: Chemicals and biochemicals.....18
Table 4: Transfection reagents.....20
Table 5: Primary antibodies.....20
Table 6: Secondary antibodies.....21
Table 7: Seperating Gel.....23
Table 8: Stacking Gel.....23
Table 9: Kits.....24
Table 10: Master mix for reverse Transcription.....29
Table 11: Protocol for reverse transcription.....29
Table 12: PCR-Mix for sqRT-PCR (HotStarTaq DNA Polymerase).....30
Table 13: Cycle protocol for sqRT-PCR (HotStartTaq DNA Polymerase).....30
Table 14: PCR-Mix for sqRT-PCR (Phire Hot Start II DNA Polymerase).....31
Table 15: Cycle protocol for sqRT-PCR (Phire Hot Start II Polymerase).....31
Table 16: PCR-Mix for qRT-PCR.....32
Table 17: Cycle-protocol for qRT-PCR.....32
Table 18: Annealing Temperatures.....34
Table 19: Primer sequences.....66

IV Abbreviations

m	mili (10^-3)
µ	micro (10^-6)
n	nano (10^-9)
p	Pico (10^-12)

A

AECII	alveolar epithelial cell type II
AIP	acute interstitial pneumonia
ALAT	Latin American Thoracic Association
ANA	antinuclear antibody
anti	antibody against
APS	Ammonium persulphate
ATF4	Activating Transcription Factor 4
ATF6	Activating Transcription Factor 6
ATS	American Thoracic Society
A.dest.	Aqua destilated

B

BAL	bronchoalveolar lavage
BCA	Bicinchoninic Acid
bp	base pair
BSA	Bovine Serum Albumin

C

° C	degree Celsius
cDNA	complementary deoxyribonucleid acid
CFA	cryptogenic fibrosing alveolitis
CHOP	C/EBP Homologous Protein
cl. Caspase	cleaved Caspase
COP	cryptogenic organizing pneumonia
Ct	threshold cycle
CVD	collagen vascular disease

D

dcSSc	diffuse cutaneous systemic sclerosis
DDB1	DNA damage binding protein 1
DIP	desquamative interstitial pneumonia
DLCO	diffusing capacity of the lung for carbon monoxide
DNA	deoxyribonucleid acid
DM	Dermatomyositis
DMEM	Dulbecco´s Modified Eagle Medium
DMSO	Dimethylsulfoxide
DMSF	Dimethylsulfoxide
dNTP	deoxyribonucleotide triphosphate
DPLD	diffuse parenchymal lung disease
ds	double strand
dsRBP	dsRNA-binding protein

E

EAA	exogenous allergic alveolitis
EDTA	Ethylendinitrilo-N,N,N',N',-tetra-acetate
eIF2α	eukaryotic initiating factor 2α
EMT	Epithelial-mesenchymal transition
ER	endoplasmic reticulum
ERS	European Respiratory Society
EtBr	ethidium bromide
eurIPFreg	european IPF registry

F

FCS	fetal calf serum
FEV1	forced expiratory volume in the first second
fNSIP	familial non-specific interstitial pneumonia
FVC	forced vital capacity

G

g	gram

H

h	hour
HisRS	histidyl-tRNA-synthetase
HPS	Hermansky-Pudlak syndrome
HPSIP	Hermansky-Pudlak syndrome-associated interstitial pneumonia
HRCT	High-resolution computed tomography

I

IB	immunoblot
ICAM-1	intercellular adhesion molecule 1
IHC	immunohistochemistry
IIP	idiopathic interstitial pneumonia
ILD	interstitial lung disease
IP	Interstitial pneumonia
IPF	idiopathic pulmonary fibrosis
IRE1α	inositol-requiring enzyme 1α

J

JRS	Japanese Respiratory Society

K

kDa	kilo Dalton

L

LC3	Light chain 3
lcSSc	limited cutaneous systemic sclerosis
LIP	lymphoid interstitial pneumonia

M

m	mean
MeOH	methanol
min	minutes
mRNA	messenger RNA

N

NaCl	sodium chloride

NAD+	nicotinamide adenide dinucleotide
NaOH	sodium hydroxide
n.s.	non significant
NSIP	non-specific interstitial pneumonia

O

OP	organizing pneumonia

P

PARP-1	poly[adenosine diphosphate (ADP)-ribose] polymerase 1
PBS	phosphate-buffered saline
PCR	polymerase chain reaction
PERK	protein kinase RNA-like endoplasmic reticulum kinase
PM	polymyositis
PVDF	polyvinylidene fluoride
PMSF	Phenylmethylsulfonylfluorid
PPIB	Peptidyl-prolyl cis-trans isomerase B
Pro SP-C	pro Surfactant protein C

Q

qRT-PCR	quantitative reverse transcription PCR

R

RB-ILD	respiratory bronchiolitis – interstitial lung diesease
RISC	RNA-induced silencing complex
RNA	ribonucleic acid
RT	room temperature or reverse Transcriptase/Transcription
RT-PCR	reverse Transcription PCR

S

SD	standard deviation
SDS	sodium dodecyl sulfate

SDS-PAGE	SDS polyacrylamide gel electrophoresis
s	second
siRNA	small interfering RNA
sqRT-PCR	semiquantitative reverse transcription PCR
ss	single strand
SSc	systemic sclerosis
ssSc	systemic sclerosis sine scleroderma

T

TAE	Tris-Acetate-EDTA
Tg	Thapsigargin
TEMED	N,N,N,N´-tetramethyl-ethane-1,2-diamine
Topo 1/2α/2β	Topoisomerase 1/2α/2β
TRIS	Tris(hydroxymethyl)-aminomethan
TBST	Tris buffered saline with Tween-20

U

UIP	usual interstitial pneumonia
UPR	unfolded protein response
UT	untreated

V

VATS	video assisted thoracic surgery
VCP	Valosin containing protein

X

XBP-1	X-box binding protein 1

V Summary

Interstitial lung diseases (ILD) or diffuse parenchymal lung diseases (DPLD) are a heterogenous group of chronic disorders that affect the distal lung. They are largely unresponsive to any currently available therapy and lead to architectural distortion of the lung parenchyma and rapid respiratory failure. The pathogenesis of the disease is not completely understood. In some ILDs like the idiopathic pulmonary fibrosis (IPF) the initial alveolar epithelial cell injury followed by ER-stress and apoptosis of alveolar epithelial cells type II (AECII) seems to be the triggering factor.

Collagen vascular diseases (CVD) are a group of immunologically mediated inflammatory disorders affecting predominantly the connective tissue and the vessels, however, quite frequently, also the lung. Especially in Polymyositis (PM), Dermatomyositis (DM) and Systemic Sclerosis (SSc), ILD determines morbidity and mortality of the disease. Autoantibody expression seems to be highly predictive for pulmonary involvement. An autoantibody frequently found in PM/DM is anti histidyl-tRNA-Synthethase (anti-HisRS), most specific autoantibodies in SSc are anti-Topoisomerase1 (anti-Topo1), anti-Topoisomerase2α (anti-Topo2α) and anti-Topoisomerase2β (anti-Topo2β).

In the present project it was hypothesized that autoantibodies cause development of ILD in CVD via alveolar epithelial cell injury leading to an ER-stress and apoptotic response in AECIIs. We supposed that the binding of pathogenetic antibody directed against HisRS and topoisomerases results in a loss of function of the respective proteins, which again causes aleveolar epithelial cell injury.

In order to evaluate such proposed mechanism, HisRS, Topo1, Topo2α and Topo2β were silenced via siRNA transfection *in vitro* in A549 cells. Furthermore, inhibition of topoisomerases was performed *in vitro* by treating A549 cells with topotecan and etoposide. ER-stress and apoptosis were analyzed employing Western Blot, semiquantitative RT-PCR and quantitative RT-PCR.

In vitro knockdown experiments (siRNA mediated) for HisRS, Topo1, Topo2α and Topo2β did not result in ER-stress or increased apoptosis markers. On the other hand it was shown that ER-stress and apoptosis occur in A549 cells after inhibition of topoisomerases with topotecan or etoposide. Performing immunohistochemistry of lung sections of a patient with SSc associated ILD revealed ER-stress and apoptosis in AECIIs. These results suggest that autoantibodies found in CVD may contribute to the development of ILD by causing ER-stress and apoptosis in AECIIs.

VI Zusammenfassung

Die interstitiellen Lungenerkrankungen (englisch: ILD- interstitial lung disease) sind eine heterogene Gruppe von chronischen Lungenerkrankungen, die das periphere Lungenparenchym betreffen. Im Falle einiger ILDs wie der idiopathischen pulmonalen Fibrose (IPF) sind diese überwiegend therapierefraktär, führen zu Zerstörung der Architektur des Lungenparenchyms und rasch zu respiratorischem Versagen.
Obwohl die Pathogenese der Erkrankung größtenteils ungeklärt ist, lassen neue Studien gerade bei der so ungünstigen IPF eine initiale Schädigung von Alveolarepithelzellen (AEC) vermuten, woraufhin es zu ER-Stress und Apoptose von Alveolarepithelzellen Typ II (AECII) kommt.
Bei Kollagenosen, einer Gruppe von Autoimmunerkrankungen, die sich bei systemischem Befall vorwiegend an Bindegewebe und Blutgefäßen abspielen, stellt die Entwicklung einer ILD eine nicht seltene Komplikation dar. Vor allem bei den Kollagenosen Polymyositis (PM), Dermatomyositis (DM) und systemischer Sklerose (SSc) bestimmt wesentlich das Vorhandensein einer ILD die Morbidität und Mortalität der Erkrankung. Die pulmonale Beteiligung ist mit dem Auftreten spezifischer Autoantikörper (AAk) assoziiert. Bei PM/DM handelt es sich um AAk gegen Histidyl-tRNA-Synthethase (HisRS), spezifische AAk bei SSc sind gegen die Topoisomerase1, 2α und 2β (Topo1/2α/2β) gerichtet.
Für das hier vorliegende Projekt wurde die Hypothese aufgestellt, dass die AAk zur Pathogenese der ILDs in Kollagenosen beitragen, indem sie das alveoläre Epithel schädigen im Sinne eines ER-Stress und so zur Apoptose der AECIIs führen. Wir postulierten, dass die Bindung der spezifischen Autoantikörper an HisRS und die Topoisomerasen zu einem Funktionsverlust der jeweiligen Proteine führt und so ein Schaden im Bereich des alveolären Epithels verursacht wird.
Daher wurden die Zielgene der genannten AAk *in vitro* in A549 Zellen mit entsprechenden siRNA gehemmt. Außerdem wurde ein Funktionsverlust der Topoisomerasen durch Behandlung von A549 Zellen mit Topotecan und Etoposide erzielt. Mittels Western Blot, semiquantitativer und quantitativer PCR wurden anschließend ER-Stress- und Apoptose-Marker analysiert.
Die *in vitro* Hemmung der AAk durch eine siRNA Transfektion ergab keinen deutlichen Effekt bezüglich ER-Stress und Apoptose. Allerdings konnte gezeigt werden, dass nach der Inhibition von Topoisomerasen durch Topotecan und Etoposide eine deutliche ER-stress- und Apoptose-Antwort in A549 Zellen stattfindet. Im Rahmen der

immunhistochemischen Untersuchung von Lungenschnitten eines Patienten mit SSc assoziierter ILD hinsichtlich zellulärer Stressmuster konnten ER-Stress und Apoptose in den AECIIs dargestellt werden.

Die vorliegenden Ergebnisse legen die Vermutung nahe, dass die in Assoziation mit genannten Kollagenosen auftretenden AAk die Entwicklung von ILDs vermitteln können, indem sie ER-Stress und Apoptose in AECIIs auslösen.

1. Introduction

1.1 Interstitial lung diseases

Interstitial lung diseases (ILD) or diffuse parenchymal lung diseases (DPLD) are a group of more than 100 different conditions mainly affecting the pulmonary interstitium, the alveolar epithelium and the capillary endothelium [1]. Characteristic features of ILD include increase of connective tissue which leads to fibrosis, reduced lung compliance and impaired gas exchange [2]. ILDs present an important cause of morbidity and mortalitiy worldwide. In the late stages of the disease patients develop a cor pulmonale. Respiratory failure is the most common reason for lethal outcome of the disorder [3]. Figure 1 shows a schematic of the general classification of the ILDs [4].

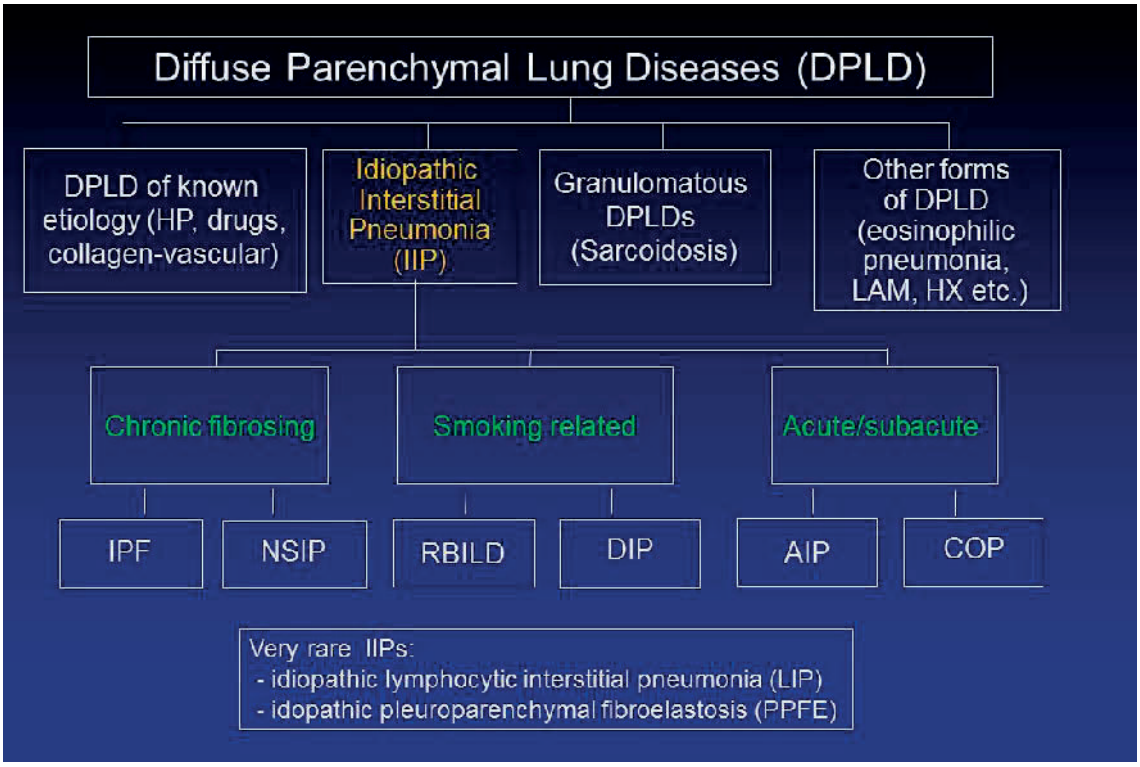

Figure 1: A schematic for the general classification of the DPLDs [4]

IPF – idiopathic pulmonary fibrosis, NSIP – non-specific interstitial pneumonia, RBILD – respiratory bronchiolitis interstitial lung disease, DIP – desquamative interstitial pneumonia, AIP – acute interstitial pneumonia, COP – cryptogenic organizing pneumonia

The complexity of classification of ILD arises from the heterogenity of the diesease. As shown in Figure 1 ILD includes either diseases with a well-defined cause such as an inhalational (e.g. asbestosis), a drug-induced (e.g. amiodarone) or a granulomatous (e.g. sarcoidosis) etiology. ILDs also occur in association with systemic disorders like vasculitis, reno-pulmonary syndromes and collagen vascular diseases (CVD). Some ILDs lack an obvious origin, e.g. the idiopathic interstitial pneumonia (IIP). The IIP presents the most common form of ILD [1]. In 2002 the American Thoracic Society/European Respiratory Society (ATS/ERS) established a classification of IIPs which was updated in 2013 [5]. Combining clinical, imaging and histopathological information, the classification of IIP now distinguishes between major IIPs, rare IIPs, and unclassifiable IIPs. The major IIPs are grouped into chronic fibrosing IPs, that include idiopathic pulmonary fibrosis (IPF) and non-specific interstitial pneumonia (NSIP), smoking-related IPs comprising respiratory bronchiolitis–interstitial lung disease (RB-ILD) and desquamative interstitial pneumonia (DIP), and acute/subacute IPs including cryptogenic organizing pneumonia (COP) and acute interstitial pneumonia (AIP) [5].

The revised classification emphasized the importance of an integrated clinical, radiological and pathological approach because of the improved diagnostic possibilities, such as the high resolution computed tomography (HRCT) and the less invasive lung biopsy via video-assisted thoracic surgery (VATS). The recognition that many of the ILDs have distinctive HRCT- appearances has greatly reduced the need for lung biopsy [1]. Already in 2011, ATS/ERS published evidence-based guidelines for diagnosis and management of IPF and specified that lung biopsy is not an essential criteria for a final diagnosis of IPF anymore in case of a definite UIP pattern in HRCT [6,7]. In such case, the diagnosis is correct in more than 90% cases, showing that surgical biopsy is no longer justified in the appropiate clinical setting [8,9,10]. Nevertheless in some cases when HRCT pattern is not explicit, lung biopsy is still needed for final diagnosis. Table 1 describes typical histologic patterns and HRCT appearances of the most frequent ILDs [3].

Pattern	Histology	CT features
UIP	Subpleural and peripheral fibrosis. Temporal and spatial heterogeneity. Scattered *fibroblastic foci* and honeycombing are key features.	Basal, subpleural reticulation and honeycombing; traction bronchiectasis; little, if any, ground-glass attenuation.
NSIP	Uniform interstitial involvement by variable degrees of fibrosis and inflammation. Honeycombing is rare.	Bilateral patchy ground-glass opacities admixed with reticulation and traction bronchiectasis / bronchiolectasis. Little or no honeycombing. Usually, predominantly basal.
OP	Connective tissue plugs within small airways and air spaces (Masson bodies). In its 'pure' form, little or no inflammation or fibrosis in the surrounding interstitium.	Airspace consolidation, with a predominantly basal/ peripheral or peri-bronchovascular distribution. Bands with air bronchograms and a perilobular pattern can also be seen.
DIP	Extensive macrophage accumulation within the distal air spaces. Mild interstitial involvement	Patchy ground-glass opacities. Microcystic change can be seen within the ground-glass. Basal, peripheral distribution frequent.
LIP	Bronchiolocentric lymphoid tissue hyperplasia.	Ground-glass attenuation is the predominant finding, with thin-walled cysts frequently present. Lung nodules and septal thickening may also be seen
RB-ILD	Bronchiolocentric macrophage accumulation. Mild bronchiolar fibrosis.	Centrilobular nodules, ground glass opacities. Diffuse or upper lung distribution

Table 1: Classification of histological and radiological patterns developed for IIP [3]

Chest HRCT and lung function tests are the most useful diagnostic items in establishing the clinical significance of an ILD. The interstitial abnormalities occuring in ILDs are associated with a restrictive pattern in lung function. Proportional reduction in forced vital capacity (FVC) and forced expiratory volume in the first second (FEV1) are detected, next to an impaired diffusion capacity, measured as a reduction in diffusing capacity of the lung for carbon monoxide (DLCO). DLCO is the most sensitive marker of ILD [11].

1.2 ILD in collagen vascular diseases

Collagen vascular diseases (CVDs) are a heterogenous group of autoimmune inflammatory disorders which include systemic sclerosis (SSc), dermatomyositis (DM), polymyositis (PM), systemic lupus erythematosus, rheumatoid arthritis, sjögren syndrome and mixed connective tissue disease [12]. Pulmonary involvement is a common, and occassionally the first manifestation in CVDs. Therefore an autoimmune screen is advised in all patients who present with ILD [13]. Especially in patients with SSc and PM/DM, the prevalent developement of ILD represents a significant cause of morbidity and mortality [14,15]. The pathogenesis of lung fibrosis in CVDs is still not

completely understood, but the involvement of an autoimmune background is hypothesized [16]. The high prevalence of lung fibrosis in patients with CVDs suggests a correlation between existence of autoantibodies and developement of lung fibrosis [17,18]. Bringing this correlation into focus may offer a chance to get a better understanding of the pathogenesis of ILD in order to develop new therapeutical options. UIP and NSIP, two histopathologic patterns of the IIPs, are also the most frequent histological patterns of ILD in SSc and PM/DM [19,20]. UIP describes the histopathologic pattern of IPF. A combination of histological patterns is quite frequent in the context of CVDs [13], especially a mixture of UIP and NSIP pattern can be detected frequently [21]. Therefore it is important to introduce the most important forms of IIP´s, namely IPF and NSIP.

1.3 Idiopathic pulmonary fibrosis

IPF represents the most common form of IIPs with the worst prognosis and a mean survival of 2–3 years after diagnosis [22,23]. It mostly affects people over 50 years of age and is more common in males. Typical clinical manifestations of IPF are dyspnea, nonproductive cough, bibasilar fine inspiratory crackles, a restrictive impairment of pulmonary function and dysfunction of gas exchange [23]. The pathogenesis of IPF remains unknown. Epithelial cell damage and apoptosis of alveolar epthelial cells type II (AECII) seem to be the triggering events for proliferation and activation of fibroblasts which transform into myofibroblasts and cause excessive production of extracellular matrix (ECM) which ultimately leads to fibrosis [22,24–26]. As shown in Figure 2, typical imaging features include subpleural reticular opacities and traction bronchiectasis that increase from the apex to the bases of the lungs [27-30]. UIP describes the histopathological pattern of IPF. As shown in Figure 3 important histologic features are temporal and spacial heterogenity, resulting in still regular appearing areas next to disease-defining areas, microscopic honeycombing and fibroblast foci consisting of activated fibroblasts [27].

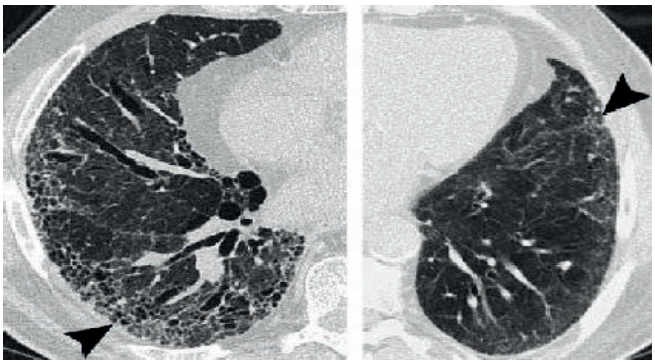

Figure 2: Comparison of high-resolution CT features between UIP and NSIP [28]

(a) IPF is characterized by heterogeneous lung abnormalities consisting of subpleural honeycombing (arrowhead), reticular opacities, and traction bronchiectasis. (b) NSIP demonstrates homogeneous lung involvement with predominance of ground-glass opacity combined with subpleural linear opacities and micronodules. The microcysts in NSIP (arrowhead) are much smaller than the honeycombing in UIP. [28]

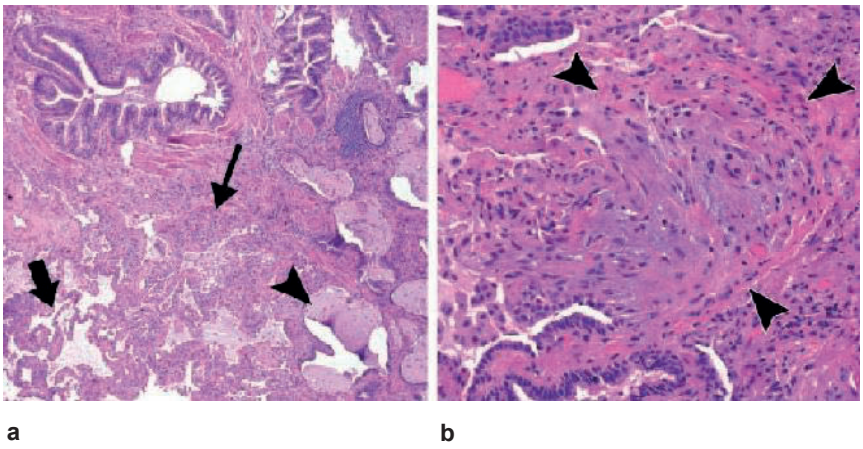

Figure 3: Histologic features of UIP [28]

(a) Photomicrograph (original magnification, 40; hematoxylin-eosin stain) shows patchy fibrosis with remodeling of the lung architecture. Interstitial chronic inflammation is mild, with only a few lymphoid aggregates (thin arrow). Cystically dilated airspaces that produce a honeycomb pattern (arrowhead) and areas of relatively unaffected lung (thick arrow) are present. (b) Photomicrograph (original magnification, 200; hematoxylin-eosin stain) shows a fibroblastic focus of loose organizing connective tissue (arrowheads). [28]

Because of its devastating character it is important to differentiate between IPF and other ILDs. In 2011 the American Thoracis Society (ATS), the European Respiratory Society (ERS), the Japanese Respiratory Society (JRS), and the Latin American Thoracic Association (ALAT) published evidence-based guidelines for diagnosis and management of IPF [6]. It was determined, that diagnosis of IPF requires following points:

- Exclusion of other known causes of ILD.
- The presence of an UIP pattern on HRCT in patients non subjected to surgical lung biopsy.
- Proof of IPF on the basis of HRCT (probable UIP; inconsistent with IPF) and surgical lung biopsy (UIP by histological criteria) in patients subjected to a surgical lung biopsy. [6]

In the last years treatment of IPF was a subject of many studies. The aim of treatment is to prevent disease progression. Therapies targeting the antifibrotic and growth factor pathways are currently being developed. Pirfenidone, a novel antifibrotic and antiinflammatory drug, was first licensed in Europe for IPF treatment in 2011, and results in attenuation of disease progression [31,32]. Moreover, Nintedanib, a novel triple-kinase inhibitor targeting receptors of fibrolast growth factor, vascular endothelial growth factor and platelet-derived growth factor seems to be another promising drug in attenuation of progression of IPF and was just licensed for treatment in IPF in 2015 [33]. Nevertheless lung transplantation still remains the only effective therapeutic option for patients suffering from advanced IPF [1,34,35]. Previous studies have reported conflicting survival rates for UIP in CVD compared to those in IPF. Interestingly some clinical studies suggest that an UIP pattern in CVD-related disease is associated with a significantly better survival rate compared to UIP pattern in the idiopathic setting [36]. In contrast to this recently Esam et al. demonstrated that the outcome of CVD-UIP patients is similar to IPF/UIP patients [37].

1.4 Nonspecific interstitial pneumonia

With a mean survival of 6-8 years after diagnosis, idiopathic nonspecific interstitial pneumonia (NSIP) has a better prognosis than IPF [23]. The mean age of patients at the onset of NSIP is about ten years younger than patients with IPF. Neither sexual

predominance nor connection with cigarette smoking could be established [3]. NSIP pattern is strongly associated with collagen vascular diseases, exogenous allergic alveolitis (EAA) and drug-induced lung fibrosis, but NSIP can occur as an idiopathic disease too [23,38]. Next to dyspnea and cough, fatigue and weight loss are usual symptoms. Abnormalities in lung function are similar to those in UIP but are often milder [3]. Pathogenesis of NSIP is still not defined [39]. The histopathologic pattern shows varying combinations of inflammation and fibrosis, sometimes predominated by chronic interstitial inflammation, named „cellular NSIP“, sometimes by interstitial fibrosis, the „fibrotic NSIP“ [19,38]. But the role of inflammation as the preceeding trigger for the development of NSIP is more emphasized than in IPF [3,40]. As shown in Figure 2 temporal and spacial homogenity is an important difference to UIP. In contrast to IPF ground glas opacitiy (GGO) combined with scattered micronodules exist frequently in NSIP [23,28]. Usually no honeycomb changes or fibroblast foci can be detected in histopathological analysis [14].

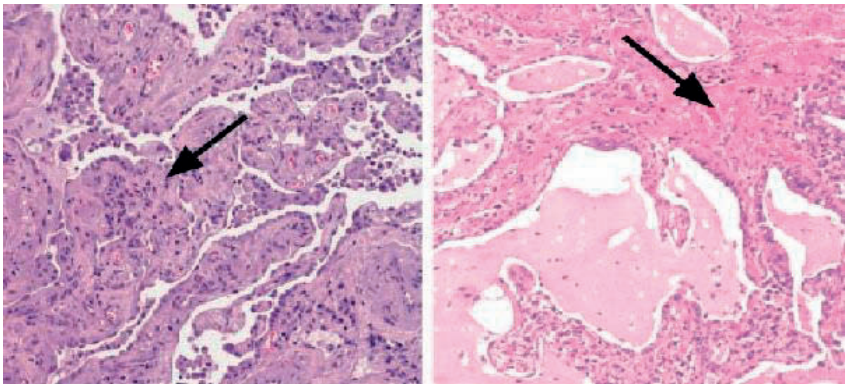

Figure 4: Histologic features of NSIP [28]

(a) Photomicrograph (original magnification, 100; hematoxylin-eosin stain) of cellular NSIP shows a uniform appearance of interstitial inflammation (arrow), which consists of lymphocytes and plasma cells. (b) Photomicrograph (original magnification, 100; hematoxylin-eosin stain) of fibrosing NSIP shows areas of fibrosis (arrow) in addition to uniform inflammation. [28]

The treamtment of NSIP is similar to the one of IPF. In patients with SSc-related NSIP Cyclophosphamid is considerered the most promising agent available today [41]. Consideration should also be given to oxygen therapy and treatment of pulmonary hypertension [1].

1.5 Molecular mechanisms underlying IPF and NSIP

The exact mechanisms responsible for initiation and perpetuation of ILD remain elusive [19,27]. According to a more recent hypothesis, epithelial cell injury followed by ER-stress induced apoptosis seem to be the triggering events in pathogenesis of IPF [2,3,22,42]. Failure to re-epithelialize the injured alveolar epithelium leads to disruption of the epithelial integrity in the alveoli and release of profibrotic cytokines and growth factors, that causes proliferation of fibroblasts, abnormal collagen deposition and finally leads to decline of lung function and impairment in gas exchange [42-44]. Increased apoptosis of AECIIs was observed at an early stage of the disease, not only in areas of remodelled regions replaced by fibrous tissue but also frequently in regions of lung with almost normal appearing alveolar structures [24,26,45]. Supporting this concept we previously demonstrated that a severe ER Stress response in the AECIIs underlies the programmed cell death in patients with IPF [42].

The older hypothesis that the development of IPF is due to chronic inflammation thus has been replaced by the hypothesis of epithelial cell injury. Yet, especially in cellular NSIP, the histolopathologic pattern is often predominated by chronic interstitial inflammation and inflammation may still play a significant role [14,38].

Therefore it has been suggested that the inflammatory concept should not be excluded from the pathogenesis of lung fibrosis, but rather be seen as an associating factor next to the alveolar epithelial injury [44].

1.5.1 Role of AECII in development of lung fibrosis

Chronic injury of AECIIs is considered as the key in pathophysiology of IPF [22,46]. AECIIs synthesize, secrete and recycle all components of surfactant. Surfactant is a lipoprotein complex that covers the alveolar interface and thereby reduces surface tension, which is necessary for breathing at normal transpulmonary pressures. The surfactant proteins SP-B and SP-C are key components of surfactant [47,48]. To prevent infections AECIIs also produce compounds of the innate immune defense system, like SP-A [49]. Furthermore AECIIs have a high potential to proliferate [48,50] and show self-renewal characteristics [51,52]. And yet they seem to be chronically injured in IPF. Risk factors for alveolar epithelial cell injury include smoking, exposure to metal or wood dust and genetic disposition, as well as age [6]. In familial forms of IPF and NSIP, mutations of surfactant proteins SP-A and SP-C, which are associated

with AECII injury and apoptosis, as well as mutations of members of the telomerase and shelterin complex, which primarily cause DNA damage, have been disclosed [53–55]. UIP, the histological pattern of IPF, can also be seen in Hermansky-Pudlak syndrome – associated interstitial pneumonia (HPSIP), which occurs in ~40% of patients with Hermansky-Pudlak syndrome (HPS), a disease caused by a lysosomal transport deficiency affecting the whole body. Mahavadi et al. [56] found, that a defective intracellular surfactant transport in AECII underlies lysosomal stress, apoptosis and development of HPSIP.

There are different theories under discussion regarding the mechanisms how injury of the AECIIs results in lung fibrosis. One of the theories involves epithelial-mesenchymal transition (EMT), where epithelial cells undergo a transdifferentiation into activated fibroblasts. Another theory suggests, that the injured AECIIs lose control over the mesenchymal cells, which leads to proliferation and production of more collagen. Furthermore it has been shown that a number of pro-fibrotic coumpounds are released by chronically injured AECIIs [47].

1.5.2 Endoplasmic reticulum (ER) -Stress and apoptosis

The endoplasmic reticulum (ER) is a subcellular compartment. Besides calcium storage and release and lipid biogenesis it plays a central role in protein synthesis and folding [57]. Impairment of protein folding and processing leads to accumulation of unfolded proteins in the ER, which triggers the so called unfolded protein respone (UPR) in order to restore ER functions [58]. UPR increases protein folding and processing capacity [59]. UPR signaling is initiated by the three transmembrane proteins inositol-requiring enzyme 1α (IRE1α), the protein kinase RNA-like endoplasmic reticulum kinase (PERK) and the activating transcription factor 6 (ATF6) [60]. PERK phosphorylates the alpha unit of the eukaryotic initiating factor 2 (eIF2α) which reduces the protein load on the ER. IREα induces splicing of x-box binding protein 1 (XBP1) mRNA in order to produce the homeostatic transcription factor XBP1s [61]. ATF6 and XBP1s increase transcription of genes which enhance ER size and function [62]. By phosphorylation of eIF2α the translation of activating transcription factor 4 (ATF4) is stimulated that again leads to transcription of different pro-survival genes [63]. However if ER-stress is too severe and prolonged, apoptosis is induced via ATF4-dependent upregulation of C/EBP Homologous Protein (CHOP) transcription

factor [60,64]. It is reported that CHOP induces cell cycle arrest and apoptosis [65].

ER-stress has been implicated in the pathogenesis of many neurodegenerative disorders like Alzheimer´s, Parkinson´s and Huntington´s disease and amyotrophic lateral sclerosis, as well as in acute pathological states of the brain as ischemia and trauma [64]. ER-stress has also been found to be caused by the above mentioned mutations of SP-A and SP-C in familial IPF [47]. Of late, a study from Korfei et al. [42] focussing on sporadic cases of IPF has demonstrated the importance of ER-stress driving the AECII apoptosis.

1.6 Collagen vascular diseases

Collagen vascular diseases (CVD) represent a heterogenous group of immunologically mediated disorders. The pathomechanism of these diseases is yet not fully settled, but the obvious dysregulation of the immune system results in the synthesis of autoantibodies affecting predominantly the connective tissue and the vessels. A large variety of organs may be affected. As mentioned before CVDs include SSc, PM/DM, systemic lupus erythematosus, rheumatoid arthritis, sjögren syndrome and mixed connective tissue disease [12]. In the following sections, PM/DM and SSc will be the CVDs of interest in view of their frequent pulmonary involvement.

1.6.1 Polymyositis and Dermatomyositis

PM is characterized by inflammation and degeneration primarily of the muscles. Clinical signs are symmetrical proximal muscle weakness, tenderness, pain and ultimately atrophy and fibrosis of the muscle. Furthermore myalgies and inflammation of pharyngeal muscles are common manifestations [66,67]. Appropiate diagnostic criteria are raised muscle enzymes, muscle biopsy consistant with a myositis and characteristic electromyographic alterations [68]. Additional to the clinical symptoms of PM, DM is clinically defined by characteristic cutaneous signs such as photosensitive erythroedema, orbital erythema, erythematosus or violaceous plaques on the dorsal surface of interphalangeal and metacarpophalangeal joints, called Gottron´s papules, and periungual erythema, the so called manicure sign [67,69]. PM and DM often occure in overlap with other CVDs [68]. PM and DM are associated with serum autoantibodies, some of which are detected almost exclusively in these diseases. The most specific

antibody is the antibody directed against histidyl-tRNA-Synthethase (anti-HisRS) [18,66,70].

Figure 5: Dermatomyositis – Typical cutaneous signs [71-73]

(a) Facial erythroedema [71] (b) Gottron´s papules: Erythematosus plaques on the surface of interphalangeal and metacarpophalangeal joints, hyperkeratosis of proximal nail fold [72] (c) Periungual erythema („manicure sign“) [73]

1.6.1.1 Jo-1 syndrome

The Jo-1 syndrome describes a subgroup of PM/DM and is characterized by the presence of anti-HisRS (=anti-Jo-1) autoantibodies and specific clinical manifestations. In addition to myositis, patients suffer from lung fibrosis, chronic polyarthritis, Raynaud´s phenomenon and fever. ILD is an early diagnostic sign [74,75].

Figure 6: Raynaud syndrome [76]

Episodic vasospasm as response to cold or emotional stress [76]

1.6.1.2 Lung involvement

Lung fibrosis is one of the most common extramuscular manifestations in PM/DM and

a common cause of morbidity and mortality in these patients [77]. ILD (histologically NSIP or UIP) is found in approximately 30% of the patients with PM and in over 60% of the patients with Jo-1 syndrome [14,75,78]. Arthritis or arthralgia, next to old age (>45 years), are significantly associated with ILD [79,80]. The existence of autoantibodies also correlates with pulmonary manifestation. Antibodies against aminoacyl-tRNA synthetases have been tigthly linked to the development of ILD. Autoantibody against histidyl-tRNA-Synthethase (anti-HisRS) is the most common antibody against aminoacyl-tRNA and shows a strong association with pulmonary involvement. It is detected in 30-75% of PM/DM associated ILD [13] and consequently serves as a marker of PM/DM associated ILD [12,81,82].

1.6.1.3 Autoantibody against histidyl-tRNA-Synthethase

The antibody considered most specific for PM/DM is the antibody against histidyl-tRNA-Synthethase (anti-HisRS = anti-Jo-1) [83]. Anti-HisRS exists in 10-30% of patients with PM/DM and is one of the conditions for the diagnosis Jo-1 syndrome. Anti-HisRS is directed against HisRS and thus probably inhibits its function. HisRS synthesizes histidyl-transfer RNA, that is fundamental for the incorporation of histidine into proteins. The amino acid histidin plays an important role in many catalytic functions of enzymes. Enzymatic decarboxylation of histidine generates the biologically important histamine. Furthermore HisRS belongs to the group of aminoacyl-tRNA synthetases that can synthesize diadenosine tetraphosphate. Diadenosine tetraphosphate is suspected to be involved in several regulatory mechanisms of cell metabolism [84]. A cleaveable form of HisRS was detected in the lung, especially in alveolar epithelium, which suggests, that autoimmunity to HisRS is initiated in the lung and thus maybe plays an important role in the developement of lung fibrosis [82].

1.6.2 Systemic sclerosis

Systemic sclerosis (SSc) is an autoimmune disease of unknown etiology that involves tissue ischemia and fibroproliferative changes in the skin and internal organs [85]. For the classification of SSc major and minor criteria exist. SSc is diagnosed if one major, and two or more minor criteria are present:
Major criterion: Symmetrical thickening, tightening, and induration of the skin of the

fingers and the skin proximal to the metacarpophalangeal, or metatarsophalangeal joints.

Minor criteria: 1. Sclerodactyly: the changes of the major criterion, but limited to the fingers
2. Digital pitting scars or loss of substance from the finger pad: depressed areas at tips of fingers or loss of digital pad tissue as a result of ischemia
3. Bibasilar pulmonary fibrosis [86]

SSc can be divided into three subgroups, diffuse cutaneous systemic sclerosis (dcSSc), limited cutaneous systemic sclerosis (lcSSc) and systemic sclerosis sine scleroderma (ssSc). DcSSc is characterized by generalized skin affection and involvement of internal organs. In lcSSc skin induration is limited to hands, face and feet. LcSSc is also known as CREST-Syndrom, which is characterized by calcinosis cutis, raynaud syndrome, esophageal dysmotility, sclerodactyly and teleangiectasia. In ssSc internal organs are affected without any cutaneous involvement [85,87]. SSc is associated with the presence of antinuclear antibodies (ANAs), which are for example directed against Topoisomerase 1 (anti-Topo1=anti-SCL-70) and Topoisomerase 2α/β (anti-Topo2α/β) [88].

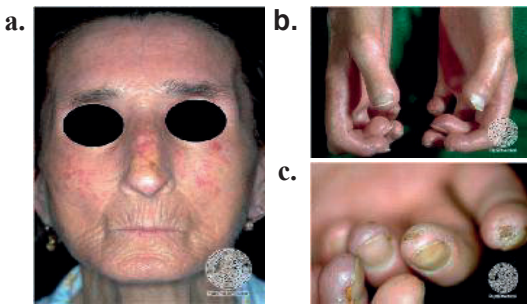

Figure 7: Systemic sclerosis – Typical cutaneous signs [89-91]

(a) Microstoma with actinomorphic wrinkles, teleangiectasia [89] (b) Sclerodactyly: thickening, tightening and induration of the skin of the fingers [90] (c) Erythema and crusted squames at the tips of the fingers [91]

1.6.2.1 Lung involvement

Lung involvement is one of the most common manifestations in SSc. Data for occurance of pulmonary disease in SSc differ from 50% to 90% [12,14,85,92,93]. ILD is the major form of pulmonary involvement associated with SSc and the leading cause of death [93]. Nevertheless the majority of SSc patients show relatively limited pulmonal

disease, which remains stable even without treatment [13]. NSIP and UIP are the most common histopathologic patterns [19,94,95]. Autoantibody-expression against topoisomerases in SSc can be considered strongly predictive for internal organ involvement, especially for the development of ILD [12,86]. Autoantibodies against topoisomerases (Anti-Topos) belong to the group of ANAs and are often associated with SSc. While anti-Topo1 is almost exclusively detected in SSc and highly predictive for internal organ involvement, anti-Topo2 can be found in different autoimmune diseases like juvenile rheumatoid arthritis (14%), systemic lupus erythematosus (1,5-31%) and systemic sclerosis (22%) [88].

1.6.2.2 Function of topoisomerases

Because of the double helical structure of DNA the problem of torsional tension arises. Solving these topologic difficulties by untangling and untwisting DNA is essential for biologic processes like replication, transcription, recombination and chromatin remodeling [96]. Topoisomerases are ubiquitous enzymes and play a crucial role in modulating DNA topology by introducing temporary single or double strand breaks in dsDNA [88]. Topoisomerases generate a transient phosphodiester bond between a tyrosine residue in the protein and one of the ends of the broken strand. This intermediate break allows the DNA to be untangled. Thus topoisomerases can relief the torsional tension between the two strands of DNA during replication and are able to relax the supercoiling in the DNA during transcription [96]. There are different classes of topoisomerases. In the following Topoisomerase type 1 and type 2 will be examined.
Topoisomerase 1 (Topo1) cleaves a single strand of DNA, no adenosine triphosphate (ATP) is necessary for the reaction. Topo1 supports the fork movement during replication and relaxes supercoils occurring during transcription [96,97].

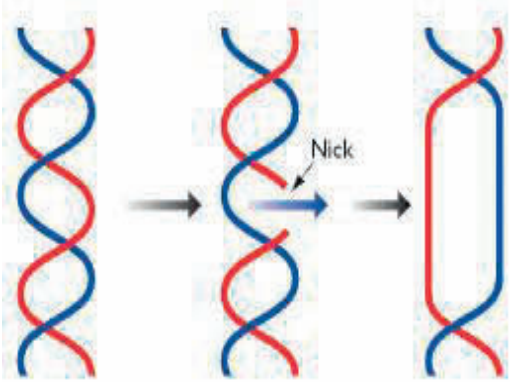

Figure 8: Schematic illustration of the action of Topoisomerase Type 1 [98]

Topoisomerases 2 (Topo2) generate transient double strand breaks in the DNA, ATP is required for this reaction. Topo2 is associated with gene promotor regions, which suggests, that they somehow play a role in transcription activation [97]. Topo2 can be subdivided in Topo2α and Topo2β, based on structural considerations. The precise roles of the two types are subject of current studies. Topo2α is essential for all cells and seems to play an important role in solving the topological problems associated with mitosis and replication [99]. The Topo2β-mediated, transient dsDNA break is required for activation of gene transcription by nuclear receptors and other classes of DNA binding transcription factors like activator protein 1 (AP-1). Furthermore it is suggested, that the dsDNA break formation, generated by Topo2β, creates a signal that leads to the activation of a poly[adenosine diphosphate (ADP)-ribose] polymerase 1 (PARP-1). PARP-1 is a nicotinamide adenide dinucleotide (NAD+)- dependent enzyme that detects and repairs damage to the DNA. Thus Topo2β probably regulates the initiation of ligand-or signal-dependant gene transcription [97].

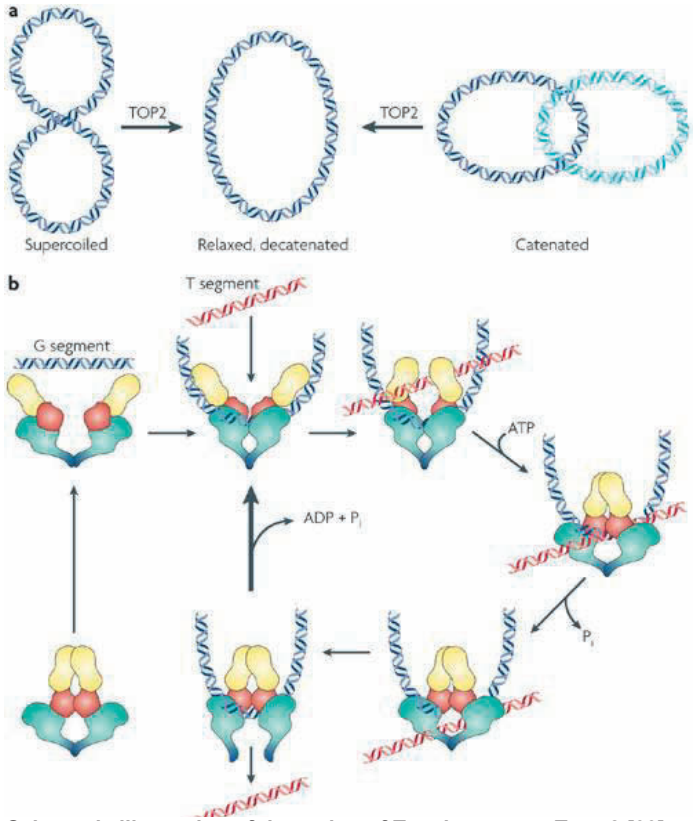

Figure 9: Schematic illustration of the action of Topoisomerase Type 2 [99]

(a) Reactions catalysed by Topo2 include decatenation of linked intact double stranded DNA and relaxation of supercoiled DNA. (b) Topo2 introduces a double strand break in one DNA strand, called G or gate segment and passes a second strand called T segment through the break. In the presence of Mg2+, the enzyme can cleave the DNA. ATP binding enables the enzyme to form a closed clamp. The closed clamp may also capture another strand (the T strand) that will pass through the break made in the G strand. ATP hydrolysis occurs at two steps in the reaction. The first hydrolysed ATP may assist in strand passage. The second hydrolysis step allows the clamp to reopen. [99]

2. Aim of the study

Lung fibrosis is a common manifestation in PM/DM and SSc and the major cause of death in these diseases [15,19,75]. Autoantibodies against HisRS, Topo1, Topo2α and Topo2β are highly predictive for the appearence of lung involvement [12,81,82,88] suggestive of a correlation between the existence of autoantibodies and developement of ILD in PM/DM and SSc. We therefore wished to explore the possibilitiy of an autoantibody induced blockade of HisRS, Topo1, Topo2α or β in alveolar epithelial cells, possibly resulting in chronic AECII injury and apoptosis. We supposed that the binding of pathogenetic antibody directed against HisRS and topoisomerases results in a loss of function of the respective proteins and hence asked:

- **Does in vitro knockdown of HisRS, respectively Topo1, Topo2α and Topo2β provoke an ER Stress or apoptotic response in AECIIs?**
- **Can AECII specific induction of ER-stress be shown in patient with SSc associated ILD?**

To answer these questions, the following approaches were considered:

- Silencing of HisRS, Topo1, Topo2α and Topo2β in A549 cells via siRNA and analysis of ER-stress and apoptosis.
- Inhibition of Topo1, Topo2α and Topo2β in A549 cells via treatment with the inhibitors topotecan and etoposide and analysis of ER-stress and apoptosis.
- Immunohistochemical analysis of ER-stress in lungs of a patient with SSc associated ILD compared to healthy donor lungs.

3. Material and Methods

3.1 Materials

3.1.1 Cell line

For all experiments a A549 cell line was used. A549 cells are adenocarcnomic human alveolar basal epithelial cells which can be used as an in vitro model of AECII.

3.1.2 Human lung sections

Immunohistochemistry was performed on serial paraffin-embedded tissue sections from one human patient with SSc associated ILD and compared to healthy donor sections. Lung sections were applied by the Biobank of the european IPF registry (eurIPFreg) and belong to the patients´ collective of Gießen. There is a vote of the ethical review committee of the Justus-Liebig-Universität Gießen regarding the eurIPFreg (AZ: 111/08). Histopathologic examination was performed by the department of pathology Universitätsklinikum Gießen und Marburg.

3.1.2.1 Patient data

Lung tissue sections of patient with SSc-ILD were obtained from a male patient born in 1954. Lung transplantation was performed in 2010. Diagnosis of SSc was settled by performing skin biopsy and barium swallow examination of the eosopagus, here scleroderma and disturbance in eosophagus-motility could be found. Lung fibrosis was diagnosed by performing lung function test, HRCT and lung biopsy. Lung function revealed a severe restrictive dysfunction of the lung. In HRCT, an UIP pattern was demonstrated. Lung biopsy confirmed UIP also histopathologically. In addition, an elevated titer of ANA´s (1:640) was detected. Further differentiation of the autoantibodies was not possible.

3.1.3 Machines / Software

MJ Mini Personal Thermal Cycler	BioRad, USA
Nanodrop ND-100 spectrophotometer	Nanodrop Technologies, USA
Trans-Blot SD Semi-dry Transfer Cell	BioRad, USA
My iQ™ Single Color Real-Time PCR Detection System	BioRad, USA
iQ5 Optical System Software	BioRad, USA
SPECTRAFlour Plus	Tecan
Magellan Tecan Inc. Software	Tecan
Molecular Imager Gel Doc™ XR	BioRad, USA
Image Lab Software	BioRad, USA
HiTrap Protein G HP column	GE Healthcare, Sweden

Table 2: Machines / Software

3.1.4 Reagents

3.1.4.1 Chemicals and reagents

Acetic Acid	Merck, Darmstadt, Germany
Acrylamide solution, Rotiphorese Gel 30	Roth, Karlsruhe, Germany
Agarose	Roth, Karlsruhe, Germany
Albumin	Roth, Karlsruhe, Germany
APS	Roth, Karlsruhe, Germany
Bromphenol Blue	Merck, Darmstadt, Germany
BSA	Roth, Karlsruhe, Germany
β-Mercaptoethanol	Sigma Aldrich, Steinheim, Germany
D-MEM	GIBCO Invitrogen, Germany
DMSF	Merck, Darmstadt, Germany
EDTA	Sigma Aldrich, Steinheim, Germany
EtBr	SERVA Electrophoresis GmbH, Heidelberg, Germany
Ethanol 70%, 95%, 99.6%	Fischer scientific, Germany
etoposide	Calbiochem, EMD Chemicals, San Diego, USA
FCS	PAA Laboratories GmbH, Marburg, Germany

Glutamin	GIBCO Invitrogen, Germany
Glycerol mounting medium	Dako cytomation, Hamburg, Germany
Glycine	Roth, Karlsruhe, Germany
Haemalaun	Roth, Karlsruhe, Germany
HCL	Roth, Karlsruhe, Germany
Methanol	Fluka Chemie, Buchs, Switzerland
NaCl	Roth, Karlsruhe, Germany
Na-Deoxycholat	Fluka Chemie, Buchs, Switzerland
Paraformaldehyde	Fischer scientific, Germany
PBS	PAA Laboratories GmbH, Marburg, Germany
PenStrep	GIBCO Invitrogen, Germany
PMSF (Proteinaseinhibitor)	SERVA Electrophoresis GmbH, Heidelberg, Germany
Saccharose	Roth, Karlsruhe, Germany
SDS	Merck, Darmstadt, Germany
Skim Milk Powder	Fluka Chemie, Buchs, Switzerland
Sodium Hydroxide Solution (NaOH)	Merck, Darmstadt, Germany
Thapsigargin	GIBCO Invitrogen, Germany
TEMED	Fluka Chemie, Buchs, Switzerland
topotecan Hydrochloride Hydrate	Sigma Aldrich, Steinheim, Germany
Tris	Roth, Karlsruhe, Germany
Triton X-100	Sigma Aldrich, Steinheim, Germany
Tween-20	Sigma Aldrich, Steinheim, Germany
Xylene	Roth, Karlsruhe, Germany

Table 3: Chemicals and biochemicals

3.1.4.2 Transfection reagents

reagent	company/catalog number
DharmaFECT non-targeting siRNA	Thermo Fisher Scientific, Germany
siGENOME Control Reagent	Thermo Fisher Scientific, Germany
HisRS siRNA	Santa Cruz Biotechnology, Germany, sc-37675
Topo I siRNA	Santa Cruz Biotechnology, Germany, sc-36694
Topo IIα siRNA	Santa Cruz Biotechnology, Germany, sc-36695
Topo IIβ siRNA	Santa Cruz Biotechnology, Germany, sc-36697

Table 4: Transfection reagents

3.1.4.3 Antibodies

Primary antibody	origin	dilution	company/catalog number
ATF4 (Creb2)	rabbit	1:1000 (WB, IHC)	Santa Cruz Biotechnology, Germany, sc-200
β-Actin	rabbit	1:15000 (WB)	Abcam, USA, ab8226
CHOP (GADD 153)	mouse	1:2000 (WB)	Abcam, USA, ab11419
CHOP	rabbit	1:50 (IHC)	Sana Cruz Biotechnology, Germany
Cleaved Caspase 3	rabbit	1:125 (WB)	Trevigan, catalog: 2305-PC-100
HisRS	mouse	1:100 (WB)	Santa Cruz Biotechnology, Germany, sc-81287
LC3B	rabbit	1:1000 (WB)	Abcam, USA, ab48394

Pro SP-C	rabbit	1:500 (IHC)	Chemicon, USA
P50 ATF6	rabbit	1:1000 (WB) 1:100 (IHC)	Abcam, USA
Topo1	mouse	1:1000 (WB)	Santa Cruz Biotechnology, Germany, sc-32736
Topo2α	mouse	1:500 (WB)	Santa Cruz Biotechnology, Germany, sc-165986
Topo2β	rabbit	1:2000 (WB)	Abcam, USA, ab72334
Topo2β	rabbit	1:2000 (WB)	Bethyl Laboratories, Texas, catalog: A300-949A

Table 5: primary antibodies

Secondary antibody	**origin**	**dilution**	company
Polyclonal Rabbit anti Mouse Immunglobulins/HRP	rabbit	1:1000	Dako, Denmark
Polyclonal Swine anti Rabbit Immunglobulins/HRP	swine	1:2000	Dako, Denmark

Table 6: Secondary antibodies

3.1.4.4 Buffer

Protein extraction:

50mM Tris, pH=7.5
5mM EDTA
150mM NaCl
1% (w/v) Triton x-100
0.5% (w/v) Na-Deoxycholat
1mM PMSF

DNA agarose gel electrophoresis:

- 1x TAE buffer: 40 mM Tris-acetate, pH = 8.0
  1 mM EDTA, pH = 8.0

Western Blot analysis:

- Seperating Gel buffer:
  1.125M Tris
  pH 8.8
  30% Saccharose
- Stacking Gel buffer:
  0.625M Tris
  pH 6.8
- 4x SDS-loading buffer:
  5g SDS
  40ml glycerin
  25ml stacking gel buffer
  0.01g bromophenolblue
  for a final volume of 100ml
- SDS-Running buffer / Electrode buffer 10:
  Tris 25mM
  Glycine 192 mM
  SDS 0.1%
- Transfer buffer:
  20mM Tris
  159mM Glycine
  20% MeOH
- Wash buffer: TBS-T 10x
  1M Tris
  4M NaCl
  1% Tween-20
  pH 7.5
- Block solution:
  Skim Milk Powder 5%
  TBS-T 1x
- Stripping buffer:
  TBS-T 1x
  2% SDS
  100mM β-mercaptoethanol

IgG-Purification:

- Binding buffer: 0.1M Glycine buffer, pH 9.0
  0.1M Glycine buffer, pH 2.5-2.7
  1M Tris-HCL buffer, pH 9.0

IHC:

- permeabilization buffer: 0.4% Triton X-100 in
  1xPBS
  pH 7.4

3.1.4.5 Gels

Agarose gel: 2% Agarose
1xTAE buffer
0.5 µg/µl EtBr

Seperating Gel:

	8%	9%	10%	12%	15%
A. dest.	3.87ml	3.53ml	3.20ml	2.53ml	1.53ml
1.125 M Tris, pH 8.8	3.33ml	3.33ml	3.33ml	3.33ml	3.33ml
Acrylamide/Bisacrylamide (30%/0.8%)	2.66ml	3.0ml	3.33ml	4.0ml	5.0ml
10% SDS	100µl	100µl	100µl	100µl	100µl
TEMED	10µl	10µl	10µl	10µl	10µl
10% APS	50µl	50µl	50µl	50µl	50µl

Table 7: Seperating Gel

Stacking Gel:

A.dest.	6.57ml
0.625M Tris, pH 6.8	2.0ml
Acrylamide/Bisacrylamide (30%/0.8%)	1.33ml
10% SDS	100µl
TEMED	10µl
10% APS	100µl

Table 8: Stacking Gel

3.1.4.6 Kits

Products	Manufacturer
Zytochem AP fast red kit, broad spectrum	Zytomed systems, Berlin, Germany.
BCA protein assay kit	Pierce, Germany.
iQ(™) SYBR Green Supermix	BioRad, USA.
Omnitranscript RT Kit (200)	Qiagen, Hilden, Germany.
HotStarTaq DNA Polymerase Kit	Qiagen, Hilden, Germany.
Phire Hot Start II DNA Polymerase	Finnzymes (Thermo Scientific), Espoo, Finland.
RNeasy Pus Mini Kit (50)	Qiagen, Hilden, Germany.

Table 9: Kits

3.2 Methods

3.2.1 Cell culture

A459 cells were cultured in D-MEM:F12, supplied with 10% FCS, 2mM Glutamin, 1% Penicillin, 1% non-essential amino acids and 1% MEM Vitamins in an atmosphere of 95-100 % air humidity, 5% CO2 at 37 °C. Passaging was carried out in a confluent stadium. After one washing step with 1x PBS, 3.5 ml of Trypsin/EDTA was added until the detachment of the cells from the underlay was catalyzed. Removing the Trypsin/EDTA and adding 2ml of Medium stopped this process. By pipetting the Medium several times up and down, the cells were stripped from the plate. In order to split the cells in a dilution of 1:20 or 1:10, 100µl or 200µl of the cell suspension was added to a new plate, containing 10ml of Medium. To use the cells for further experiments they were seeded accordingly to respective protocols.

3.2.2 siRNA Transfection

In order to analyze the consequence of a loss of function of specific genes on RNA and protein level, the technique of small interfering RNA (siRNA) was used. siRNA consists of short double strand ribonucleic molecules and is directed against a complementary gene sequence that is meant to be silenced. It enters the cell via lipid-based

transfection and binds the so called RNA-induced silencing complex (RISC). RISC is a ribonucleoprotein complex which has not been completely identified yet. Nucleases such as Dicer, Argonaute proteins and a dsRNA-binding protein (dsRBP) play an important role in this complex. Binding the RISC leads to a separation of the RNA strands and an activation of the complex. The activated RISC/siRNA-complex associates with the complementary mRNA and cleaves it. Thus the translation of the target mRNA can be inhibited and the expression of the specific gene is silenced [100]. For silencing, cells were plated in a 6-well-plate and incubated until they reached more than 90% confluency. In order to prepare a 20µM stock solution, each siRNA was resuspended in RNase free water. Cells transfected with non targeting siRNA served as a negative control. To exclude a potential effect of transfection reagent on the cells, a mock transfection (transfection with transfection reagent without any siRNA) was also included. To get a 2µM siRNA working solution, the 20µM stock solution was diluted 1:10 in PBS. The preparation of the transfection reagents was calculated for triplicate transfection. Solution A, consisting of 350µl siRNA working solution plus 350µl serum free medium, was carefully mixed wih a pipette and incubated at RT for 5min. For solution B 28µl of transfection reagent Dharmafect and 672µl of serum free medium were carefully mixed with a pipette. After a 5min incubation at RT, solution A was added to solution B, carefully mixed with a pipette and incubated for 20min. Finally 5.6ml serum containing culture medium was added to this solution. For mock transfection, solution A was prepared with PBS instead of siRNA solutions. Medium was removed from the cells and 2ml/well of siRNA solution was added. Cells were harvested after 48h, 72h or 96h respectively.

3.2.3 Protein Inhibition

In order to inhibit activity of topoisomerases, the protein inhibitors etoposide and topotecan were used.

Etoposide is a semisynthetic derivative of podophyllotoxin that exhibits antitumor activity. It causes error in DNA synthesis and prevents re-ligation of DNA strands by forming a complex with Topo2 and DNA. Thus repair of DNA by Topo2 is inhibited and apoptosis of cancer cells can be promoted [101].

Topotecan is an antineoplastic agent used to treat ovarian cancer. It works by inhibiting function of Topo1. Topotecan binds to the Topo1-DNA-complex and thus prevents religation of the single strand breaks [102–104].

To prepare a stock solution of 100µM of protein inhibitors, respective amounts were solved in 200µl Dimethylsulfoxide (DMSO) and filled up with culture medium to 50ml.
Cells were treated with protein-inhibitor-solution in different concentrations and at different time points. After treatment endpoints cells were harvested and protein expression was checked by Immunoblotting.
Medium containing only DMSO without inhibitors served as vehicle.
In order to get a positiv control for apoptosis and ER-stress some cells were treated with a 1µM solution of Thapsigargin instead of etoposide or topotecan. Thapsigargin is an enzyme known for triggering apoptosis and ER-stress.

3.2.4 Protein extraction and quantification

After transfection or inhibition endpoints, proteins were lysed in 100µl lysis buffer. Plates were dipped twice in liquid nitrogen for a few seconds and harvested with a cell scraper. The suspensions were transfered to Eppendorf tubes. After destroying DNA with Sono Rex the tubes were centrifugated at 4°C and 13000rpm for 5min. The supernatant was obtained and used for protein concentration determination by Bicinchoninic acid (BCA) method, a colorimetric detection system of cuprous cation. A BCA/copper complex is formed which exhibits a linear absorbance at 562nm with increasing protein concentrations. To construct a standard curve 2mg/ml bovine serum albumin (BSA) was mixed with 0.9% NaCl respectively in order to get different dilutions of BSA (1500µg/ml, 1000µg/ml, 750µg/ml, 500µg/ml, 250µg/ml, 125µg/ml, 62.5µg/ml, 31.25µg/ml, 15.625µg/ml, 7.813µg/ml). For the measurement BSA solutions and 1:10 diluted protein probes were transfered in duplication to a 96 well plate and mixed with 200µl of Pierce BCA dye. After 45min incubation at 37°C absorbance was measured at 565nm in a ELISA plate reader. The corresponding protein concentrations were calculated by interpolation using the standard curve.

3.2.5 Polyacrylamide Gel Electrophoresis of Protein (SDS-Page)

In order to perform Western Blot analysis, protein extracts were seperated by SDS polyacrylamide gel electrophoresis (SDS-Page). SDS denatures the proteins and binds to the polypeptides. Thus a negative charge to the polypeptides is provided that leads to the migration of the polypeptides to the positive electrode. The mobilitiy of the

proteins increases linear to the protein size. The smaller the molecule the faster it migrates. In this way protein can be seperated according to their molecular weight. Proteins were mixed with 4x SDS-loading buffer reduced by adding 10% β-mercaptoethanol and denatured in a water bath at 98°C for 15min. The samples were collected by brief centrifugation. After loading a proteinladder and 20µg or 25µg of each protein sample onto the gel (stacking and seperating gel were produced as described in table 7 and 8), electrophoresis was performed in presence of SDS-running buffer at 90V till the bromphenol blue reached the bottom of the seperating gel.

3.2.6 Immunoblotting

The separated proteins on the SDS polyacrylamide gel were transfered to a polyvinylidene fluoride (PVDF) membrane by electro blotting to visualize specific proteins. The PVDF membrane was activated with methanol before using. Two layers of Whatmann 3mM filter paper washed with Transfer buffer followed by PVDF membrane were placed onto the electroblotting chamber. On the PVDF membrane, the gel and two other filter paper washed with Transfer buffer were placed. The transfer was performed at constant current (2mA/cm²) for 1.5h. After this step the membrane was blocked in 5% Skim Milk solution for 1h at RT. To dissolve the Skim Milk Powder, TBSTx1 was used. After blocking respective primary antibodies, diluted in 5% Skim Milk, were added to the membrane and incubated at 4°C overnight. Concentrations of different antbodies are listed in table 5 . The next day the membrane was washed in TBSTx1 4 times for 15min, followed by incubation with appropriate secondary antibody (refer to table 6) at RT for 1h. After washing with TBSTx1, the protein was detected by ECL (Enhanced Chemi-luminescence) treatment and exposure of the membrane to ECL films in dark. Bands on the film were finally visualized by diping them in developing and fixing solutions. Where necessary, the membranes were re-probed with another antibody by stripping it with stripping buffer at 58°C for 2h. After washing with TBSTx1 and blocking with 5% Skim Milk at RT for 1h, appropriate primary antibody was added, followed by further steps as described before.

3.2.7 Densitometry

To perform densitometric analysis, the spot denso software from Alpha Innotech was used. Values of target protein were normalized to actin values and are given as a percentage of the respective scrambled controls.

3.2.8 RNA isolation and measurement

Isolation of RNA from A549 cells was performed by using the RNeasy Pus Mini Kit (50). Steps were accomplished according to the instructions of the manufacturer. Obtained RNA solutions were stored at -80°C. Concentration and purity of the obtained RNA was determined with a Nanodrop ND-100 spectrophotometer via measuring the optical density at 260nm and 280nm of the obtained solutions. The wavelenght for maximal absorption of nucleid acids is 260nm, known as Optical Density at 260nm (OD260nm). An OD of 1 at 260nm corresponds to 40µg RNA/ml. Proteins, that often form a contamination source, have an absorption maximum of 280nm (OD280nm). Therefore the quotient of the OD at 260nm and at 280nm is a measure of RNA purity. In a pure RNA and protein-free solution the ratio OD260nm/280nm is 2. Due to protein contaminations this coefficient is usually lower. In the experiments of this study it was between 1.8 and 2.

3.2.9 cDNA synthesis

In order to perform semiquantitave reverse transcription polymerase chain reaction (sqRT-PCR) or quantitative reverse transcription PCR (qRT-PCR), RNA was transcribed into comlentary cDNA using the Omnitranscript RT Kit (200). The reverse transcription of mRNA to cDNA is catalyzed by reverse Transcriptase (RT) and RNA-dependent DNA polymerase. By using Oligo dT-Primer, which hybridize to the poly(A) 3 ´tail of mRNA all mRNAs could be primed simultaneously.
For the preparation of cDNA, 2µg RNA was used. For 20µl reaction 11µl of the following master mix was added to 2µg/9µl RNA. For 40µl reaction 22µl of the following master mix was added to 2µl/18µl RNA.

reagent	20µl reaction	40µl reaction
10x Buffer	2µl	4µl
dNTPs (5mM each dNTP)	2µl	4µl
Oligo-dT Primer (10 µM)	0.5µl	1µl
RNAse Inhibitor (10 units/µl)	0.5µl	1µl
Reverse Transcriptase (4 units/µl)	1µl	2µl
RNase free water	5µl	10µl

Table 10: Master mix for reverse Transcription

Reverse transcription was performed in a Thermo Cycler, using the following protocol:

1. Attachment of the Oligo-dT Primer	25°C for 10min
2. Reverse Transcription	37°C for 65min
3. Cooling	4°C

Table 11: Protocol for reverse transcription

Obtained cDNA was stored at -20ºC.

3.2.10 Reverse transcription polymerase chain reaction (RT-PCR)

PCR is a method which allows the amplification of DNA sequences in order to detect them. This procedure uses two specific oligonucleotides, which function as primers, four deoxyribonucleotide triphosphates (dNTP´s) and a heat-stable DNA polymerase. Each reaction cycle consists of three reactions that take place under different temperatures:

1. Denaturation at 94°C: The double-stranded DNA is converted into two single strands.
2. Hybridization at 50-65°C: Cooling of the reaction allows the annealing of the primers to the complementary DNA sequence.
3. DNA synthesis at 72°C: thermo-stable DNA polymerase extends both DNA strands starting from the primers.

In 20-50 reaction cycles the target DNA product increases exponentially and can be detected. PCR products were analysed either semiquantitatively or quantitatively.

3.2.10.1 Semiquantitative reverse transcription polymerase chain reaction

Semiquantitative reverse transcription polymerase chain reaction (sqRT-PCR) analyzes the PCR products via gelelectrophoresis, it is an endpoint determination.

For sqRT-PCR following PCR-Mix was used:

HotStarTaq DNA Polymerase Kit:

reagent	**25µl reaction**
d10xBuffer	2.5µl
NTP (10 mM of each)	0.5µl
forward primer (10 pM)	1µl
reverse primer (10 pM)	1µl
H2O	17.75µl
Taq-Polymerase (5 units/µl)	0.25µl
cDNA (20µl reaction)	2µl
Total volume	25µl

Table 12: PCR-Mix for sqRT-PCR (HotStarTaq DNA Polymerase)

The PCR was performed in a thermo-cycler, programmed as follows:

Activation of HotStart Taq		20min	94°C
Denaturation	30cycles	30s	94°C
Annealing		30s	Refer to table 18
Extension		1min	72°C
Final Extension		10min	72°C

Table 13: Cycle protocol for sqRT-PCR (HotStartTaq DNA Polymerase)

Phire Hot Start II DNA Polymerase:

reagent	**25µl reaction**
PhireBuffer	5µl
DNTPs (10 nM)	0.5µl
forward primer (10 pM)	2µl
reverse primer (10 pM)	2µl
H2O	13µl
Taq-Polymerase (5 units/µl)	0.5µl
cDNA (40µl reaction)	2µl
Total volume	25µl

Table 14: PCR-Mix for sqRT-PCR (Phire Hot Start II DNA Polymerase)

The PCR was performed in a thermo-cycler, programmed as follows:

Activation of Phire Hot Start II Polymerase		30s	98°C
Denaturation	25cycles	5s	98°C
Annealing		5s	Refer to table 18
Extension		15s	72°C
Final Extension		1min	72°C

Table 15: Cycle protocol for sqRT-PCR (Phire Hot Start II Polymerase)

After amplification PCR products were analyzed via agarose gel electrophoresis.

3.2.10.2 Quantitative reverse transcription polymerase chain reaction

Unlike the sqRT-PCR, which is an endpoint analysis of the PCR products, the quantitative reverse transcription polymerase chain reaction (qRT-PCR) performs simultaneous quantification of the initial amount of amplified sequence next to the amplification. The process is monitored in „real time“, means products are measured during the reaction and at the end of each cycle respectively. For this, fluorescent dyes, which conduct proportional to the product accumulation, are used [105].
Following PCR-Mix was used:

reagent	**20µl reaction**
BIORAD Sybergreen Mix	10µl
forward primer 10 pmol/µl	0.5µl
reverse primer 10pmol/µl	0.5µl
water	8µl
cDNA (10ng/µl)	1µl

Table 16: PCR-Mix for qRT-PCR

The PCR was performed with iQ™ Single Color Real-Time PCR Detection System programmed as follows:

	1x	3min	95°C
Denaturation	40 cycles	15s	95°C
Annealing		30s	58°C
	1x	10s	Meltingcurve analysis

Table 17: Cycle-protocol for qRT-PCR

3.2.10.3 DNA agarose gel electrophoresis

DNA agarose gel electrophoresis is used to analyze DNA fragments obtained in sqRT-PCR. Agarose gelelectrophoresis can seperate and visualize DNA fragments according to their size. An electric field causes a movement of negatively charged DNA from the cathode (-) to the anode (+). After a certain time period shorter molecules have covered a longer distance than longer ones, as the shorter molecules move faster through the gel. For the electrophoresis a 2% agarose gel was prepared with 1xTAE buffer mixed with respective amounts of agarose. To visualize DNA, the gel was treated with 0,5µg/ml ethidium bromide (EtBr). EtBr intercalates between the bases of DNA double strands and fluoresces under ultraviolet light. The DNA sample was mixed with 5x loading buffer and 10µl of this solution was loaded onto the agarose gel that was covered by 1xTAE buffer. Electrophoresis was performed for 45-60min at 80V/cm. Finally the gel was visualized with Molecular Imager Gel Doc™ XR system. The size of amplified DNA was determined by a DNA molecular weight standard.

3.2.10.4 Measurement of fluoresecence with SYBR-Green

Measurement of fluorescence is necessary to analyze products obtained during qRT-PCR. One possibility of detection is to measure the fluoresecence with SYBR-Green, a dsDNA-specific asymmetric cyanine dye. It binds sequence independently to the minor groove of dsDNA. The fluoresecence of the bound dye is 1000-fold higher than that of free dye, which is the reason why product accumulation during PCR can be well monitored. Fluoresecence is measured at the end of the elongation phase of each cycle, when the amount of dsDNA reach their maxima and fluoresecence is at the highest point. It is possible, that non-specific products like primer dimer occur, which alters the amplification efficiency. This can lead to a quantification error and the quantitative analysis has to be optimized [105].

3.2.10.5 Melting curve analysis

SYBR Green binds to any dsDNA. Melting of the product means, that SYBR-Green is released and fluoresecence signal decreases rapidly. A melting curve identifies the PCR product because of temperatue-dependant signal decrease as a result of melting of the product. The melting temperature (Tm) is defined as the temperature at which the decrease of temperature occurs and half of the DNA is present as a denatured single strand. Tm is characterized by the lenght of the dsDNA. After the PCR cycles were performed, the samples were heated to 95°C. This leads to denaturation of the samples and thus an abrupt decrease of fluorescence. Timepoint of fluoresecence decline allows the conclusion of Tm. Nonspecific products have deviating melting temperatures. For example primer dimers have a lower melting temperature as they are shorter. Thererfore the amplification of the correct sequence can be confirmed. The area under the curve (AUC) of the peak is proportional to the product amount [105].

3.2.10.6 Analysis of data

To analyze the data, the fluroscence signal is plotted against the number of cycles (amplifiaction plot). The baseline of this graph is determined by the initial phase that corresponds to the cycles in which the fluroescence has not yet started to increase considerably. The crucial point for quantification is the exponential phase of product

accumulation, the so-called “threshold“ regarding the fluorescence signal has to be assessed. The cycle number when the signal reaches this threshold is called Ct (theshold cycle) or crossing point. It depends linear on the logarithm of the inital product concentration and therefore allows its determination.

For the comparative Ct method of relative quantification to be valid, the efficiency of the reaction of the target gene and the efficiency of the reaction of the reference/ housekeeping gene must be approximately equal. Amplification efficiancy was determined by running serial dilutions of a template, the results were used to generate a standard curve. Amplification efficiency was calculated from the slope of the standard curve. Ideally, the amount of PCR product will perfectly double during each cycle of exponential amplification. This translates to a reaction efficiency of 2. ß-Actin, an ubiquitously and constitutively expressed gene in human cells was used as a reference/ housekeeping gene.

In order to get a relative quantification of the mRNA level of the target gene, their Ct values were analyzed as the difference to the housekeeping gene: ΔCt = Ct house keeping gene – Ct target gene. β-Actin was used as the housekeeping gene. To judge the effects of silencing on gene expression, mRNA level changes of samples transfected with non targeting siRNA (Scrambled) were compared with untreated samples (UT), mock transfections (Mock) and samples transfected with target siRNA. The difference was expressed as $\Delta\Delta$Ct and determined as follows: $\Delta\Delta$Ct UT = ΔCt Scrambled - ΔCt UT; $\Delta\Delta$Ct Mock=ΔCt Scrambled - ΔCt Mock; $\Delta\Delta$Ct siRNA=ΔCt Scrambled - ΔCt siRNA. The $\Delta\Delta$Ct corresponds to the binary logarithm of the fold change.

Primer	Annealing Temperature (Hot Star Taq Polymerase)	Annealing Temperature (Phire Hot Start II Polymerase)
ATF4	62°C	65°C
β-Actin	60°C	62°C
CHOP	60°C	65°C
DDB1	61°C	63°C
HisRS	58°C	61°C
PPIB	60°C	63°C
Topo1	60°C	63°C
Topo2α	61°C	63°C
Topo2β	59°C	59°C
VCP	62°C	65°C
XBP1 (first set)	61°C	64°C
XBP1 (second set)	60°C	62°C

Table 18: Annealing Temperatures

3.2.11 Immunohistochemistry

Immunohistochemistry (IHC) is the localization of antigens in tissue sections by the use of labeled antibody as specific reagents through antigen-antibody interactions that are visualized by a marker such as fluorescent dye, enzyme, radioactive element or colloidal gold. Since immunohistochemistry involves specific antigen-antibody reaction, it has apparent advantages over other traditionally used special enzyme staining techniques that identify only a limited number of proteins, enzymes and tissue structures. There are numerous immunohistochemistry methods that may be used to localize antigens. The selection of a suitable method should be based on parameters such as the type of specimen under investigation and the degree of sensitivity required. Lungs were fixed in paraformaldehyde and sections of 3µm thickness were used for immunohistochemical analysis in this study. Sections were deparaffinized at 60°C for 2 hours and then in xylene for 10 minutes. They were then rehydrated in descending alcohol concentrations (99.6%>96%>80%>70%>50%). Sections were washed in washing buffer (1x PBS) to remove traces of ethanol. Heat mediated antigen retrival was performed by boiling the section for 3x5 minutes at 500W, followed by washing in PBS. The AP fast red kit (Zytomed Berlin) was used for further steps. The sections were blocked for 10 minutes in the blocking solution followed by washing.

Primary antibody solutions were prepared in 3% BSA solution with respective dilutions. A negative control was always used where primary antibody was omitted. Isotype controls served as confirmation of the specifity of used antibodies (Fig. 25 of appendix). For this purpose samples were incubated with antibody diluent, supplemented with a non-immune immunoglobulin of the same isotype and concentration as the primary antibody. Sections were placed in a humid chamber and incubated with primary antibody overnight at 4°C, followed by washing for 5 times. 50µl of biotinylated secondary antibody was added to each section and incubated for 10 min at RT, followed by washing. Few drops of enzyme conjugate (streptavidin / alkalic-phosphatase conjugate) were added to each section with 10 min incubation at RT, followed by washing. Fast red tablets were used as substrate which was freshly prepared by dissolving one fast red tablet in one substrate buffer (naphtol-phosphate buffer). 50µl of this substrate solution was given to each section and allowed to develop in the dark, with constant monitoring for the pink colour development under light microscope. Enough care was taken that all sections, control sections and negative control sections were treated in the same way, and developed for the same time in order to avoid false results. After developing, the reaction was stopped by immersing the slides in aqua.dest. Counterstaining was performed with haemalaun for 2 minutes followed by washing the slides under running tap water, which resulted in blue nuclei. Sections were then mounted with glycerol mounting medium and allowed to dry.

3.2.12 Statistical analysis

Unless otherwise stated, three independent experiments were conducted for all in vitro studies. Statistical significance was assessed employing Mann-Whitney U-test (Graph Pad Prism 4.0). Significance is indicated as # $p < 0.05$ between two different groups as indicated in the respective figure legends. Values were considered not significant where no symbols are indicated.

4. Results

4.1 Gene silencing in A549 cells

ER-stress induced apoptosis in AECII seems to represent a common pathomechanistic principle in ILD [9]. ER stress means a disruption of ER homeostasis which leads to accumulation of misfolded or unfolded proteins and is often followed by apoptotic cell death [60,64,106,107]. In order to investigate a possible relation between autoantibody expression against HisRS, Topo1, Topo2α and Topo2β and development of ILD, respective genes were silenced via siRNA transfection and occurance of ER-stress and apoptosis was checked in A549 cells.

4.1.1 HisRS – Silencing and analysis of ER-stress and DNA-damage

4.1.1.1 HisRS - Silencing

To assess the success of HisRS-Silencing on mRNA level, sqRT-PCR was performed after 72h of transfection. PCR products were visualized by DNA agarose electrophoresis. Downregulation of HisRS mRNA after transfection with a specific siRNA directed against HisRS could be shown (Fig.10a). To further corroborate the knockdown of HisRS, expression of the HisRS gene was quantified by qRT-PCR. The results are presented as mean of ΔΔCT ± SD The mRNA expression of HisRS after transfection with siRNA was significantly decreased (-3,93 ± 0.33), proving the knockdown (Fig.10b). Western blot analysis also showed a decrease in HisRS protein after siRNA transfection and thus confirms the success of HisRS-Silencing as well on protein level (Fig.10c), although there still was HisRS protein visible. Densitometric analysis from the immunoblots showed, that approximately 37% of HisRS is left post silencing (Fig. 10d).

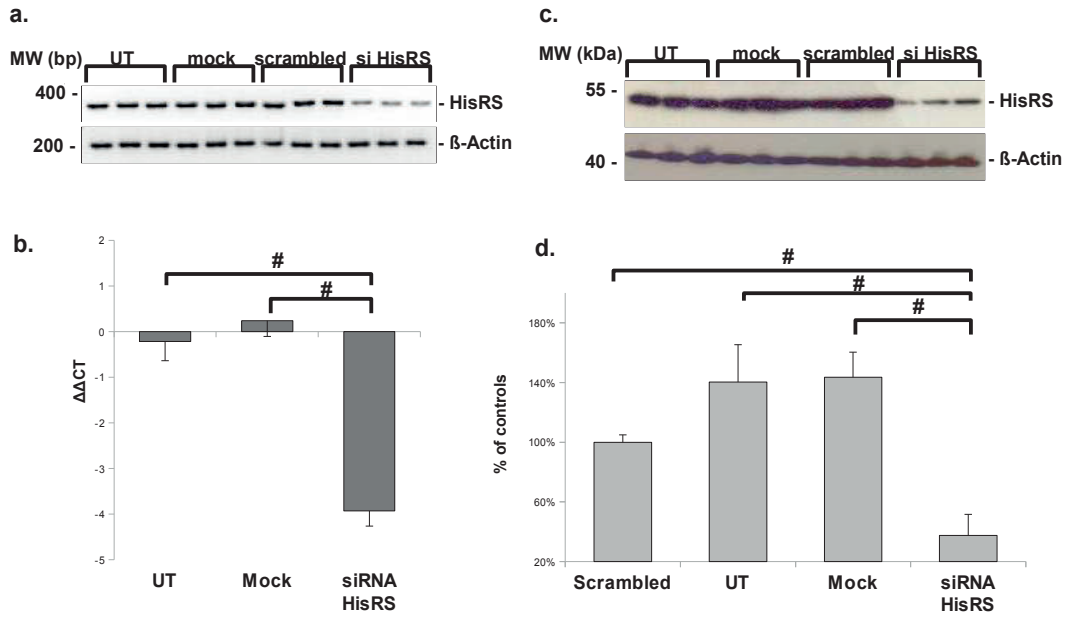

Figure 10: HisRS – Silencing

A549 cells were transfected with siRNA directed against HisRS, knockdown of HisRS was checked by RT-PCR and Immunoblot (IB) 72h after transfection. Mock (transfection with transfection reagent without any siRNA) and scrambled (non targeting) siRNA served as negative controls: Pictures are each representative for three independant experiments. (a) sqRT-PCR analysis for the expression of HisRS, 30 cycles were performed, β-Actin served as loading control. (n=3) (b) qRT-PCR analysis for the expression of HisRS, results are presented as mean of ΔΔCT ± SD (n=3; #p<0.05). (c) IB analysis for the expression of HisRS, β-Actin served as loading control. (n=3) (d) Densitometry was performed from IB analysis. The target protein/ß-Actin ratio was calculated (scrambled=100%) (n=3; # p<0.05).

4.1.1.2 Analysis of ER-stress and DNA-damage after HisRS knockdown

After successful silencing of HisRS, a possible existence of an ER-stress response, apoptosis or DNA-damage was investigated. For this purpose markers involved in ER-stress such as CHOP [60,64,65], Peptidyl-prolyl cis-trans isomerase B (PPIB) [108], Valosin containing protein (VCP) [109], ATF4 [60,64,65] and XBP-1 [60,64], as well as the marker DNA damage binding protein 1 (DDB1), which indicates DNA-damage, were analyzed.

As evident from Figure 11, we could, however, not detect any kind of significant ER stress response or DNA damage on RNA as well as on protein level 48 and 72h after transfection.

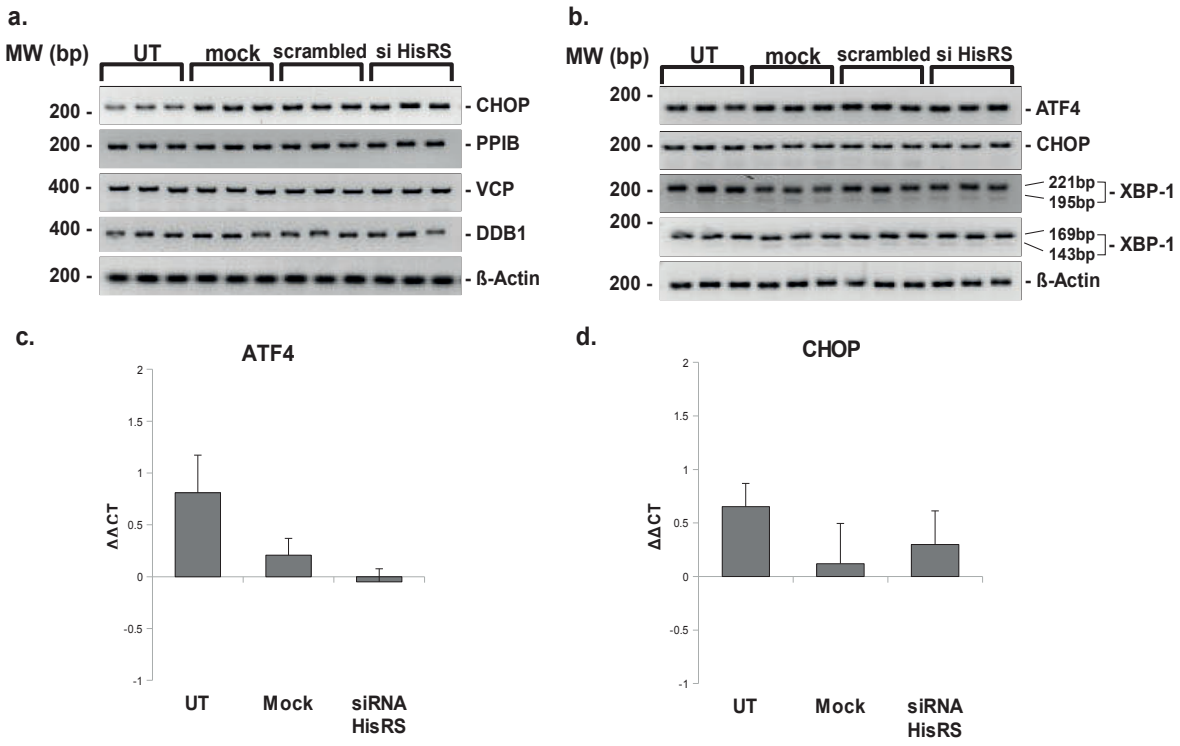

Figure 11: No ER-stress or DNA damage 72h after HisRS knockdown

(a) sqRT-PCR analysis of CHOP, PPIB, VCP and DDB1 48h after transfection with siRNA directed against HisRS, 30 cycles were performed, β-Actin served as control. (n=2) (b) sqRT-PCR analysis of ATF4, CHOP and XBP-1 (221/169bp: unspliced = inactive, 195/143bp: spliced = active) 72h after transfection with siRNA directed against HisRS, 30 cycles were performed, β-Actin served as loading control. (n=2) (c-d) qRT-PCR analysis of ATF4 and CHOP 72h after transfection with siRNA directed against HisRS, results are presented as mean of ΔΔCT ± SD (n=3). Significance level was not reached. Pictures are each representative for two independant experiments.

4.1.2 Topoisomerase 1 – Silencing and analysis of ER-stress

4.1.2.1 Topoisomerase 1 – Silencing

SiRNA mediated knockdown of Topo1 was checked in the same manner as for HisRS. After 72h of transfection with siRNA against Topo1, sqRT-PCR showed a decrease in Topo1 expression (Fig. 12a) and qRT-PCR (-3,2 ± 0,36) and western blot analysis clearly confirmed the silencing of Topo1 (Fig. 12b+c), again with some residual Topo1 being visible on protein level. Densitometric analysis revelaed about 14% of Topo1 being left after silencing (Fig. 12d).

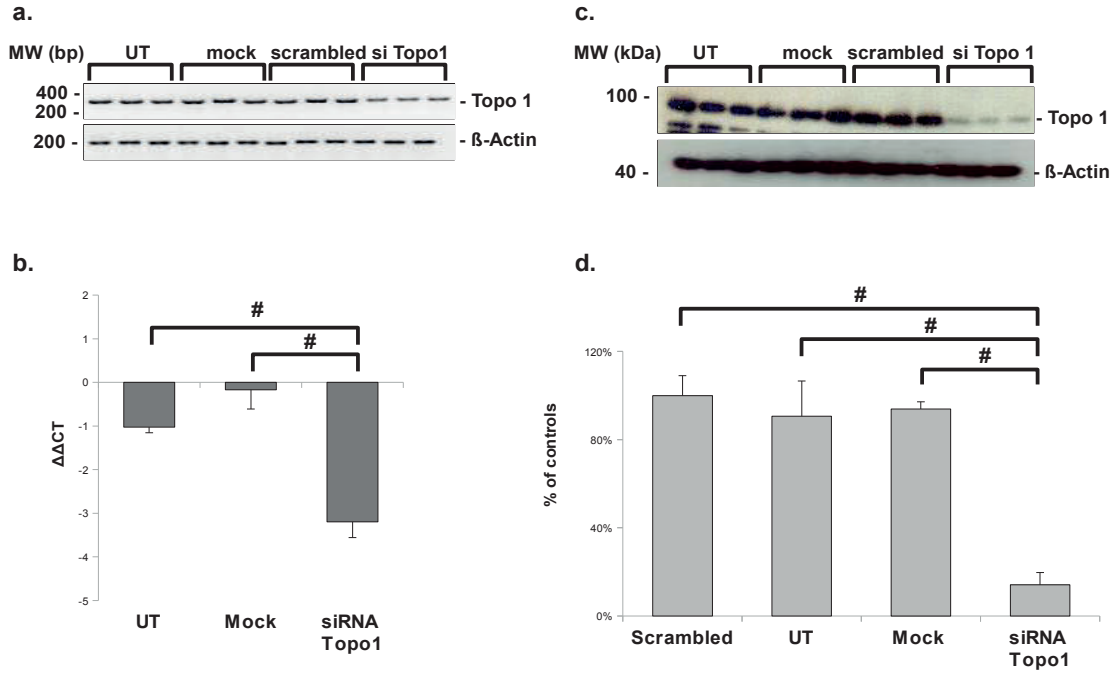

Figure 12: Topoisomerase 1 – Silencing

A549 cells were transfected with siRNA directed against Topo1, knockdown of Topo1 was checked by RT-PCR and IB 72h after transfection. Mock (transfection with transfection reagent without any siRNA) and scrambled (non targeting siRNA) served as negative controls: (a) sqRT-PCR analysis for the expression of Topo1, 30 cycles were performed, β-Actin served as loading control. (n=3) (b) qRT-PCR analysis for the expression of Topo1, results are presented as mean of ΔΔCT ± SD (n=3; #p<0.05). (c) IB analysis for the expression of Topo1, β-Actin served as loading control. (n=3) (d) Densitometry was performed from IB analysis. The target protein/ß-Actin ratio was calculated (scrambled=100%) (n=3; # p<0.05). Pictures are each representative for three independant experiments.

As shown in Figure 23a of the appendix a slight decrease of Topo1 expression on mRNA level could be observed already after 48h of transfection with siRNA against Topo1.

4.1.2.2 Analysis of ER-stress after Topoisomerase 1 knockdown

After successfully silencing the Topo1, a possible existence of an ER-stress response was investigated. For this purpose ATF4, CHOP and XBP-1, which are markers that indicate ER-stress, were analysed. Knockdown of Topo1 did not result in a significant induction of ER stress marker 72h after knockdown (Fig. 13 a-c).

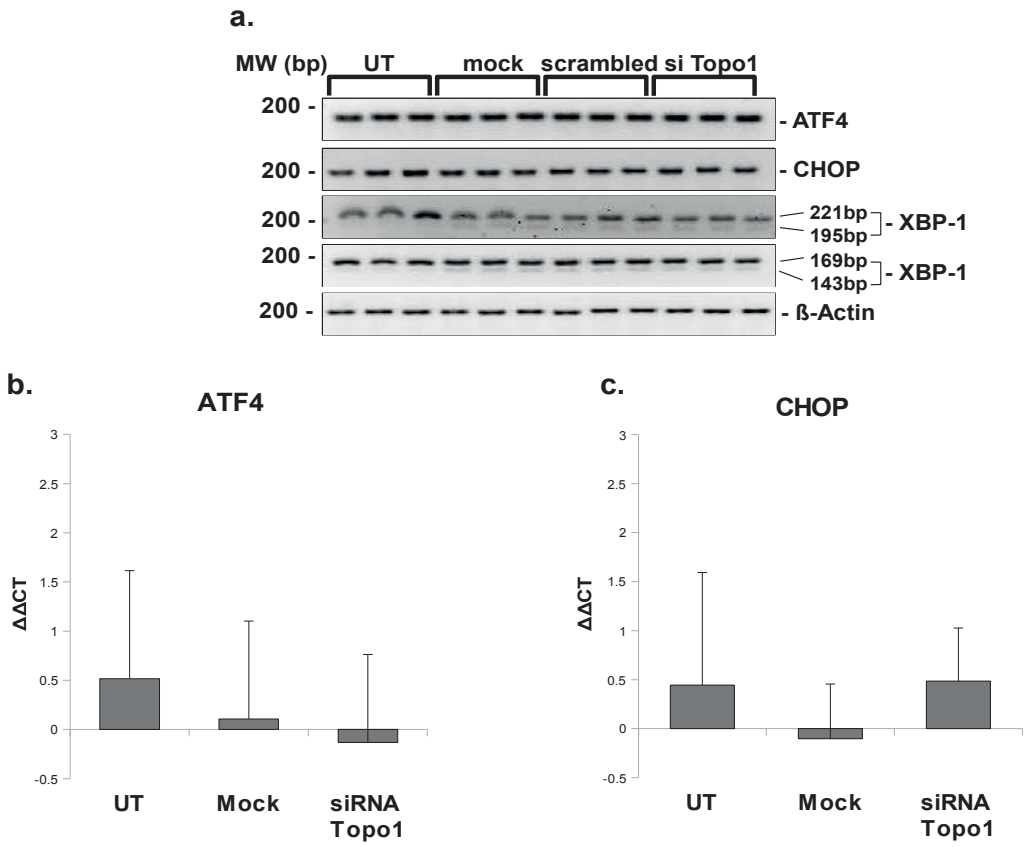

Figure 13: No ER-stress after Topoisomerase 1 knockdown

(a) sqRT-PCR analysis of ATF4, CHOP, XBP-1 (221/169bp: unspliced = inactive, 195/143bp: spliced = active) 72h after transfection with siRNA directed against Topoisomerase 1, 30 cycles were performed, β-Actin served as loading control. (n=2) (b-c) qRT-PCR analysis of ATF4 and CHOP 72h after transfection with siRNA directed against Topoisomerase 1, results are presented as mean of ΔΔCT ± SD (n=3). Significance level was not reached. Pictures are each representative for two independant experiments.

4.1.3 Topoisomerase 2α – Silencing and analysis of ER-stress

4.1.3.1 Topoisomerase 2α – Silencing

After 72h of transfection with siRNA against Topo2α sqRT-PCR revealed a slight decrease of Topo2α expression (Fig.14a). Analysis of qRT-PCR (-5,48 ± 0,06) and western blot corroborates the Topo2α-knockdown by showing a considerable downregulation of Topo2α (Fig.14 b+c). On protein level (Fig. 14c), there was no Topo2α visible anymore. In densitometric analysis only 0.88% of Topo2α were left after silencing with siRNA (Fig. 14d).

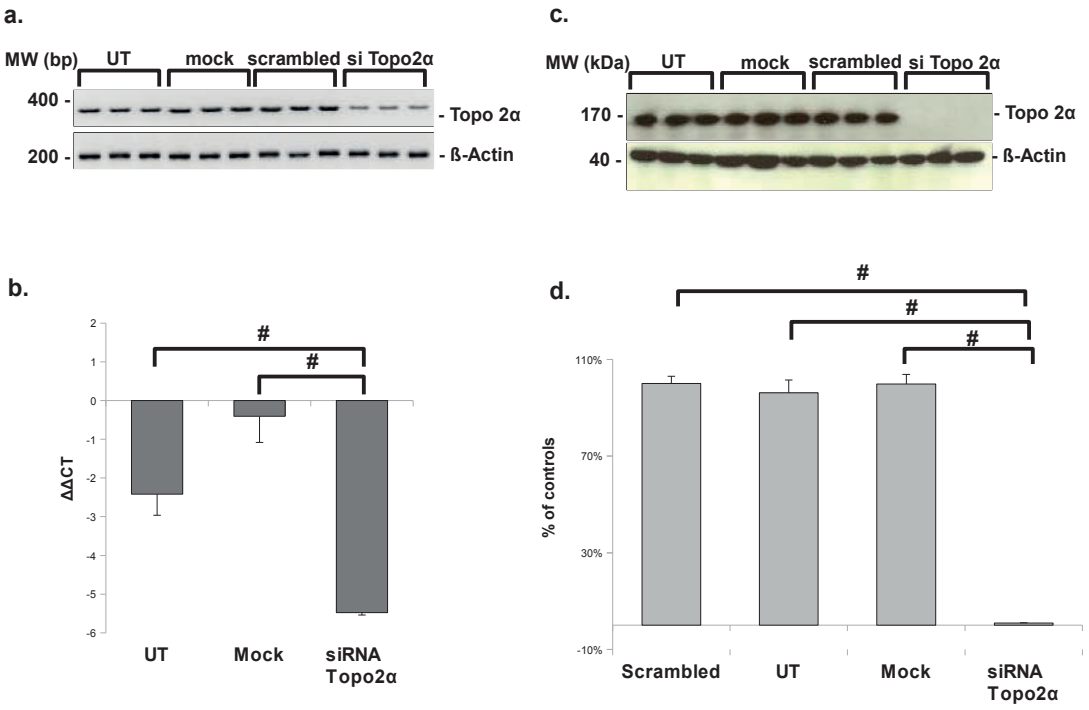

Figure 14: Topoisomerase 2α – Silencing

A549 cells were transfected with siRNA directed against Topo2α, knockdown of Topo2α was checked by RT-PCR and IB 72h after transfection. Mock (transfection with transfection reagent without any siRNA) and scrambled (non targeting siRNA) served negative controls: (a) sqRT-PCR analysis for the expression of Topo2α, 30 cycles were performed, β-Actin served as loading control. (n=3) (b) qRT-PCR analysis for the expression of Topo2α, results are presented as mean of ΔΔCT ± SD (n=3; #p<0.05; * indicates significance between siRNA Topo2α and scrambled). (c) IB analysis for the expression of Topo2α, β-Actin served as loading control. n=3 (d) Densitometry was performed from IB analysis. The target protein/ß-Actin ratio was calculated (scrambled=100%) (n=3; # p<0.05). Pictures are each representative for three independent experiments.

After 48h of transfection with siRNA against Topo2α a very modest decrease of Topo2α expression could be revealed after performing sqRT-PCR (Fig. 23b of appendix).

4.1.3.2 Analysis of ER-stress after Topoisomerase 2α knockdown

After successfully silencing the Topo2α, a possible existence of an ER-stress response was investigated. For this purpose ATF4, CHOP and XBP-1 were analysed. As illustrated in Figure 15 sqRT-PCR analysis did not reveal any ER-stress response 72h after knockdown of Topo2α (Fig.15 a). Quantification of ATF4 and CHOP via qRT-PCR suggests a slight, but not significant ER-stress response after Topo2α-knockdown (Fig. 15 b-c).

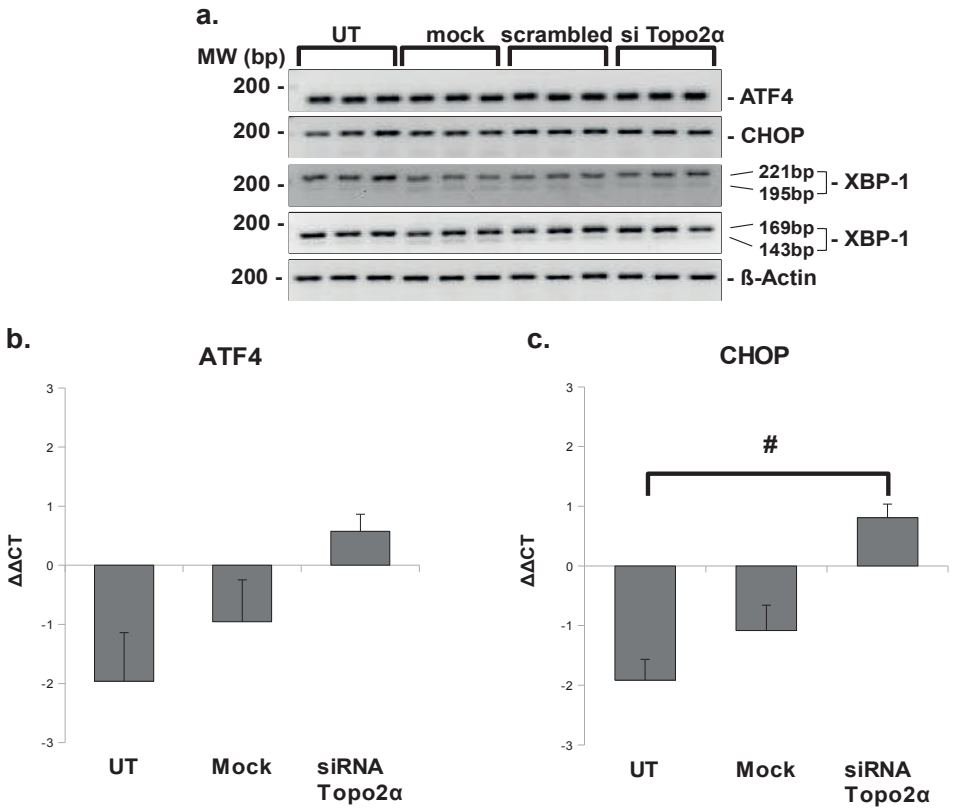

Figure 15: No ER-stress after Topoisomerase 2α knockdown

(a) sqRT-PCR analysis of ATF4, CHOP, XBP-1 (221/169bp: unspliced = inactive, 195/143bp: spliced = active) 72h after transfection with siRNA directed against Topoisomerase 2α, 30 cycles were performed, β-Actin served as loading control. (n=2) (b-c) qRT-PCR analysis of ATF4 and CHOP 72h after transfection with siRNA directed against Topoisomerase 2α, results are presented as mean of ΔΔCT ± SD (#p<0.05). Values were considered not significant where no symbols are indicated. Pictures are each representative for two independent experiments.

4.1.4 Topoisomerase 2β – Silencing and analysis of ER-stress

4.1.4.1 Topoisomerase 2β – Silencing

Transfection with siRNA against Topo2β was performed for 72h followed by analysis of Topo2β expression on mRNA and protein level. SqRT-PCR and qRT-PCR (-6,05 ± 0,46) as well as western blot analysis showed a clear downregulation of Topo2β and thus confirmed successfully silencing of Topo2β (Fig.16a-c). In densitometric analysis magnitude of remaining protein was measured approximately 22.5%, given as a percentage of the respective scrambled controls (Fig. 16d).

A549 cells were transfected with siRNA directed against Topo2β, knockdown of Topo2β was checked by RT-PCR and IB 72h after transfection. Mock (transfection with transfection reagent without any siRNA) and scrambled (non targeting siRNA) served as negative controls. (a) sqRT-PCR analysis for the expression of Topo2β, 30 cycles were performed, β-

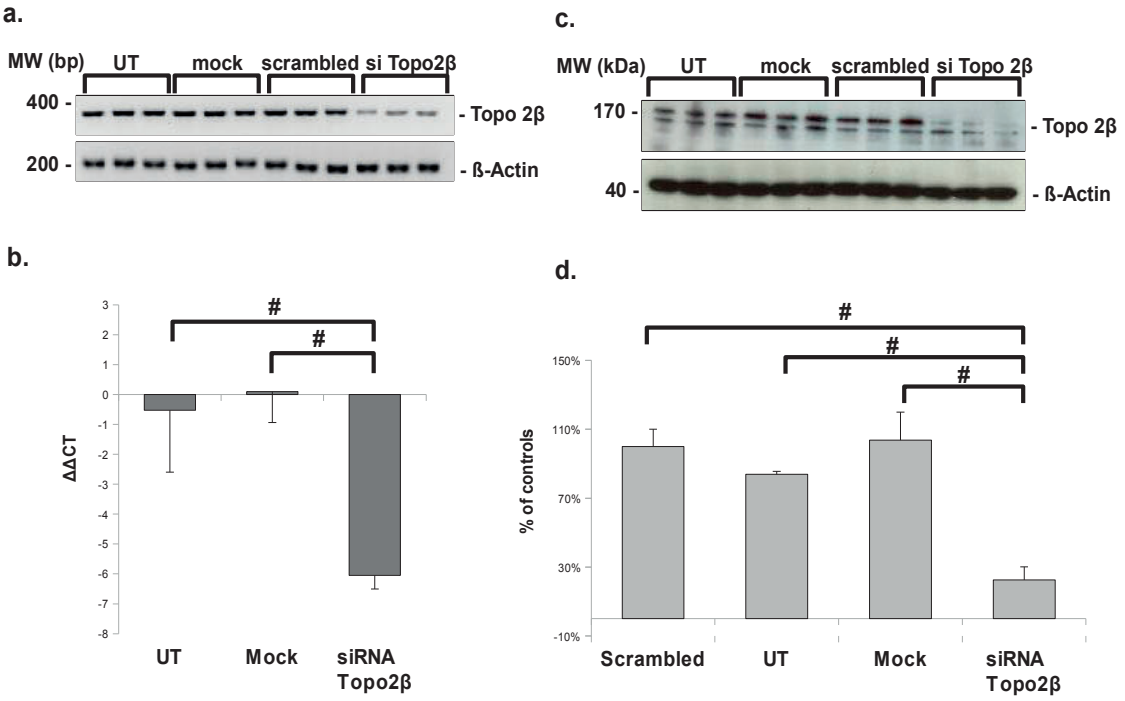

Figure 16: Topoisomerase 2β – Silencing

Actin served as loading control. (n=3) (b) qRT-PCR analysis for the expression of Topo2β, results are presented as mean of ΔΔCT ± SD (n=3; #p<0.05). (c) IB analysis for the expression of Topo2β, β-Actin served as loading control. (n=3) (d) Densitometry was performed from IB analysis. The target protein/ß-Actin ratio was calculated (scrambled=100%) (n=3; # p<0.05). Pictures are each representative for three independent experiments.

Figure 23c of appendix shows a downreglation of Topo2β in sqRT-PCR after transfection with siRNA directed against Topo2β already after 48h of transfection.

4.1.4.2 Analysis of ER-stress after Topoisomerase 2β knockdown

Despite a successful knockdown of Topo2β no increase in ER-stress markers ATF4, CHOP or sXBP-1 could be observed in sqRT-PCR and RT-PCR analysis 72h after transfection (Fig.17 a-c).

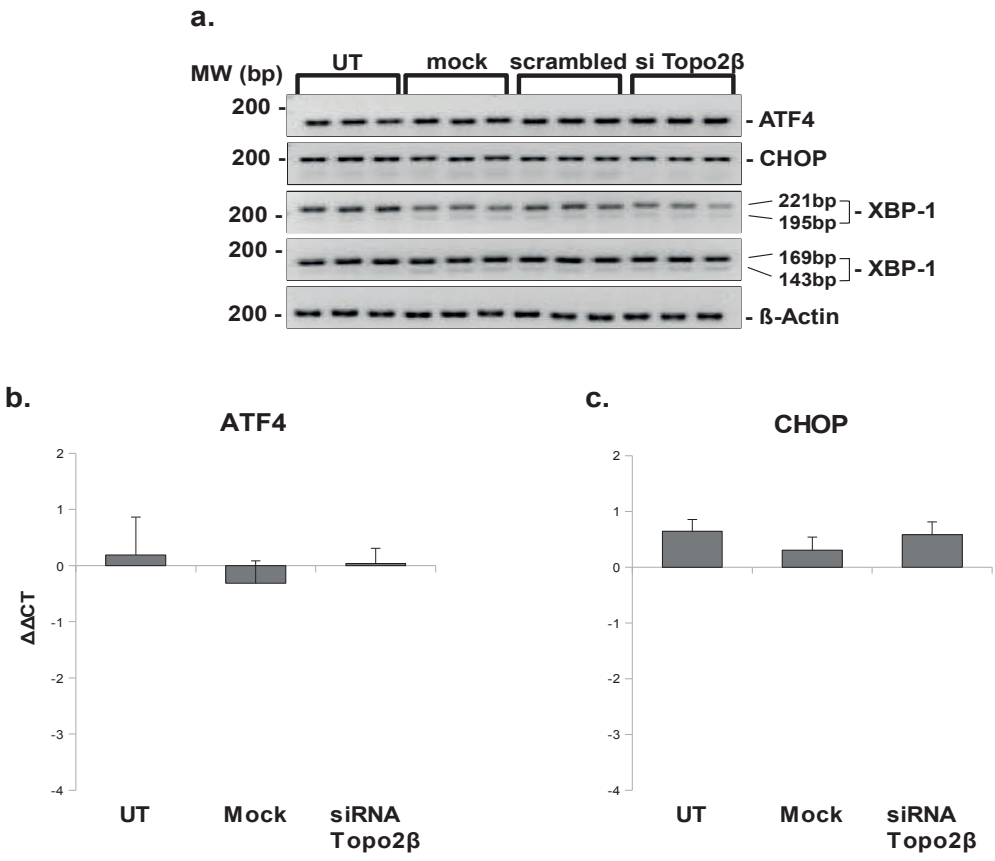

Figure 17: No ER-stress after Topoisomerase 2β knockdown

(a) sqRT-PCR analysis of ATF4, CHOP and XBP-1 (221/169bp: unspliced = inactive, 195/143bp: spliced = active) 72h after transfection with siRNA directed against Topoisomerase 2β, 30 cycles were performed, β-Actin served as loading control. (n=2) (b-c) qRT-PCR analysis of ATF4 and CHOP 72h after transfection with siRNA directed against Topoisomerase 2β, results are presented as mean of ΔΔCT ± SD (n=3). Significance level was not reached. Pictures are each representative for two independent experiments.

4.2 Protein Inhibition with topotecan and etoposide in A549 cells

Although silencing of HisRS, Topo1, Topo2α and Topo2β worked out very well, no ER-stress could be detected after knockdown of the named target genes. To investigate whether direct inhibition of respective proteins provokes any ER-stress or apoptosis, treatment of A549 cells with topotecan and etoposide was analysed. Additionally a treatment of A549 cells with a 1μM solution of Thapsigargin was performed in order to get a positive control for apoptosis and ER-stress. As mentioned in 3.2.3, topotecan inhibits the activity of Topo1, while function of Topo2α and Topo2β can be inhibitied by the protein inhibitor etoposide.

4.2.1 Analysis of ER-stress and apoptosis after topotecan treatment in A549 cells

A549 cells were treated with different concentrations of topotecan, from 50μM up to 300μM, and incubated for 24h and 48h in each case. Surprisingly immunoblot analysis of Topo1 showed a clear decrease in Topo1 protein expression on protein level for all concentrations and timepoints (Fig. 18). Interestingly, after 48h of incubation, also a downregulation of Topo2α and Topo2β could be detected. To analyze apoptosis, the terminal cleaved caspase form of caspase 3 was studied. In the apoptotic cell caspase 3 is activated to its cleaved forms (17kDa and 12kDa) [110]. Already after 24h of incubation, a slight increase in cleaved caspase 3 could be observed for all concentrations. After 48h of incubation an impressive upregulation of cleaved caspase 3 was detected. Surprisingly, ATF4 expression, which marks ER-stress, seemed to be decreased after 48h of incubation, whereas the ER-stress marker CHOP showed a slight upregulation after 24h of incubation for all concentrations and after 48h for the higher concentrations (100-300μM) of topotecan (Fig. 18).

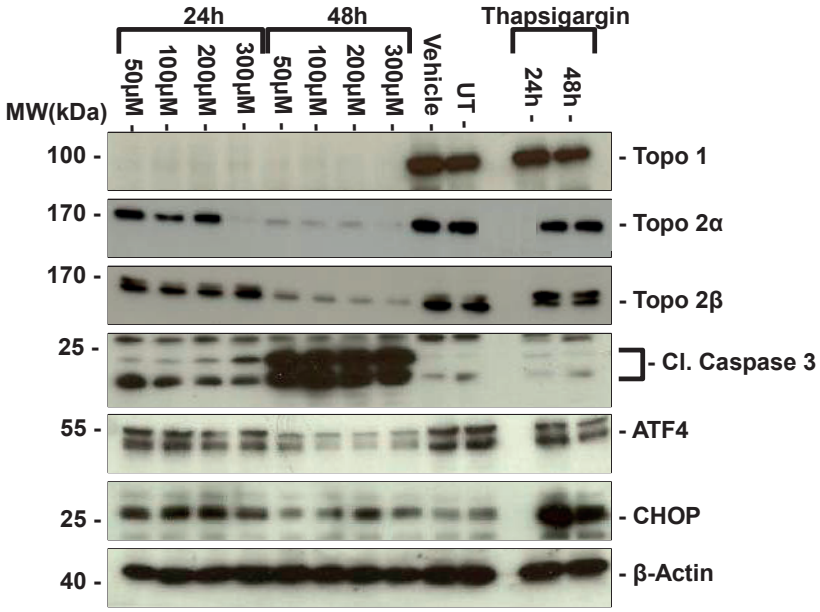

Figure 18: Inhibition of Topoisomerase 1 and induction of apoptosis and ER-stress after topotecan treatment in A549 cells

IB analysis of Topo 1, Topo 2α, Topo 2β, Cleaved Caspase 3, ATF4 and CHOP 24h and 48h after treatment with different concentrations (50µM - 300µM) of topotecan, Vehicle served as negative control, Thapsigargin served as positive control for apoptosis and ER-stress, β-Actin served as loading control. Picture is representative for two independent experiments. (n=2)

To analyze effects of protein inhibition on mRNA level, sqRT-PCR and qRT-PCR were performed after treatment of A549 cells with topotecan. As Figure 24 in Appendix shows, inhibition of Topo 1 could allready be detected in IB analysis after 8h of treatment and at a concentration of 2µM of topotecan. Therefore, concentration and incubation time were adapted respectively and inhibition studies were performed with 2µM and 5µM of topotecan for 4h, 8h, 16h and 24h. In contrast to IB analysis (Fig. 24 of appendix), inhibition of Topo1 could neither be visualized in sqRT-PCR (Fig. 19a) nor in qRT-PCR (Fig. 19b). As Topo2α seemed to be inhibited by topotecan on protein level (shown in Figure 18), expression of Topo2α was also studied on mRNA level via qRT-PCR, but no significant downregulation of Topo2α could be quantified. With respect to ER-stress, no increase of ATF4 expression could be visualized in sqRT-PCR (Figure 19a) and only a slight upregulation of ATF4 in qRT-PCR was detectable (Fig. 19d). However, increasing expression of CHOP, the known marker for ER-stress induced apoptosis, could be shown impressively by sqRT-PCR (Fig. 19a) and qRT-PCR (Fig. 19e). We were able to observe that longer incubation times went along with ascending expression of CHOP for both concentrations of topotecan (2µM and 5µM). After 4h of

topotecan treatment only a slight increase of CHOP could be observed (2µM 4h: 0,21± 0,02; 5µM 4h: 1,21± 0,33) and after 24h highest level of CHOP expression was detected (2µM 24h: 3,69 ± 0,26; 5µM 24h: 3,83 ± 0,3), which were significantly altered as compared to untreated A549 cells (UT: 0,38 ± 0,27) (Figure 19e).

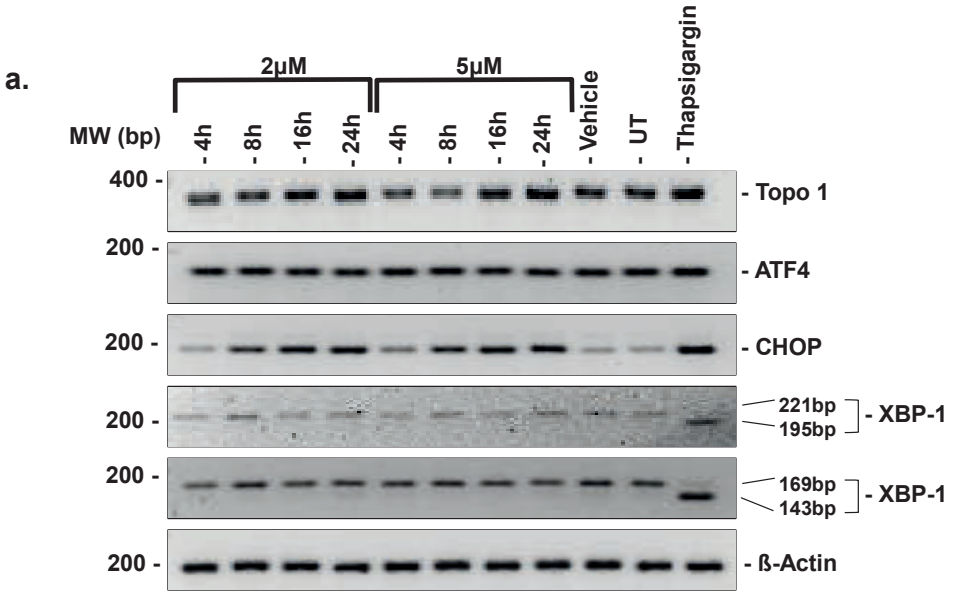

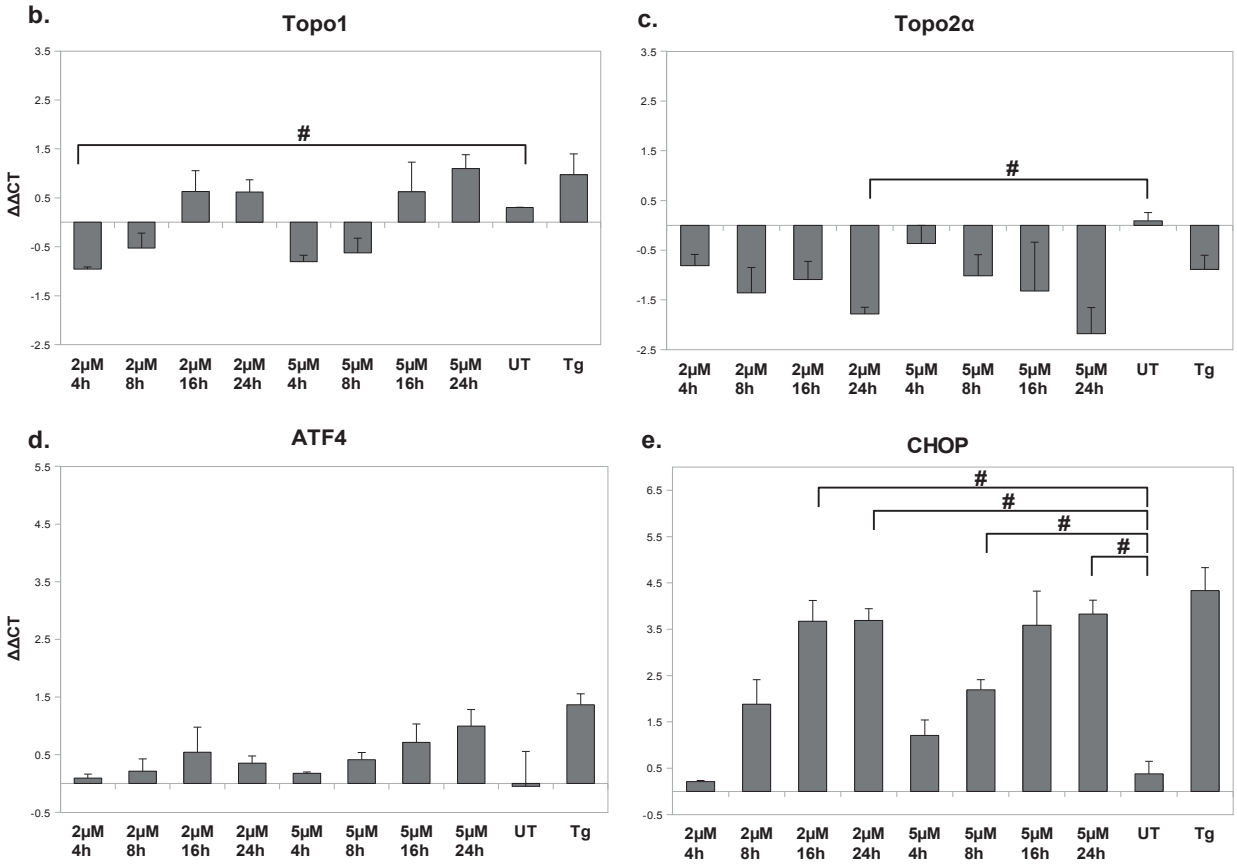

Figure 19: Induction of CHOP after topotecan treatment in A549 cells

(a) sqRT-PCR analysis of Topo1, ATF4, CHOP and XBP-1 (221/169bp: unspliced = inactive, 195/143bp: spliced = active) after treatment with 2µM and 5µM of topotecan and different timepoints (4 - 24h), Vehicle served as negative control, Thapsigargin served as positive control for Apoptosis and ER-stress, β-Actin served as loading control, 25 cycles were performed n=2) (b-e) qRT-PCR analysis of Topo1, Topo2α, ATF4 and CHOP after treatment with 2µM and 5µM of topotecan and different timepoints (4 – 24h), Thapsigargin served as positive control for apoptosis and ER-stress, results are presented as mean of ΔΔCT ± SD (n=3; #p<0.05). Values were considered not significant where no symbols are indicated. Pictures are representative for two independent experiments.

4.2.2 Analysis of ER-stress and apoptosis after etoposide treatment in A549 cells

A549 cells were treated with different concentrations of etoposide, from 50μM up to 300μM, and incubated for 24h and 48h in each case. Immunoblot analysis of Topo2α showed a decrease of Topo2α expression for 200μM and 300μM of etoposide after 24h treatment and an even more downregulation of Topo2α for all concentrations after 48h of incubation. Regarding Topo2β, only a slight decrease in protein level was detected following etoposide treatment. Expression of Topo1 remained unchanged after etoposide treatment (Fig.20a). To study apoptosis, expression of cleaved caspase 3 was studied. Increase of cl. caspase 3 was revealed at 24h and 48h where 100μM and 200μM of etoposide was used (Fig.20a). Again ATF4 expression, which marks ER-stress, seemed to be decreased after 48h of incubation, whereas the ER-stress marker CHOP showed a slight upregulation after 24h of incubation for all concentrations. Immunoblot analysis for 200μM and 300μM of etoposide and shorter incubation times from 4h to 24h, as shown in Figure 20b, revealed decreasing expression of Topo2α and Topo2β with longer exposure to etoposide, although Topo2α was inhibited more clearly than Topo2β. In the course of analyzing ER-stress, no difference in ATF4 expression could be shown, whereas the apoptotic marker CHOP seemed to be increased slightly after 16h and 24h for both concentrations (Fig.20b).

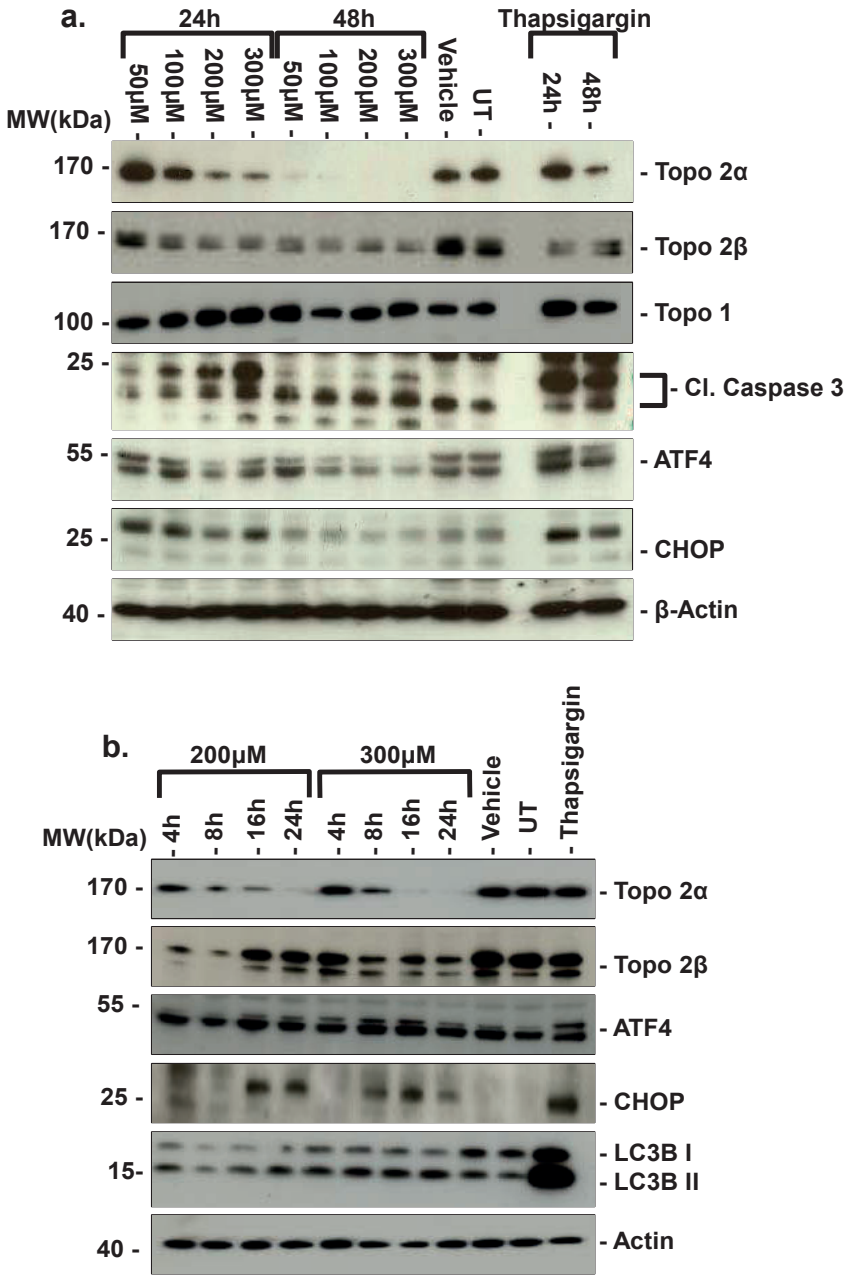

Figure 20: Inhibition of Topoisomerase 2 and induction of apoptosis and ER-stress after etoposide treatment in A549 cells.

(a) IB analysis of Topo2α, Topo2β, Topo1, Cleaved Caspase 3, ATF4 and CHOP 24h and 48h after treatment with different concentrations (50µM-300µM) of etoposide, Vehicle served as negative control, Thapsigargin served as positive control for apoptosis and ER-stress, β-Actin served as loading control. n=2) (b) IB analysis of Topo2α, Topo2β, ATF4, CHOP and LC3 after treatment with 200µM and 300µM of topotecan with different timepoints (4-24h), Thapsigargin served as positive control for apoptosis and ER-stress, β-Actin served as loading control. (n=2). Pictures are each representative for two independent experiments.

In order to analyze the effects of etoposide treatment on mRNA level, qRT-PCR and sqRT-PCR were performed and expression of topoisomerases as well as ER-stress and apoptotic markers were studied. In sqRT-PCR a decrease of Topo2α after 16h and 24h of incubation could be shown, expression of Topo2β seemed to remain unchanged (Fig. 21a). Longer treatment periods with etoposide revealed increased expression of CHOP, whereas no difference in ATF4 expression could be visualized (Fig.21a). Increase in another ER-stress marker XBP-1 was also not observed after etoposide treatment (Fig.21a). As shown in Figure 21b, qRT-PCR and sqRT-PCR revealed a significant decrease in Topo2α after treatment with 300µM etoposide for 24h compared to untreated A549 cells (300µM 24h: -3,9 ± 0,56, UT: -0,59 ± 0,7). For Topo2β and Topo1 no clear decrease after etoposide treatment could be shown. Analysis of ATF4 and CHOP via qRT-PCR again showed no difference in ATF4 expression, confirming the observation of sqRT-PCR (Fig.21e). However longer incubation of cells with etoposide went along with ascending increase of CHOP expression (Fig.21f). Significant upregulation of CHOP compared to UT cells could be quantified for 300µM of etoposide for 16h (300µM 16h: 2,07 ± 0,17, UT: 0,17 ± 0,06) (Fig.21f).

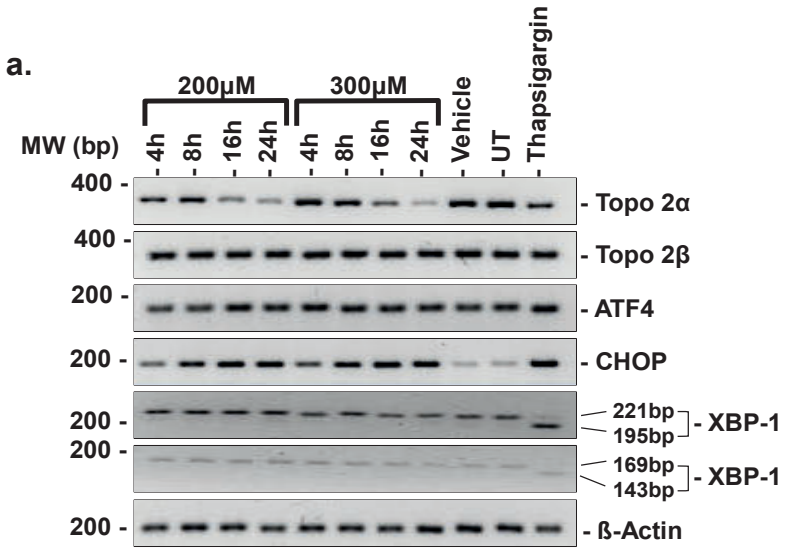

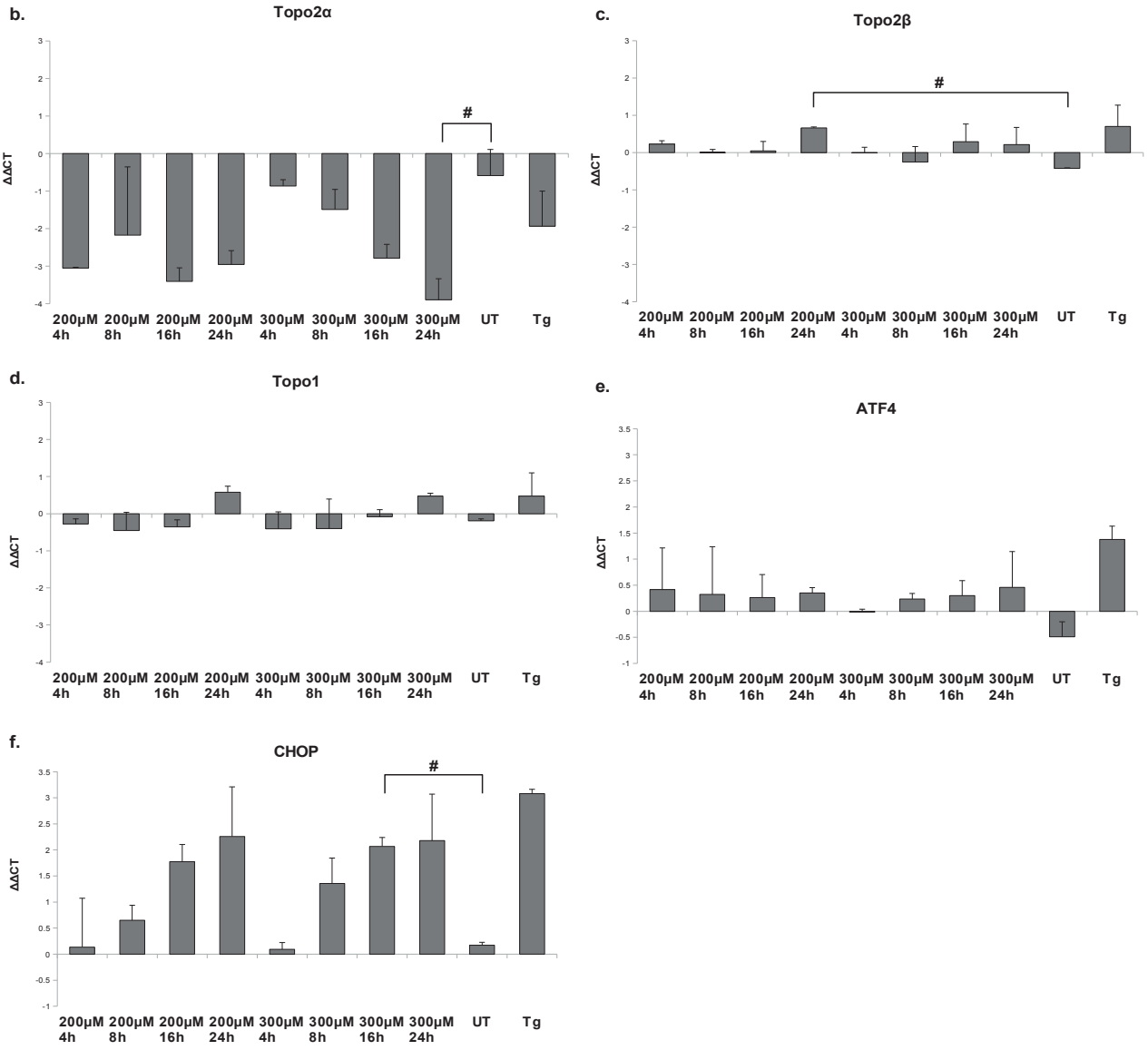

Figure 21: Induction of CHOP after etoposide treatment in A549 cells

(a) sqRT-PCR analysis of Topo2α, Topo2β, ATF4, CHOP and XBP-1 (221/169bp: unspliced = inactive, 195/143bp: spliced = active) after treatment with 200µM and 300µM of etoposide and different timepoints (4 - 24h), 25 cycles were performed, Vehicle served as negative control, Thapsigargin served as positive control for apoptosis and ER-stress, β-Actin served as loading control. (n=2) (b-f) qRT-PCR analysis of Topo2α, Topo2β, Topo1, ATF4 and CHOP after treatment with 200µM and 300µM of etoposide and different timepoints (4 – 24h), Thapsigargin served as positive control for apoptosis and ER-stress, results are presented as mean of ΔΔCT ± SD (n=3; #p<0.05). Values were considered not significant where no symbols are indicated. Pictures are representative for two independent experiments.

4.3 Analysis of ER-stress in a patient with SSc associated ILD

To analyze ER-Stress and apoptosis in CVD-ILD, immunohistochemistry was performed on lung sections of a patient with SSc associated ILD and compared to healthy donor lung sections. Diagnosis of SSc associated ILD was settled by skin biopsy, barium swallow examination, lung function test, HRCT and lung biopsy. Radiologically and histopathologically an UIP pattern was detected. To identify ER-stress and apoptosis in AECIIs, immunohistochemistry was realized for p50 ATF6, ATF4, pro SP-C and CHOP on serial sections. SP-C is a protein exclusively synthesized by AECII and hence was used as a marker for AECII.

To confirm the specifity of primary antibody binding that is not a result of non-specific Fc receptor binding or other cellular protein interactions isotype controls with a non-immune immunoglobulin of the same isotype and concentration as the primary antibody were performed (Fig. 25 of appendix).

Analysis by immunohistochemistry revealed that pro SP-C positive cells stained positive also for p50 ATF6, ATF4 and CHOP and thus revealed a serious induction of ER stress markers within AECII of patient with SSc-ILD, compared to healthy donor lung sections (Fig. 22 a-d).

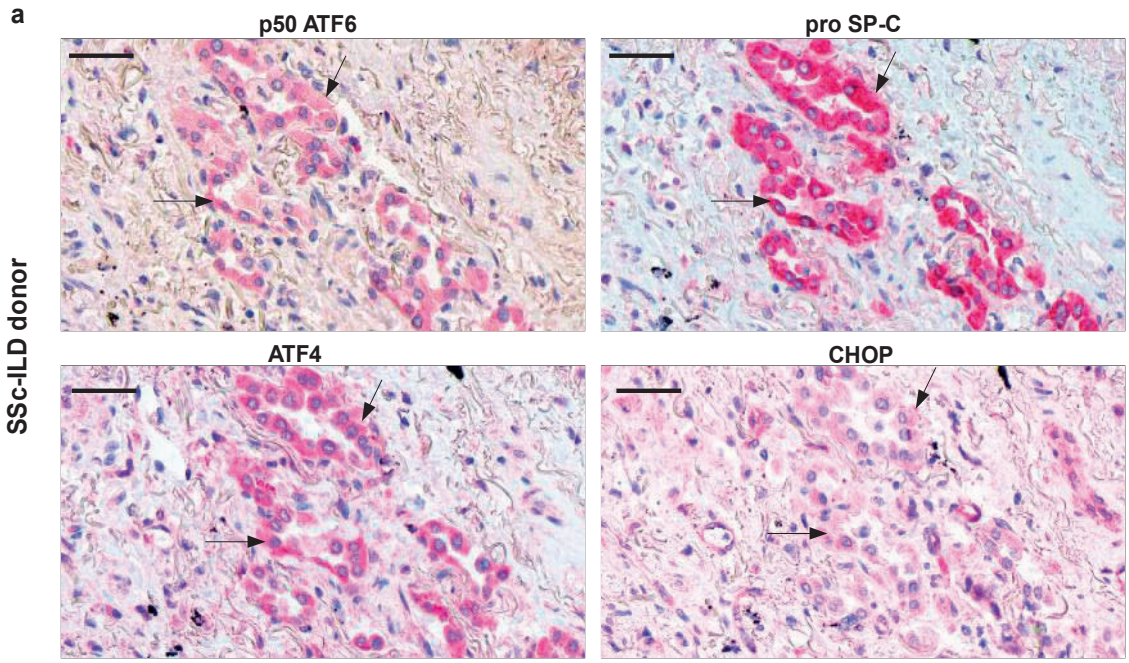

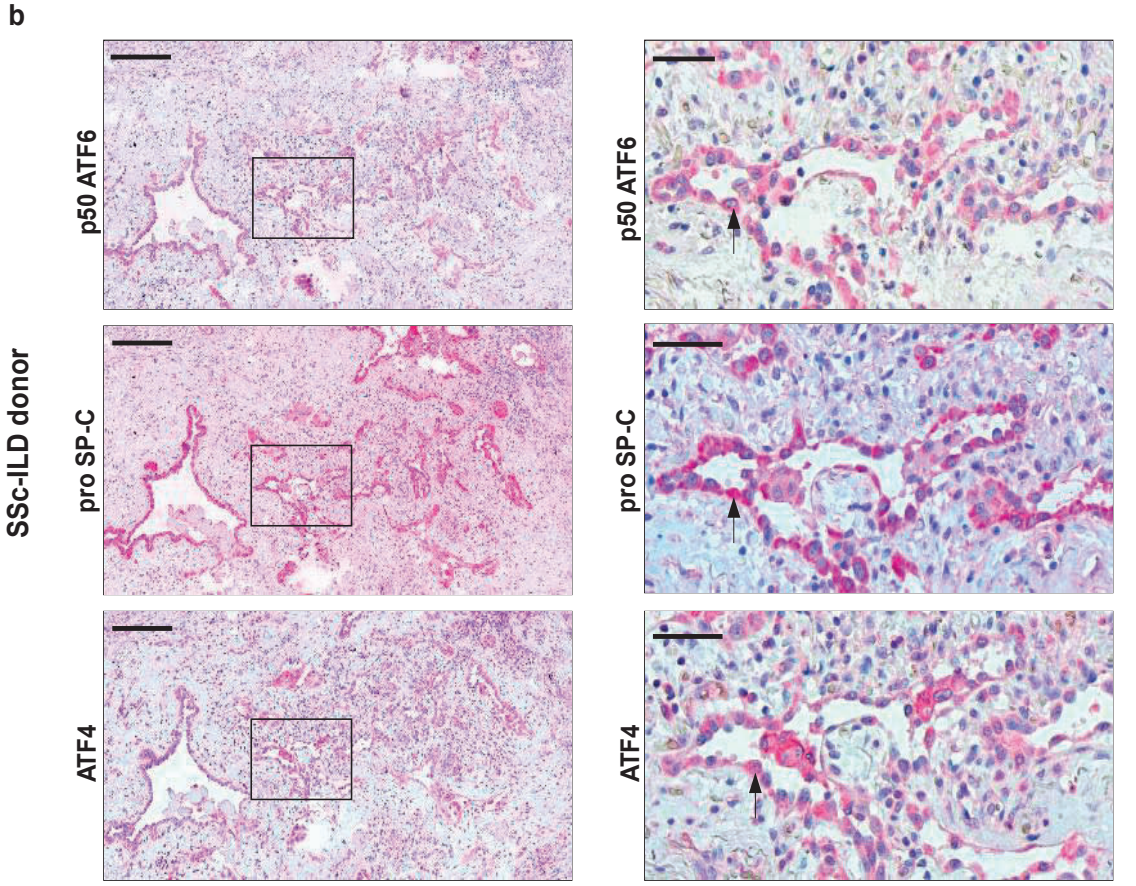
b
SSc-ILD donor
p50 ATF6
pro SP-C
ATF4
p50 ATF6
pro SP-C
ATF4

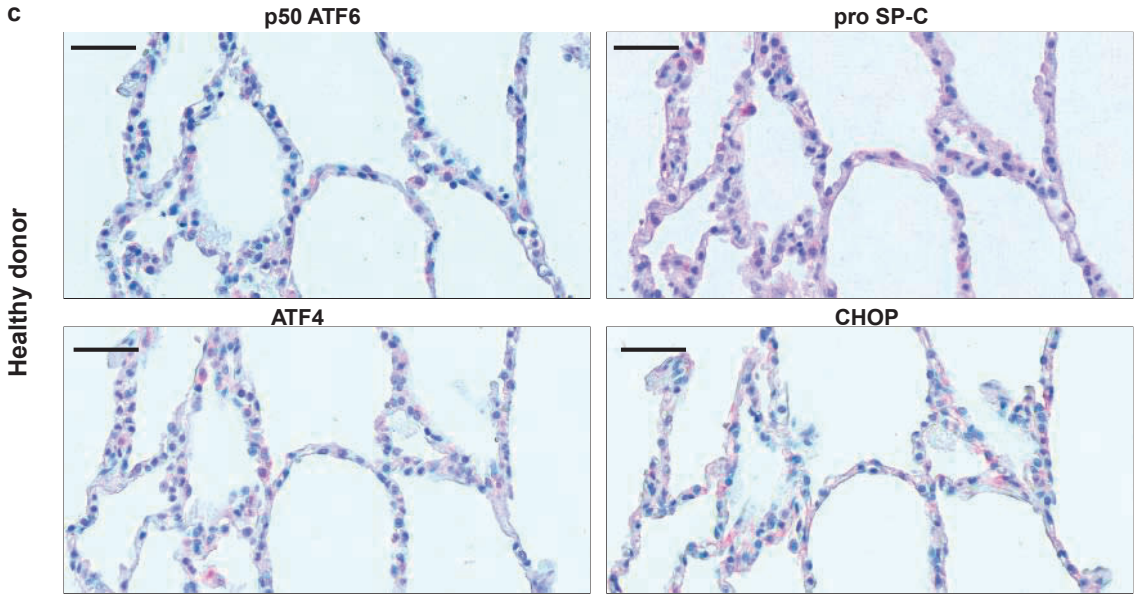
c
Healthy donor
p50 ATF6
pro SP-C
ATF4
CHOP

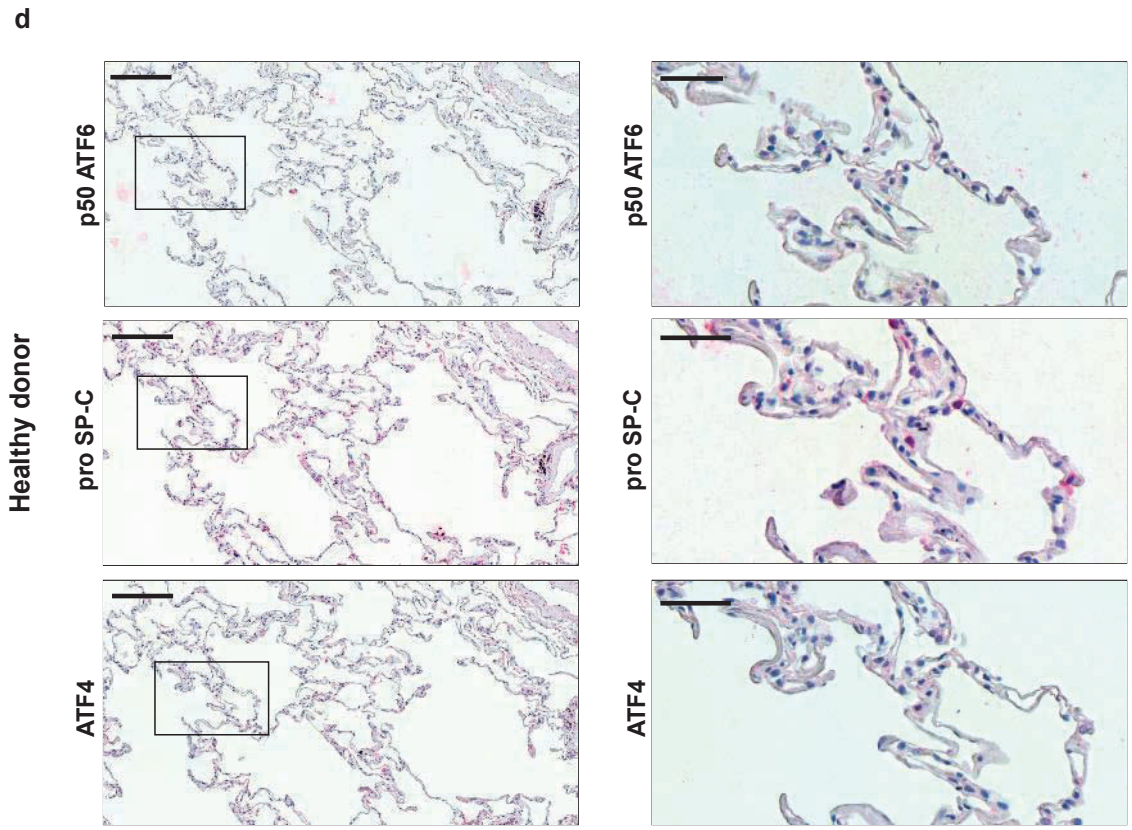

Figure 22: AECII specific induction of ER stress in patient with Ssc-ILD

Immunhistochemistry performed on serial paraffin-embedded lung tissue sections from human patient with SSc-ILD (a, b) and healthy donors (c,d) stained for p50 ATF6, pro SP-C, ATF4 and CHOP. Arrows indicate the same AECII stained for all four proteins. (a,c) Original magnification: 400x, scalebar, 50µm. (b,d) left: Original magnification: 100x, scalebar, 200µm; right: Original magnification: 400x, scalebar, 50µm.

5. Discussion

5.1 ILD associated with collagen vascular diseases

ILDs refer to a group of chronic lung diseases that mainly affect the epithelial, interstitial and vascular compartment of the lung. ILDs are characterized by fibroblast proliferation, collagen deposition and architectural remodeling [22]. While mechanisms that result in lung fibrosis are still not fully understood, there is a strong suggestion that ER-stress induced apoptosis caused by alveolar epithelial cell injury is the triggering event in pathogenesis of some forms of ILD, especially the idiopathic IIPs IPF and NSIP [3,19,22]. ILD is a common pulmonary complication of CVDs, which represent a group of immunologically mediated inflammatory disorders. Especially in patients with SSc and DM/PM the developement of ILD represents a significant cause of morbidity and mortality [14,15,77,93, 111]. The incidence of ILD in CVD varies between 20-54% [79,112]. In view of frequent pulmonary involvement the present study was focussed on PM/DM and SSc associated ILD.

To define diagnosis of ILD, an integrated clinical, radiological and pathological approach is necessary [3]. The most important items to determine entitiy and clinical significance of ILD are lung function, HRCT and lung biopsy [13].

Autoantibodies to aminoacyl tRNA synthetase (mostly anti-HisRS) are the strongest predictive factor for ILD in PM/DM [71]. Autoantibodies to a glycoprotein KL-6 is also considered as another risk factor for ILD in PM/DM [113]. Similarly, autoantibodies to Topo1, Topo2α and Topo2β are strongly predictive for the development of ILD in SSc [7,82]. In the present study, we wished to explore the possibilitiy of an autoantibody induced blockade of HisRS, Topo1, Topo2α or β in alveolar epithelial cells, possibly resulting in chronic AECII injury and apoptosis.

We supposed that the binding of pathogenetic antibody directed against HisRS and topoisomerases results in a loss of function of the respective proteins.
Anti-HisRS is described as an antibody directed against the cytoplasmic protein HisRS. Autoantibody against topoisomerases are anti-nuclear-antibodies. They bind to contents of the cell nucleus, and thus seem to inhibit the activity of the respective enzymes [114].
In Sjögren´s syndrome, an autoimmune rheumatic disease that targets salivary and

lacrimal glands, it was found that autoantibodies mediate apoptosis in the human salivary gland cells in a caspase-3 dependent manner [115]. Furthermore it was shown, that autoantibodies to dsDNA and ribosomal P proteins, which are often found in SLE, are potent inhibitors of protein synthesis and are likely to mediate cellular dysfunction via this pathway [116]. However, blockade of HisRS and Topo 1, 2α or β by antibody-binding has not been shown yet. Other mechanisms, how these autoantibodies may contribute to development of ILD in CVD, have to be taken into consideration. To this end, immune complexes might perpetuate a positive feedback loop amplifying inflammatory responses [117]. IgG-mediated activation of complement is an important defense mechanism of the innate immune system to protect against infections. However, the same mechanisms can drive severe and harmful inflammation, when IgG antibodies react with self-antigens in solution or tissues, as described for several autoimmune diseases. More specifically, IgG immune complexes can activate all three pathways of the complement system, resulting in activation a panel of different complement receptors on innate and adaptive immune cells. Importantly, complement is often co-expressed on inflammatory immune cells such as neutrophils, monocytes, macrophages or dendritic cells and act in concert to mediate the inflammatory response in autoimmune diseases [118].

It is currently unclear, how the presence of autoantibodies contributes to the development of CVD-ILD, but like in other forms of ILDs like IPF, which is the most common form of idiopathic ILD, chronic injury of the alveolar epithelium is currently discussed as a possible event [21,45]. In full agreement, it was reported that patients with SSc associated ILD demonstrated breach of the epithelial barrier [119]. The increase in KL-6, a glycoprotein that is exclusively found on the surface of alveolar epithelial cells in serum and bronchoalveolar lavage (BAL) of patients with different forms of CVD-ILD is also indicative of severe epithelial injury. On the same line, it was suggested that the alveolar epithelial cell-endothelial cell compartment is the site of the initial injurious process in SSc associated ILD [86].

Due to the scarce patient material and the need for *in vitro* studies to identify and understand the molecular mechanisms underlying different ILD associated CVD, we focused our study primarily on HisRS, Topo1, Topo2α and Topo2β, being the autoantibody targets in DM/PM and in SSc, asking for the possibility that loss of

function of these proteins could cause alveolar epithelial stress similar to IPF.

5.2 ER-stress and apoptosis of AECII in CVD-ILD

As Günther et al. [47] reported, chronic injury of AECIIs is increasingly accepted as an elementary event in pathogenesis of IPF. In 1988 Myers and Katzenstein [24] already emphasized the role of epithelial necrosis and alveolar collapse in pathogenesis of UIP. However the hypothesis that development of IPF was due to an inflammatory process [40] prevailed until 2006, when Selman and Pardo [120] reintroduced the topic of epithelial cell injury in IPF. Now it is assumed that injury to epithelial alveolar cells, in particular AECII, underlies abnormal epithelial repair in IPF [46]. On this line, Korfei et al. [42] recently showed that AECII undergo ER-stress and apoptosis in sporadic IPF.

The ER plays a central role in folding and secretion of newly synthesized proteins [57]. Accumulation of unfolded proteins in the ER caused by impairment of protein folding and processing, activates the UPR with the primary purpose of aiding the cell to improve the protein folding and to attain homeostasis again [55,59]. UPR involves activation of IRE1α, PERK and ATF6 [60]. PERK phosphorylates eIF2α which reduces the protein load on the ER. IREα induces splicing of XBP1 in order to produce the homeostatic transcription factor XBP1s [61]. ATF6 and XBP1s increase transcription of genes which enhance ER size and function [62]. By phosphorylation of eIF2α the translation of ATF4 is stimulated, which again leads to transcription of different pro-survival genes [63]. This ER-stress reaction generally helps the cell to survive. However, if the stress condition is overwhelming or prolonged, the cell will be driven to apoptosis [60,64].

The initial focus of this study was to downregulate expression of HisRS, Topo1, Topo2α and Topo2β and to analyze the subsequent effects on A549 cells like ER-stress and apoptosis. In spite of quite successful silencing of the respective genes, no induction of ER-stress could be detected in A549 cells. Such observation deserves further discussion: Firstly, it has to be noted that the still remaining protein after respective gene knockdown might be sufficient to perform its functions in the cell. Densitometric analysis revealed a considerable magnitude of remaining protein after silencing of HisRS, Topo1 and Topo2ß. In case of Topo2α, only a very small amount of remaining

protein could be measured densitometrically (0.88%). Nevertheless, only a slight and non-significant ER-stress response could be revealed after knockdown of Topo2α. Secondly, even in case of a complete loss of the target protein, it may take some additional more time until cellular stress evolves. Thirdly, it should be taken into account that the autoantibodies in CVD-ILD may only provoke a moderate level of cellular stress and secondary hits such as infection and smoking may be needed for apoptosis and development of lung fibrosis. Kropski et al. [121] recently emphasized the role of herpesvirus infection as a second hit in IPF and reported that herpesvirus infection induces or worsens lung fibrosis when combined with immunodeficiency or other injurious stimuli. They consider induction or modulation of ER stress responses as one potential mechanism through which herpesvirus infection may contribute to the pathogenesis of IPF.

We then directed our experiments towards pharmacological inhibition of the proteins of interest. A549 cells were treated with etoposide and topotecan in order to inhibit function of Topo1 and Topo2. Etoposide is a semisynthetic derivative of podophyllotoxin that exhibits antitumor activity. It impairs DNA synthesis and prevents re-ligation of DNA strands by forming a complex with Topo2 and DNA. Thus, repair of DNA by Topo2 is inhibited and apoptosis of cancer cells can be promoted [101]. Topotecan is an antineoplastic agent used to treat ovarian cancer. It works by inhibiting function of Topo1. Topotecan binds to the Topo1-DNA-complex and thus prevents religation of the single strand breaks [102–104]. Due to the lack of appropriate pharmacological inhibitors, inhibition of HisRS could not be realized.

Treatment of A549 cells with topotecan lead to a decrease in Topo1 expression on protein level, whereas RNA levels of Topo1 seemed to be unaffected by such approach. Interestingly, after 48h of incubation, also a downregulation of the proteins Topo2α and Topo2β could be detected. Up to now topotecan was only known as an inhibitor of Topo1. Impressive upregulation of cleaved Caspase 3 and CHOP in A549 after treatment with topotecan strongly suggested an apoptotic response. Caspases are crucial mediators of programmed cell death. Among them, caspase-3 is a commonly activated death protease, catalyzing the specific cleavage of many key cellular proteins [110]. Especially the observed upregulation of CHOP on RNA level lead to the assumption, that topotecan provokes an ER-stress mediated apoptotic response in A549 cells. Recent studies revealed that CHOP is one of highest inducible genes during ER stress [122,123]. Also, inhibition of Topo2α and Topo2β following treatment of A549 cells with etoposide showed significant increase of CHOP on RNA

level and thus again provided indication of ER-stress induced apoptosis. Surprisingly, after treatment of A549 cells with etoposide, downregulation in Topo2α was also noticed on RNA level. Effects of etoposide on Topo2 mRNA are not described yet and require further studies.

Significant induction of CHOP after treatment with topotecan and etoposide indicated that ER-stress and apoptosis are triggered after inhibition of topoisomerases. Su and Kilberg [65] identified CHOP as an interacting partner of ATF4. Previously Bruhat et al. [124] showed that expression of CHOP is rapidly induced through ATF4-dependent transcription. Surprisingly, our experiments showed that CHOP is induced despite unaffected expression of ATF4. Upregulation of CHOP next to seemingly unchanged ATF4 expression may arise from an inhibitory effect of CHOP on ATF4 function, as already discussed by Su and Kilberg [65]. Another possible reason for exclusive induction of CHOP could be the existence of other pathways playing a role in activation of CHOP. Gotah et al. [125] as well as Paschen et al. [64] mentioned ATF6 to be another activator of CHOP. Bruhat et al. [124] demonstrated that at least two pathways, one leading to ATF4 induction, and one leading to ATF2 phosphorylation, are necessary to induce CHOP expression. To gain certainty concerning the mechanism of CHOP activation after treatment of A549 cells with topotecan and etoposide, other mechanisms like induction of ATF4, ATF6 and ATF2 have to be investigated intensively in future experiments.

To examine whether AECIIs are actually the cells of interest in developement of CVD associated lung fibrosis, lung sections of patient with SSc associated ILD were immunhistochemically analyzed. Chronic injury of AECIIs is considered key in pathogenesis of IPF [22,46]. The injured alveolar epithelium can not be re-epithelized which leads to disruption of the epithelial integrity in the alveoli. As a consequence profibrotic cytokines and growth factors are released by the damaged epithelial cells [40,44]. Korfei et al. [42] demonstrated that a severe ER Stress response in the AECIIs underlies apoptosis in patients with IPF. By performing IHC in lung sections of patient with SSc-ILD the present study confirmed AECIIs to be also of interest in CVD associated ILD. We identified AECII specific induction of ER-stress and apoptosis in CVD-ILD. Showing that ER-stress and apoptotic responses in AECIIs also play a key role in CVD associated ILD and the positive ER-stress response in A549 cells after protein inhibition with topotecan and etoposide entail the strong assumption that autoantibodies found in CVD somehow trigger the cellular stress mechanisms in AECII, which in turn contribute majorly to the development of lung fibrosis.

5.3 Conclusions and future perspectives in regard to CVD-ILD pathogenesis

Experiments of this study were performed in order to test the hypothesis that autoantibodies against HisRS, Topo1, Topo2α and Topo2β cause ER-stress and apoptosis in AECII by blocking respective target genes and thus trigger development of lung fibrosis. Data are received from *in vitro* experiments with A549 cells. The used cell line is well established in culture and frequently used for basic research indicating reactions of the human AECIIs.

It has to be emphasized, that the obtained results are preliminary data. First of all, it was important to realize successfull gene silencing and protein inhibition. To gain certainty regarding the effects on apoptosis and ER-stress after respective gene silencing and protein inhibition, a higher number of independent experiments is required in further studies.

One issue which also has to be clarified in future is if binding of autoantibodies against HisRS and topoisomerases indeed results in a loss of function of the target proteins. Other mechanisms caused by the antigen-antibody-complexes, like complement activation or other, more complex, immunological reactions, also have to be taken into consideration concerning development of ILD in CVD.

To identify, if ER-stress and apoptosis in AECIIs are indeed caused by autoantibodies against HisRS, Topo1, Topo2α or Topo2β and thus lead to developement of ILD, a worthwile research focus would be to check binding pattern of purified autoantibodies against HisRS, Topo1, Topo2α or Topo2β in order to confirm AECIIs to be the target cells for the autoantibodies in the lung.

Another interesting issue would be to check, if alveolar epithelial knockdown of HisRS, Topo1, Topo2α or Topo2β triggers developement of ILD by analyzing the consequeces of gene silencing on fibroblastproliferation and matrixproduction. Furthermore the need for secondary hits in development of lung fibrosis such as viral infections have to be investigated.

Further experiments are required to analyze if, in case of a complete loss of target protein, there still exists some secretory activity in the cell and if more time is needed until cellular stress evolves. Therefore transient and stable transfections *in vitro* and *in vivo* have to be performed. Future plan of our group is to work with inducible, AECII

specific knock out mice and check, if silencing of Topo 1/2 and HisRS *in vivo* can contribute to development of lung fibrosis.

From the results of the present study it can be concluded that pathogenesis of CVD associated ILD may include ER-stress and apoptosis of AECIIs. This is reinforced by the finding of an induction of ER-stress and apoptosis after inhibition of topoisomerases *in vitro*. The further elucidation of the precise mechanisms, how the autoantibodies mediate these reactions in AECIIs, still deserves further investigations.

6. Appendix

6.1 Additional figures

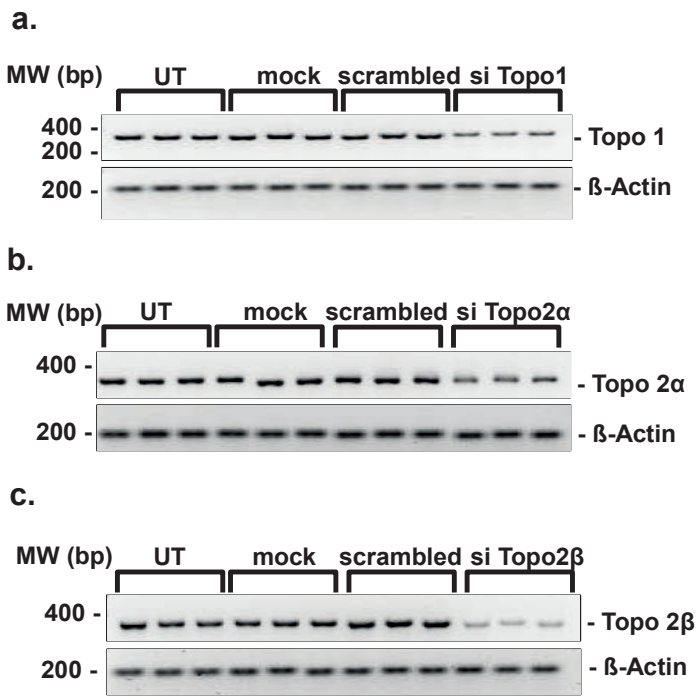

Figure 23: Silencing of Topo1, Topo2α and Topo2β

A549 cells were transfectes with siRNA directed against Topo1 (a), Topo2α (b) and Topo2β (c) and knockdown of respective genes was checked by sqT-PCR 48h after transfection. Mock (transfection with transfection reagen without any siRNA and scrambled (non targeting siRNA) served as negative controls, 30 cycles were performed, β-Actin served as loadig control.

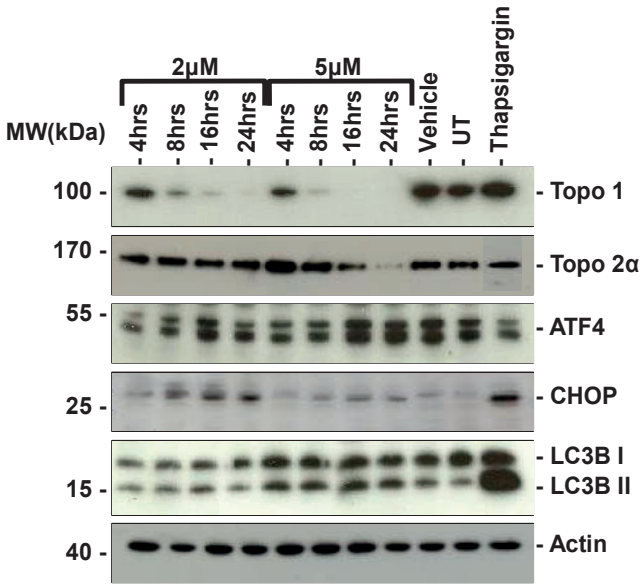

Figure 24: Inhibition of Topo1 after topotecan treatment in A549 cells.

IB analysis of Topo 1, Topo 2α, ATF4, CHOP and LC3 after treatment with 2µM and 5µM of topotecan and different timepoints (4-24h), Vehicle served as negative control, Thapsigargin served as positive control for apoptosis and ER-stress, β-Actin served as loading control.

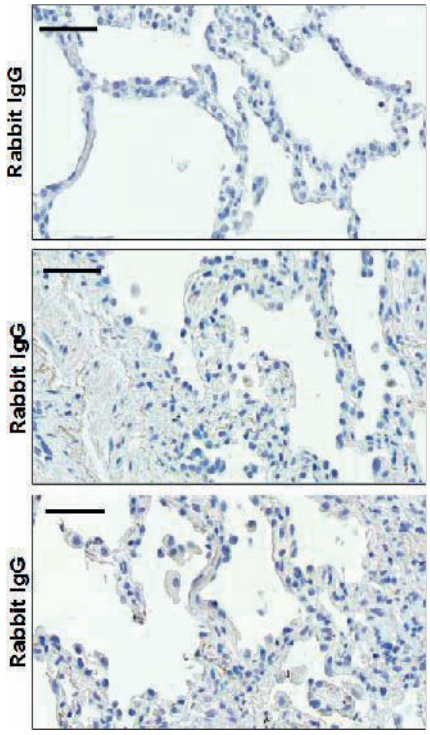

Figure 25: Isotype controls

Immunhistochemistry performed on serial paraffin-embedded lung tissue sections from healthy donors stained for isotype control antibodies. Original magnification: 400x, scalebar: 50µm

6.2 Primer sequences

Gene		Sequences (5' → 3')
ATF4	for	GAT AGG AAG CCA GAC TAC ACT G
	rev	GAG ACC CCA GAT AGG ACT CTG
β-Actin (sqRT-PCR)	for	ACC CTG AAG TAC CCC ATC
	rev	CAG CCT GGA TAG CAA CGT AC
β-Actin (qRT-PCR)	for	CAG AGC CTC GCC TTT GCC G
	rev	GAC GAG CGC GGC GAT ATC AT
CHOP	for	ACT CTC CAG ATT CCA GTC AGA G
	rev	GCC TCT ACT TCC CTG GTC AG
DDB1	for	TAT CCA GAT CAC TTC AGC ATC G
	rev	GAT GGA GCG AGG AAT GAT CTC
HisRS	for	CTA TGA GGC AGT GCT GCT AC
	rev	CAG CAG CTC AGC CTT GAT C
p53	for	GCA CAT GAC GGA GGT TGT G
	rev	AGT GTG ATG ATG GTG AGG ATG
Topo1	for	CCA CAA CGA TTC CCA GAT CG
	rev	TGG ACT AGA GAA GCC ATT TTC C
Topo2α	for	TGG TGA TAA ATG GTG CTG AAG G
	rev	GTT ATG AGA GGA GGT GTC TTC TC
Topo2β	for	ATG CTA GAT GGC CTG GAT CC
	rev	GTC CAG CAG CTT CTG CTT G
VCP	for	CCA AGG GAG TTC TGT TCT ATG G
	rev	GAG GAT GGC AGG ATC AAT GAT G
XBP1	for	GTT GAG AAC CAG GAG GAG TTA AGA
	rev	CAG ACT CTG AAT CTG AAG AGT C
XBP1	for	GAT GCC CTG GTT GCT GAA
	rev	GAG TCA ATA CCG CCA GAA TCC

Table 19: Primer sequences

6.3 Dissociation curves

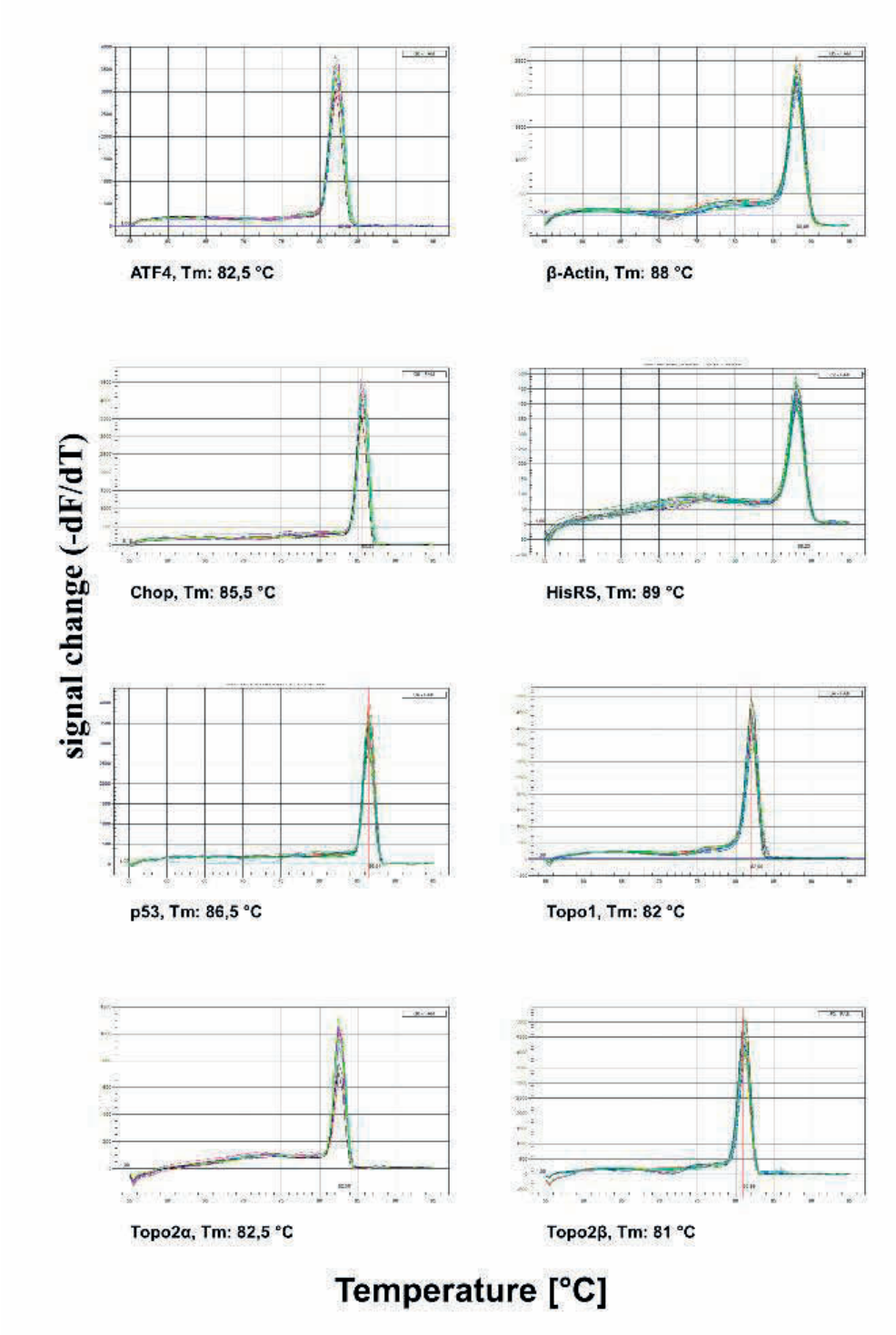

Figure 26: Dissociation curves

7. References

1. Maher Toby M: Diffuse parenchymal lung diseaes. *Medicine* 2012, 40:6, 314-321

2. Chapman HA: Disorders of lung matrix remodeling. *J. Clin. Invest* 2004, 113:148- 157.

3. American Thoracic Society/European Respiratory Society International Multidisciplinary Consensus Classification of the Idiopathic Interstitial Pneumonias. This joint statement of the American Thoracic Society (ATS), and the European Respiratory Society (ERS) was adopted by the ATS board of directors, June 2001 and by the ERS Executive Committee, June 2001. *Am. J. Respir. Crit.Care Med* 2002, 165:277-304.

4. Travis, WD; Costabel, U; Hansell, DM; King TE, Jr; Lynch, DA; Nicholson, AG; Ryerson, CJ; Ryu, JH; Selman, M; Wells, AU; Behr, J; Bouros, D; Brown, KK; Colby, TV; Collard, HR; Cordeiro, CR; Cottin, V; Crestani, B; Drent, M; Dudden, RF; Egan, J; Flaherty, K; Hogaboam, C; Inoue, Y; Johkoh, T; Kim, DS; Kitaichi, M; Loyd, J; Martinez, FJ; Myers, J; Protzko, S; Raghu, G; Richeldi, L; Sverzellati, N; Swigris, J; Valeyre, D: ATS/ERS Committee on Idiopathic Interstitial, Pneumonias (15 September 2013). "An official American Thoracic Society/European Respiratory Society statement: Update of the international multidisciplinary classification of the idiopathic interstitial pneumonias.". *American journal of respiratory and critical care medicine* 2013, **188** (6): 733–48.

5. American Thoracic Society/European Respiratory Society International Multidisciplinary Consensus Classification of the Idiopathic Interstitial Pneumonias. This official statement of the American Thoracic Society (ATS), and the European Respiratory Society (ERS) was approved by the ATS board of directors, June 2013 and by the ERS Steering Committee, March 2013. *Am Respir Crit Care Med.* 2013, 188 (6): 733-748.

6. Raghu G, Collard HR, Egan JJ, Martinez FJ, Behr J, Brown KK, Colby TV, Cordier J, Flaherty KR, Lasky JA, Lynch DA, Ryu JH, Swigris JJ, Wells AU, Ancochea J, Bouros D, Carvalho C, Costabel U, Ebina M, Hansell DM, Johkoh T, Kim DS, King TE, Kondoh Y, Myers J, Müller NL, Nicholson AG, Richeldi L, Selman M, Dudden RF *et al.*: An official ATS/ERS/JRS/ALAT statement: idiopathic pulmonary fibrosis: evidence-based guidelines for diagnosis and management. *Am. J. Respir. Crit. Care Med.* 2011, 183:788-824.

7. Walsh SLF, Hansell DM: Diffuse interstitial lung disease: overlaps and uncertainties. *Eur Radiol* 2010, 20:1859-1867.

8. Flaherty KR, Thwaite EL, Kazerooni EA, Gross BH, Toews GB, Colby TV, et al.: Radiological versus histological diagnosis in UIP and NSIP: survival implications. *Thorax* 2003*,* 58:143-148.

9. Hunninghake GW, Zimmerman MB, Schwartz DA, King TEJ, Lynch J, Hegele R, et al.: Utility of a lung biopsy for the diagnosis of idiopathic pulmonary fibrosis. *Am J Respir Crit Care Med* 2001, 164:193-196.

10. Raghu G, Mageto YN, Lockhart D, Schmidt RA, Wood DE and Godwin JD: The accuracy of the clinical diagnosis of new-onset idiopathic pulmonary fibrosis and other interstitial lung disease: A prospective study. *Chest 1999,* 116:1168-1174.

11. Wells AU, Hansell DM, Rubens MB, King AD, Cramer D, Black CM et al.: Fibrosing alveolitis in systemic sclerosis: indices of lung function in relation to extent of disease on computed tomography. *Arthritis Rheum* 1997, 40:1229-1236.

12. Lamblin C, Bergoin C, Saelens T, Wallaert B: Interstitial lung diseases in collagen vascular diseases. *Eur Respir J Suppl* 2001, 32:69s-80s.

13. De Lauretis A, Veeraraghavan S, Renzoni E: Review Series: Aspects of Interstitial lung disease: Connective tissue disease-associated interstitial lung disease: How does it differ frim IPF? How should the clinical approach differ? *Chronic respiratory Disease* 2011, 8:53.

14. Schnabel A, Reuter M: Interstitielle Lungenkrankheit bei Kollagenosen. *Z. Rheumatol* 2009, 68:650-657.

15. Kang EH, Lee EB, Shin KC, Im CH, Chung DH, Han SK, Song YW: Interstitial lung disease in patients with polymyositis, dermatomyositis and amyopathic dermatomyositis. *Rheumatology (Oxford)* 2005, 44:1282-1286.

16. Takahashi T, Wada I, Ohtsuka Y, Munakata M, Homma Y, Kuroki Y: Autoantibody to alanyl-tRNA synthetase in patients with idiopathic pulmonary fibrosis. *Respirology* 2007, 12:642-653.

17. Crystal RG, Gadek JE, Ferrans VJ, Fulmer JD, Line BR, Hunninghake GW: Interstitial lung disease: current concepts of pathogenesis, staging and therapy. *Am. J. Med.* 1981, 70:542-568.

18. Wasicek CA, Reichlin M, Montes M, Raghu G: Polymyositis and interstitial lung disease in a patient with anti-Jo1 prototype. *Am. J. Med.* 1984, 76:538-544.

19. Veraldi KL, Hsu E, Feghali-Bostwick CA: Pathogenesis of pulmonary fibrosis in systemic sclerosis: lessons from interstitial lung disease. *Curr Rheumatol Rep* 2010, 12:19-25.

20. Bouros D, Wells AU, Nicholson AG, Colby TV, Polychronopoulos V, Pantelidis P, Haslam PL, Vassilakis DA, Black CM, Du Bois RM: Histopathologic subsets of fibrosing alveolitis in patients with systemic sclerosis and their relationship to outcome. *Am. J. Respir. Crit. Care Med* 2002, 165:1581-1586.

21. Strollo D, Goldin J: Imaging lung disease in systemic sclerosis. *Curr Rheumatol Rep* 2010, 12:156-161.

22. Visscher DW, Myers JL: Histologic spectrum of idiopathic interstitial pneumonias. *Proc Am Thorac Soc* 2006, 3:322-329.

23. Kim DS, Collard HR, King TE: Classification and natural history of the idiopathic interstitial pneumonias. *Proc Am Thorac Soc* 2006, 3:285-292.

24. Myers JL, Katzenstein AL: Epithelial necrosis and alveolar collapse in the pathogenesis of usual interstitial pneumonia. *Chest* 1988, 94:1309-1311.

25. Noble PW, Homer RJ: Back to the future: historical perspective on the pathogenesis of idiopathic pulmonary fibrosis. *Am. J. Respir. Cell Mol. Biol* 2005, 33:113-120.

26. Barbas-Filho JV, Ferreira MA, Sesso A, Kairalla RA, Carvalho CR, Capelozzi VL: Evidence of type II pneumocyte apoptosis in the pathogenesis of idiopathic pulmonary fibrosis (IFP)/usual interstitial pneumonia (UIP). *J. Clin. Pathol* 2001, 54:132-138.

27. Katzenstein AL, Myers JL: Idiopathic pulmonary fibrosis: clinical relevance of pathologic classification. *Am. J. Respir. Crit. Care Med* 1998, 157:1301-1315.

28. Mueller-Mang C, Grosse C, Schmid K, Stiebellehner L, Bankier AA: What Every Radiologist Should Know about Idiopathic Interstitial Pneumonias. Radiographics 2007, 27:595-615.

29. Chandler PW, Shin MS, Friedman SE, Myers JL, Katzenstein AL: Radiographic manifestations of bronchiolitis obliterans with organizing pneumonia vs usual interstitial pneumonia. *AJR Am J Roentgenol* 1986, 147:899-906.

30. Hunninghake GW, Lynch DA, Galvin JR, Gross BH, Müller N, Schwartz DA, King TE, Lynch JP, Hegele R, Waldron J, Colby TV, Hogg JC: Radiologic findings are strongly associated with a pathologic diagnosis of usual interstitial pneumonia. *Chest* 2003, 124:1215-1223.

31. Maher TM: Pirfenidone in idiopathic pulmonary fibrosis. *Drugs Today* 2010, 46:473–482.

32. Jackson RM, Gomez-Martin O: Development and utility of pirfenidone in the treatment of idiopathic pulmonary fibrosis: review of preclinical science and recent clinical trials. *Transplant Res Risk Manage* 2011, 3: 55–63.

33. Richeldi L, Costabel U, Selman M, et al: Efficacy of a tyrosine kinase inhibitor in idiopathic pulmonary fibrosis. *N Engl J Med* 2011, 365: 1079–1087.

34. Noble PW, Albera C, Bradford WZ, et. Al: Pirfenidone in patients with idopathic pulmonary fibrosis (CAPACITY): two randomised trials. *Lancet* 2011, 4377:1760-9.

35. Idiopathic Pulmonary Fibrosis Research Network, Zisman DA, Schwarz M, et al.: A controlled trial of sildenafil in advanced idiopathic pulmonary fibrosis. *N Engl J Med* 2010, 363:620-8.

36. Park JH, KimDS, Park I, Jang SJ, Kitaichi M, Nicholson AG, et al.: Prognosis of fibrotic interstitial pneumonia: idiopathic versus collagen vascular disease-related subtypes. *Am J Respir Crit Care Med* 2007; 175:705-711.

37. Esam H. Alhamad: Clinical characteristics and survival in idiopathic pulmonary fibrosis and connective tissue disease-associated usual interstitial pneumonia. J Thorac Dis. 2015, 7(3): 386–393.

38. Günther A, Ermert L, Breithecker A, Hackstein N, Eickelberg O, Morr H, Grimminger F, Velcovsky H, Seeger W: Klassifikation, Diagnostik und Therapie der idiopathischen interstitiellen Pneumonien: Eine kritische Bestandsaufnahme der gegenwärtig in Deutschland geübten Praxis. *Deutsches Ärzteblatt* 2003, 100.

39. Kinder BW, Collard HR, Koth L, Daikh DI, Wolters PJ, Elicker B, Jones KD, King TE: Idiopathic nonspecific interstitial pneumonia: lung manifestation of undifferentiated connective tissue disease? *Am. J. Respir. Crit. Care Med.* 2007, 176:691-697.

40. Selman M, King TE, Pardo A: Idiopathic pulmonary fibrosis: prevailing and evolving hypotheses about its pathogenesis and implications for therapy. *Ann. Intern. Med* 2001, 134:136-151.

41. Tashkin DP, Elashoff R, Clements PJ, et al.: Cycloposphamide versus placebo in scleroderma lung disease. *N Engl J Med* 2006, 354: 2655-66.

42. Korfei M, Ruppert C, Mahavadi P, Henneke I, Markart P, Koch M, Lang G, Fink L, Bohle R, Seeger W, Weaver TE, Guenther A: Epithelial endoplasmic reticulum stress and apoptosis in sporadic idiopathic pulmonary fibrosis. *Am. J. Respir. Crit.Care Med.* 2008, 178:838-846.

43. Pardo A, Selman M: Idiopathic pulmonary fibrosis: new insights in its pathogenesis. *Int. J. Biochem. Cell Biol* 2002, 34:1534-1538.

44. Selman M, Pardo A: Idiopathic pulmonary fibrosis: an epithelial/fibroblastic cross-talk disorder. *Respir. Res* 2002, 3:3.

45. Uhal BD, Joshi I, Hughes WF, Ramos C, Pardo A, Selman M: Alveolar epithelial cell death adjacent to underlying myofibroblasts in advanced fibrotic human lung. *Am. J. Physiol.* 1998, 275:L1192-9.

46. Du Bois RM: Strategies for treating idiopathic pulmonary fibrosis. *Nat Rev Drug Discov* 2010, 9:129-140.

47. Günther A, Korfei M, Mahavadi P, Beck D von der, Ruppert C, Markart P: Unravelling the progressive pathophysiology of idiopathic pulmonary fibrosis. *Eur Respir Rev* 2012, 21:152-160.

48. Fehrenbach H: Alveolar epithelial type II cell: defender of the alveolus revisited. *Respir. Res.* 2001, 2:33-46.

49. Pison U, Max M, Neuendank A, Weissbach S, Pietschmann S: Host defence capacities of pulmonary surfactant: evidence for 'non-surfactant' functions of the surfactant system. *Eur. J. Clin. Invest.* 1994, 24:586-599.

50. Uhal BD: Cell cycle kinetics in the alveolar epithelium. *Am. J. Physiol.* 1997, 272:L1031-45.

51. Daniels CB, Lopatko OV, Orgeig S: Evolution of surface activity related functions of vertebrate pulmonary surfactant. *Clin. Exp. Pharmacol. Physiol.* 1998, 25:716-721.

52. Hills BA: An alternative view of the role(s) of surfactant and the alveolar model. *J. Appl. Physiol.* 1999, 87:1567-1583.

53. Thomas AQ, Lane K, Phillips J, Prince M, Markin C, Speer M, Schwartz DA, Gaddipati R, Marney A, Johnson J, Roberts R, Haines J, Stahlman M, Loyd JE: Heterozygosity for a surfactant protein C gene mutation associated with usual interstitial pneumonitis and cellular nonspecific interstitial pneumonitis in one kindred. *Am. J. Respir. Crit. Care Med.* 2002, 165:1322-1328.

54. Cameron HS, Somaschini M, Carrera P, Hamvas A, Whitsett JA, Wert SE, Deutsch G, Nogee LM: A common mutation in the surfactant protein C gene associated with lung disease. *J. Pediatr.* 2005, 146:370-375.

55. Alder JK, Chen JJ, Lancaster L, Danoff S, Su S, Cogan JD, Vulto I, Xie M, Qi X, Tuder RM, Phillips JA, Lansdorp PM, Loyd JE, Armanios MY: Short telomeres are a risk factor for idiopathic pulmonary fibrosis. *Proc. Natl. Acad. Sci. U.S.A.* 2008, 105:13051-13056.

56. Mahavadi P, Korfei M, Henneke I, Liebisch G, Schmitz G, Gochuico BR, Markart P, Bellusci S, Seeger W, Ruppert C, Guenther A: Epithelial stress and apoptosis underlie Hermansky-Pudlak syndrome-associated interstitial pneumonia. *Am. J. Respir. Crit. Care Med.* 2010, 182:207-219.

57. Anelli T, Sitia R: Protein quality control in the early secretory pathway. *EMBO J.* 2008, 27:315-327.

58. Kaufman RJ: Stress signaling from the lumen of the endoplasmic reticulum: coordination of gene transcriptional and translational controls. *Genes Dev.* 1999, 13:1211-1233.

59. Wu J, Kaufman RJ: From acute ER stress to physiological roles of the Unfolded Protein Response. *Cell Death Differ.* 2006, 13:374-384.

60. Shore GC, Papa FR, Oakes SA: Signaling cell death from the endoplasmic reticulum stress response. *Curr. Opin. Cell Biol.* 2011, 23:143-149.

61. Calfon M, Zeng H, Urano F, Till JH, Hubbard SR, Harding HP, Clark SG, Ron D: IRE1 couples endoplasmic reticulum load to secretory capacity by processing the XBP-1 mRNA. *Nature* 2002, 415:92-96.

62. Yamamoto K, Sato T, Matsui T, Sato M, Okada T, Yoshida H, Harada A, Mori K: Transcriptional induction of mammalian ER quality control proteins is mediated by single or combined action of ATF6alpha and XBP1. *Dev. Cell* 2007, 13:365-376.

63. Harding HP, Zhang Y, Zeng H, Novoa I, Lu PD, Calfon M, Sadri N, Yun C, Popko B, Paules R, Stojdl DF, Bell JC, Hettmann T, Leiden JM, Ron D: An integrated stress response regulates amino acid metabolism and resistance to oxidative stress. *Mol. Cell* 2003, 11:619-633.

64. Paschen W, Mengesdorf T: Endoplasmic reticulum stress response and neurodegeneration. *Cell Calcium* 2005, 38:409-415.

65. Su N, Kilberg MS: C/EBP homology protein (CHOP) interacts with activating transcription factor 4 (ATF4) and negatively regulates the stress-dependent induction of the asparagine synthetase gene. *J. Biol. Chem.* 2008, 283:35106-35117.

66. Chérin P.: Polymyositis [http://www.orpha.net/data/patho/GB/uk-PM.pdf].

67. Briani C, Doria A, Sarzi-Puttini P, Dalakas MC: Update on idiopathic inflammatory myopathies. *Autoimmunity* 2006, 39:161-170.

68. Dalakas MC and Hohlfeld R: Polymyositis and dermatomyositis. *Lancet* 2003, 362: 971-982.

69. Chérin P.: Dermatomyositis [http://www.orpha.net/data/patho/Pro/en/Dermatomyositis-FRenPro701.pdf].

70. Bernstein RM, Morgan SH, Chapman J, Bunn CC, Mathews MB, Turner-Warwick M, Hughes GR: Anti-Jo-1 antibody: a marker for myositis with interstitial lung disease.

71. DermIS-Dermatomyositis (image) [http://www.dermis.net/dermisroot/en/39526/image.htm].

72. DermIS-Dermatomyositis (image) [http://www.dermis.net/dermisroot/en/39484/image.htm].

73. DermIS-Dermatomyositis (image) [http://www.dermis.net/dermisroot/en/39571/image.htm].

74. Häussermann A, Gillissen A, Seidel W: Das Anti-Jo-1-Syndrom – eine Sonderform der Myositis mit interstitieller Lungenerkrankung. *Pneumologie* 2010, 64:496-503.

75. Tzioufas AG: Antisynthetase syndrome 2001.

76. DermIS-Raynaud'sDisease(image) [http://www.dermis.net/dermisroot/en/25163/image.ht

77. Arakawa H, Yamada H, Kurihara Y, Nakajima Y, Takeda A, Fukushima Y, Fujioka M: Nonspecific interstitial pneumonia associated with polymyositis and dermatomyositis: serial high-resolution CT findings and functional correlation. *Chest* 2003, 123:1096-1103.

78. Ikezoe J, Johkoh T, Kohno N, Takeuchi N, Ichikado K, Nakamura H: High-resolution CT findings of lung disease in patients with polymyositis and dermatomyositis. *J Thorac Imaging* 1996, 11:250-259.

79. Chen I, Jan Wu Y, Lin C, Fan K, Luo S, Ho H, et al.: Interstitial lung disease in polymyositis and dermatomyositis. *Clin Rheumatol* 2009, 28:639-646.

80. Schnabel A, Reuter M, Biederer J, Richter C, and Gross WL. Interstitial lung disease in polymyositis and dermatomyositis: clinical course and response to treatment. Semin Arthritis Rheum 2003, 32: 273-284.

81. Labirua A, Lundberg I: Interstitial lung disease and idiopathic inflammatory myopathies: progress and pitfalls. *Curr Opin Rheumatol* 2010, 22:633-638.

82. Levine SM, Raben N, Xie D, Askin FB, Tuder R, Mullins M, Rosen A, Casciola-Rosen LA: Novel conformation of histidyl-transfer RNA synthetase in the lung: the target tissue in Jo-1 autoantibody-associated myositis. *Arthritis Rheum* 2007, 56:2729-2739.

83. Targoff IN: Autoantibodies in polymyositis. *Rheum. Dis. Clin. North Am.* 1992, 18:455-482.

84. Freist W, Verhey JF, Ruhlmann A, Gauss DH, Arnez JG: Histidyl-tRNA synthetase. *Biol Chem* 1999, 380:623-646.

85. Vlachoyiannopoulos PG: Systemicsclerosis (scleroderma) [http://www.orpha.net/data/patho/GB/uk-SSc.pdf].

86. Du Bois RM: State of the Art. Mechanisms of Scleroderma-induced Lung Disease. *Proceedings of the American Thoracic Society* 2007, 4:434-438.

87. LeRoy EC, Black C, Fleischmajer R, Jablonska S, Krieg T, Medsger TA, Rowell N, Wollheim F: Scleroderma (systemic sclerosis): classification, subsets and pathogenesis. *J. Rheumatol.* 1988, 15:202-205.

88. Hayakawa I, Hasegawa M, Takehara K, Sato S: Anti-DNA topoisomerase II autoantibodies in localized scleroderma. *Arthritis & Rheumatism* 2004, 50:227-232.

89. DermIS - Progressive Systemic Scleroderma (image) [http://www.dermis.net/dermisroot/en/39101/image.htm].

90. DermIS - Progressive Systemic Scleroderma (image) [http://www.dermis.net/dermisroot/en/39207/image.htm].

91. DermIS - Progressive Systemic Scleroderma (image) [http://www.dermis.net/dermisroot/en/39151/image.htm].

92. Ostojic P, Cerinic MM, Silver R, Highland K, Damjanov N: Interstitial lung disease in systemic sclerosis. *Lung* 2007, 185:211-220.

93. Arroliga AC, Podell DN, Matthay RA: Pulmonary manifestations of scleroderma. *J Thorac Imaging* 1992, 7:30-45.

94. Strollo D, Goldin J: Imaging lung disease in systemic sclerosis. *Curr Rheumatol Rep* 2010, 12:156-161.

95. Cottin V: Interstitial lung disease. *Eur Respir Rev* 2013, 22:26-32.

96. Champoux JJ: DNA TOPOISOMERASES. *Annu. Rev. Biochem* 2001, 70:369-413.

97. Ju B, Lunyak VV, Perissi V, Garcia-Bassets I, Rose DW, Glass CK, Rosenfeld MG: A topoisomerase IIbeta-mediated dsDNA break required for regulated transcription. *Science* 2006, 312:1798-1802.

98. rep2.24.gif (GIF-Grafik, 639x216 Pixel) [http://biosiva.50webs.org/rep2.24.gif].

99. Nitiss JL: DNA topoisomerase II and its growing repertoire of biological functions. *Nat Rev Cancer* 2009, 9:327-337.

100. Paroo Z, Liu Q, Wang X: Biochemical mechanisms of the RNA-induced silencing complex. *Cell Res* 2007, 17:187-194.

101. DrugBank: etoposide (DB00773) [http://www.drugbank.ca/drugs/DB00773].

102. Buckwalter CA, Lin AH, Tanizawa A, Pommier YG, Cheng YC, Kaufmann SH: RNA synthesis inhibitors alter the subnuclear distribution of DNA topoisomerase I. *Cancer Res.* 1996, 56:1674-1681.

103. Winter S, Weller M: Potentiation of CD95L-induced apoptosis of human malignant glioma cells by topotecan involves inhibition of RNA synthesis but not changes in CD95 or CD95L protein expression. *J. Pharmacol. Exp. Ther.* 1998, 286:1374-1382.

104. DrugBank: topotecan (DB01030) [http://www.drugbank.ca/drugs/DB01030].

105. Wilhelm J, Pingoud A: Real-time polymerase chain reaction. *Chembiochem* 2003, 4:1120-1128.

106. Basseri S, Austin RC: Endoplasmic Reticulum Stress and Lipid Metabolism: Mechanisms and Therapeutic Potential. *Biochemistry Research International* 2012, 2012:1-13.

107. Szegezdi E, Logue SE, Gorman AM, Samali A: Mediators of endoplasmic reticulum stress-induced apoptosis. *EMBO Rep* 2006, 7:880-885.

108. Kim J, Choi TG, Ding Y, Kim Y, Ha KS, Lee KH, Kang I, Ha J, Kaufman RJ, Lee J, Choe W, Kim SS: Overexpressed cyclophilin B suppresses apoptosis associated with ROS and Ca2+ homeostasis after ER stress. *J. Cell. Sci.* 2008, 121:3636-3648.

109. Wójcik C, Rowicka M, Kudlicki A, Nowis D, McConnell E, Kujawa M, DeMartino GN: Valosin-containing protein (p97) is a regulator of endoplasmic reticulum stress and of the degradation of N-end rule and ubiquitin-fusion degradation pathway substrates in mammalian cells. *Mol. Biol. Cell* 2006, 17:4606-4618.

110. Porter AG, Jänicke RU: Emerging roles of caspase-3 in apoptosis. *Cell Death Differ.* 1999, 6:99-104.

111. Strange C, Highland KB: Interstitial lung disease in the patient who has connective tissue disease. *Clin. Chest Med.* 2004, 25:549-59, vii.

112. Hayashi S, Tanaka M, Kobayashi H, et al.: High-resolution computed tomography characterization of interstitial lung diseases in polymyositis/dermatomyositis. *J Rheumatol* 2008, 35:260-269

113. Kubo M, Ihn H, Yamane K, Kikuchi K, Yazawa N, Soma Y, Tamaki K: Serum KL-6 in adult patients with polymyositis and dermatomyositis. *Rheumatology* 2000, 39:632-636.

114. Samuels DS, Tojo T, Homma M, Shimizu N: Inhibition of topoisomerase I by antibodies in sera from scleroderma patients. *FEBS Lett.* 1986, 209 (2): 231– 4.

115. Lisi A, et al.: Sjögren´s syndrome: anti-Ro and anti-La autoantibodies trigger apoptotic mechanism in the human slaivary gland cell line, A-253, *Med* 2007, 49, 103-8

116. Morris Reichlin: Cellular Dysfunction Induced by Penetration of Autoantibodies into Living Cells: Cellular Damage and Dysfunction Mediated by Antibodies to dsDNA and Ribsomal P Proteins. *Journal of Autoimmunity* 1998, 11:557-561.

117. Elkon K, Casali P: Nature and functions of autoantibodies. *Nat Clin Pract Rheumatol* 2008, 4(9):491-8.

118. Karsten CM, Köjl J: The immunoglobulin, IgG Fc receptor and complement triangle in autoimmune diseases. *Immunibiology* 2012, 217(11):1067-79.

119. Wells AU, Hansell DM, Harrison NK, Lawrence R, Black CM, du Bois RM: Clearance of inhaled 99mTc-DTPA predicts the clinical course of fibrosing alveolitis. *Eur Respir J*. 1993, 6:797-802.

120. Selman M, Pardo A: Role of epithelial cells in idiopathic pulmonary fibrosis: from innocent targets to serial killers. *Proc Am Thorac Soc* 2006, 3:364-372.

121. Kropski JA, Lawson WE, Blackwell TS: Right place, right time: the evolving role of herpesvirus infection as a "second hit" in idiopathic pulmonary fibrosis. *Am. J. Physiol. Lung Cell Mol. Physiol.* 2012, 302:L441-4.

122. Okada T, Yoshida H, Akazawa R, Negishi M, Mori K: Distinct roles of activating transcription factor 6 (ATF6) and double-stranded RNA-activated protein kinase-like endoplasmic reticulum kinase (PERK) in transcription during the mammalian unfolded protein response. *Biochem. J.* 2002, 366:585-594.

123. Oyadomari S, Mori M: Roles of CHOP/GADD153 in endoplasmic reticulum stress. *Cell Death Differ.* 2004, 11:381-389.

124. Averous J, Bruhat A, Jousse C, Carraro V, Thiel G, Fafournoux P: Induction of CHOP expression by amino acid limitation requires both ATF4 expression and ATF2 phosphorylation. *J. Biol. Chem.* 2004, 279:5288-5297.

125. Gotoh T, Terada K, Oyadomari S, Mori M: hsp70-DnaJ chaperone pair prevents nitric oxide- and CHOP-induced apoptosis by inhibiting translocation of Bax to mitochondria. *Cell Death Differ.* 2004, 11:390-402.

8. Erklärung

„Hiermit erkläre ich, dass ich die vorgelegte Dissertation selbstständig und ohne unzulässige Hilfe oder Benutzung anderer als der angegebenen Hilfsmittel angefertigt habe. Alle Textstellen, die wörtlich oder sinngemäß aus veröffentlichten oder nichtveröffentlichten Schriften entnommen sind, und alle Angaben, die auf mündlichen Auskünften beruhen, sind als solche kenntlich gemacht. Bei den von mir durchgeführten und in der Dissertation erwähnten Untersuchungen habe ich die Grundsätze guter wissenschaftlicher Praxis, wie sie in der „Satzung der Justus-Liebig-Universität Gießen zur Sicherung guter wissenschaftlicher Praxis“ niedergelegt sind, eingehalten sowie ethische, datenschutzrechtliche und tierschutzrechtliche Grundsätze befolgt. Ich versichere, dass Dritte von mir weder unmittelbar noch mittelbar geldwerte Leistungen für Arbeiten erhalten haben, die im Zusammenhang mit dem Inhalt der vorgelegten Dissertation stehen, oder habe diese nachstehend spezifiziert. Die vorgelegte Arbeit wurde weder im Inland noch im Ausland in gleicher oder ähnlicher Form einer anderen Prüfungsbehörde zum Zweck einer Promotion oder eines anderen Prüfungsverfahrens vorgelegt. Alles aus anderen Quellen und von anderen Personen übernommene Material, das in der Arbeit verwendet wurde oder auf das direkt Bezug genommen wird, wurde als solches kenntlich gemacht. Insbesondere wurden alle Personen genannt, die direkt und indirekt an der Entstehung der vorliegenden Arbeit beteiligt waren. Mit der Überprüfung meiner Arbeit durch eine Plagiatserkennungssoftware bzw. ein internetbasiertes Softwareprogramm erkläre ich mich einverstanden.“

9. Danksagung

Professor Dr. med. Werner Seeger danke ich für die Möglichkeit der Durchführung dieser Arbeit.

Ich bedanke mich bei meinem Doktorvater Prof. Dr. med. Andreas Günther für die Chance, in seinem Team Einblicke in wissenschaftliches Denken und Arbeiten zu erlangen. Seine wissenschaftliche Kompetenz und Leidenschaft für das Thema waren mir eine Stütze und Motivation bei der Erstellung dieser Arbeit.

Ein ganz besonderer Dank geht an Dr. rer. nat. Poornima Mahavadi für die ausgezeichnete und nette Betreuung. Zu jeder Zeit konnte ich mich auf ihre Unterstützung verlassen. Danke für die schöne und lehrreiche Zeit!

Ich danke allen Mitarbeitern des Labors für die Hilfsbereitschaft und viele gute Ratschläge.

Bei Dr. Jasmin Wagner bedanke ich mich für die freundliche Unterstützung bei der Erstellung der Arbeit.

Abschließend danke ich meiner Familie und Arne für stetigen Rückhalt und Geduld.

édition scientifique
VVB LAUFERSWEILER VERLAG

VVB LAUFERSWEILER VERLAG
STAUFENBERGRING 15
D-35396 GIESSEN

Tel: 0641-5599888 Fax: -5599890
redaktion@doktorverlag.de
www.doktorverlag.de

ISBN: 978-3-8359-6542-3